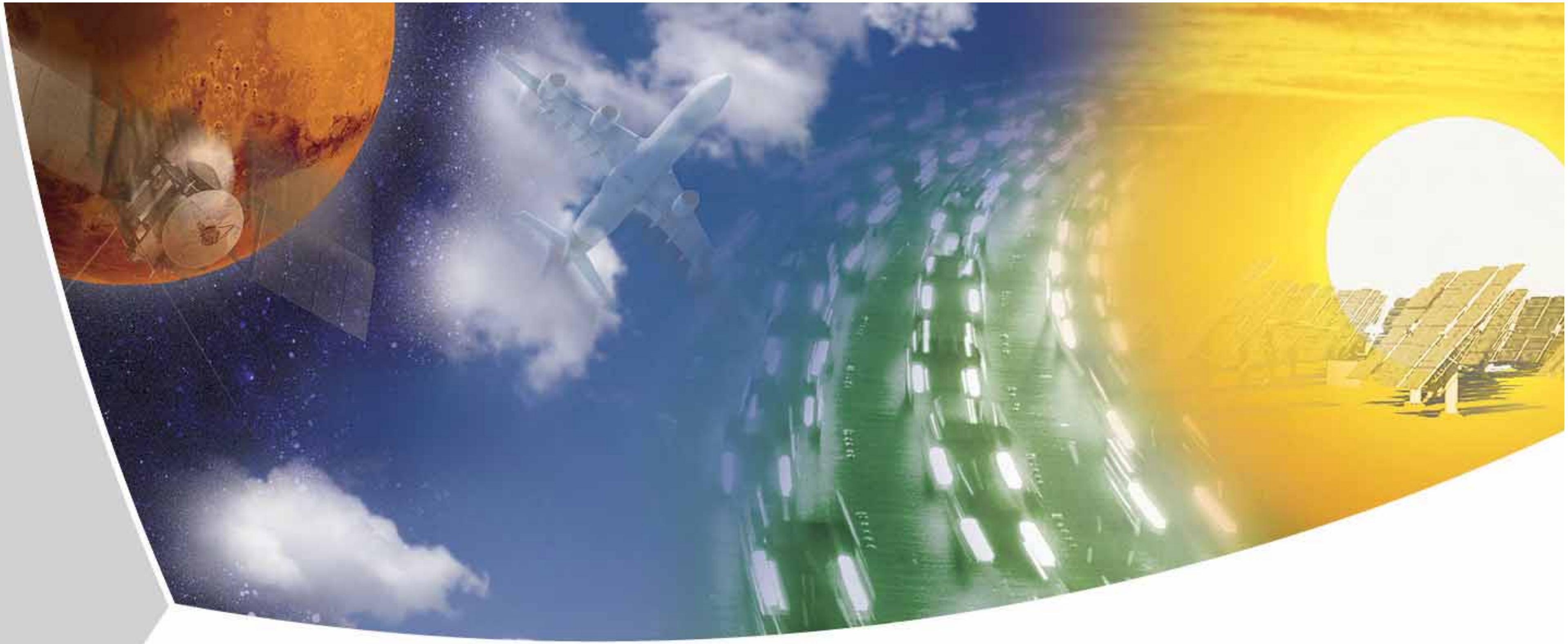

Advanced Bistatic and Multistatic SAR Concepts and Applications

Gerhard Krieger

Microwaves and Radar Institute, DLR

DLR Deutsches Zentrum für Luft- und Raumfahrt e.V.
in der Helmholtz-Gemeinschaft

Future SAR Systems: Motivation

Application Areas for SAR Data Products

Agriculture

Precision Farming Suite
Crop Ripeness
Crop Inventory
Yield Prediction Cereals

Risk / Disaster

Flood Damage Assessment
Fire Damage Assessment
Storm Damage Assessment

Forestry

Strategic Forestry Inventory
Reconnaissance Inventory
Inventory Update

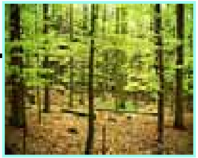

Security

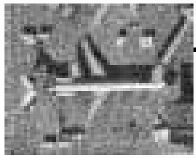

Reconnaissance Imagery
(VHR-SAR)

Cartography

Topo Map
Regional Planing Map
Environmental Planing Map
Infrastructure Planing Map

Geology

Geology Structure Map
Geology Image Map
Geology Elevation Map
Oil Seep Detection

Marine

Ship Detection Service
Oil Spill Monitoring
Sea Ice Monitoring

Transportation

Dynamic Traffic Monitoring
Maps of Roads, Channels, ...

Requirements

- ***wide area coverage and short revisit times***
- ***high radiometric and geometric resolution***
- ***new data products:***
  - ***high precision DEMs***
  - ***3-D volume images (biomass, soil, ice, …)***
  - ***dynamic maps (ocean currents, traffic, …)***
  - ***…***
- ***high reliability and cost efficiency***

Microwaves and Radar Institute
gerhard.krieger@dlr.de

Future SAR Systems: Paradigm Shift to Satellite Clusters

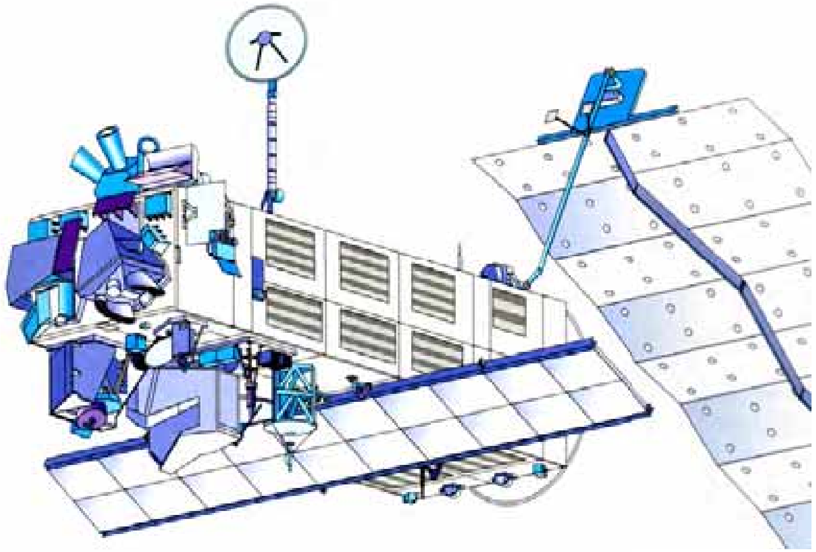

Paradigm Shift

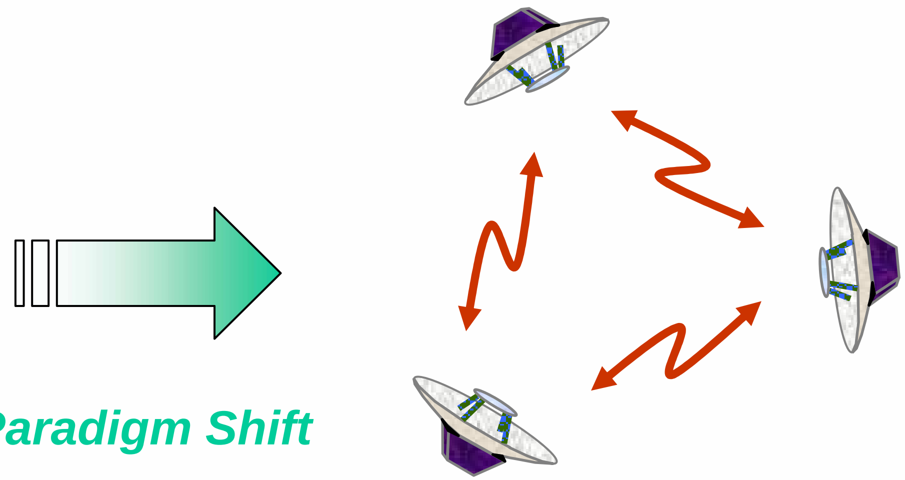

Large, multi-functional satellites

Virtual satellite -
web of cooperating satellites

- Smaller, simpler satellites → reduced cost & time
- Modular design → upgradable, improved reliability
- Spatially distributed → improved revisit time / coverage / adaptability
- Separated, sparse apertures → improved performance and resolution

Microwaves and Radar Institute
gerhard.krieger@dlr.de

Bistatic and Multistatic SAR Systems

Definitions:
- Radar systems with a spatial separation between transmitter and receiver are called ***bistatic***.
- Systems with multiple receivers are called ***multistatic.***

Fully active system

(TechSAT21, Radarsat 2/3, TanDEM-X)

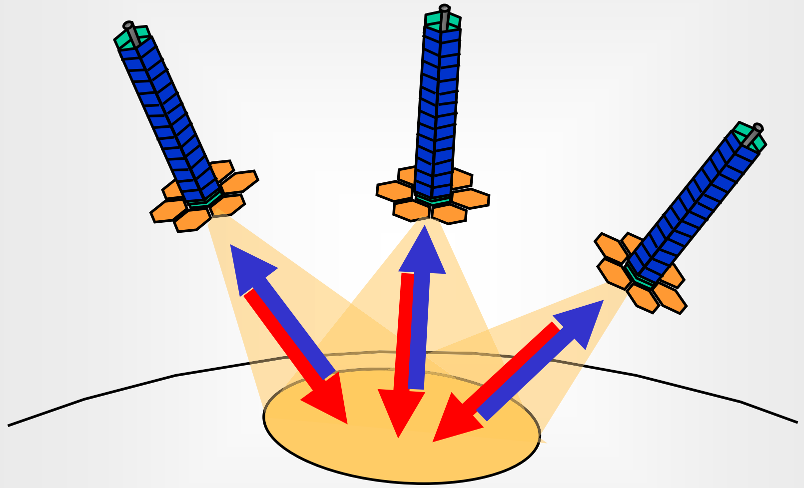

+ more observables & baselines
+ phase synchronisation in ping/pong mode
+ high redundancy & great flexibility

Semi active system

(BISSAT, Cartwheel, Pendulum)

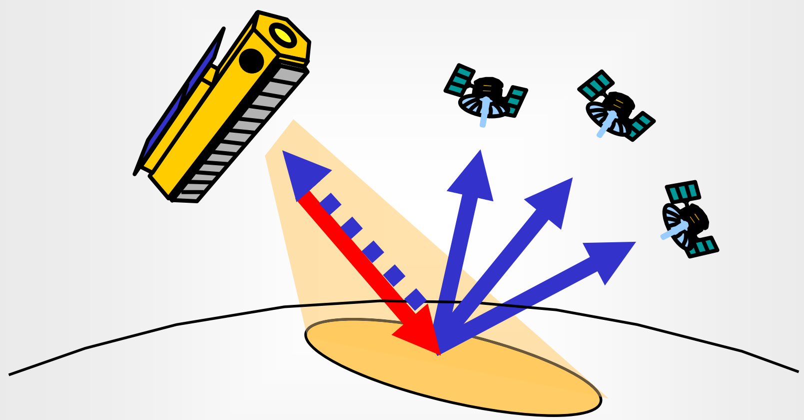

+ reduced size, weight and costs
+ increased sensitivity (no Tx/Rx switches)
+ receiver camouflage, robustness to jamming

Microwaves and Radar Institute
gerhard.krieger@dlr.de

Examples for Suggested Missions

TanDEM-X (Germany)

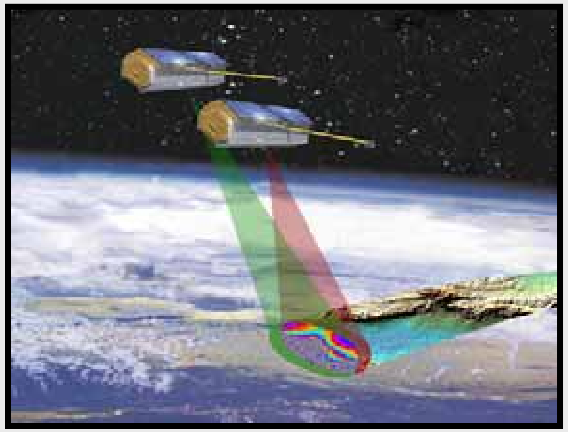

Radarsat 2/3 (Canada)

TechSat 21 (USA)

BISSAT (Italy)

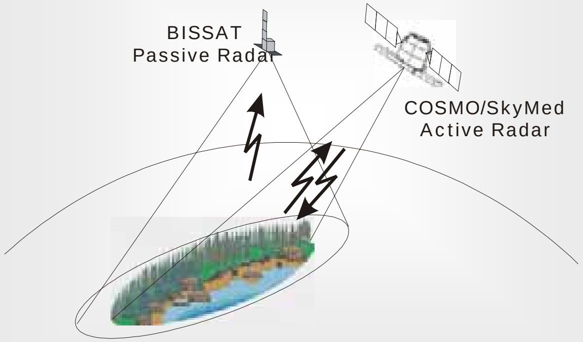

TerraSAR-L Cartwheel (ESA)

Voice, Habitat (Earth Explorer Proposals)

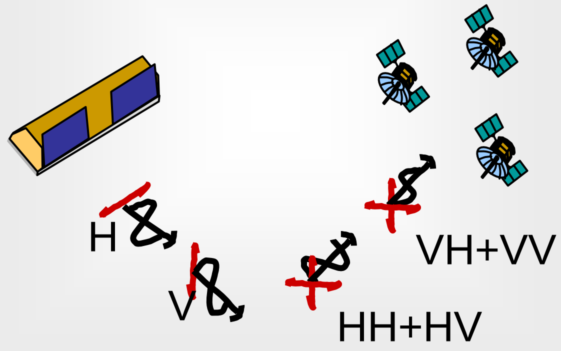

Microwaves and Radar Institute
gerhard.krieger@dlr.de

Potentials of Bistatic and Multistatic SAR Systems

Bistatic Imaging

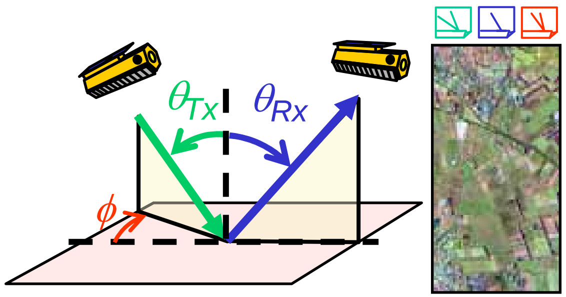

Cross-Track Interferometry

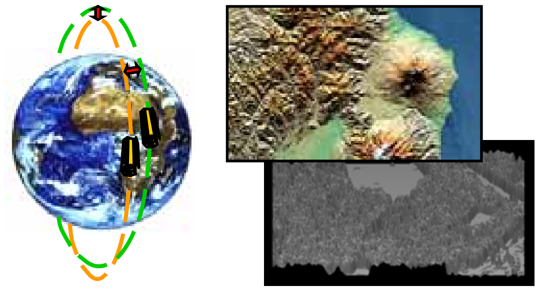

Along-Track Interferometry

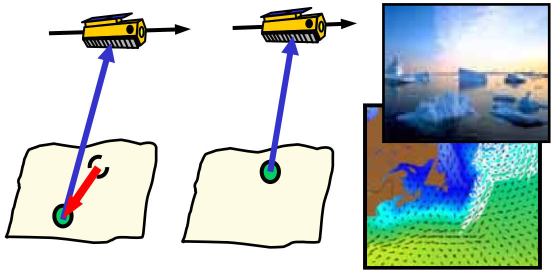

Moving Target Indication

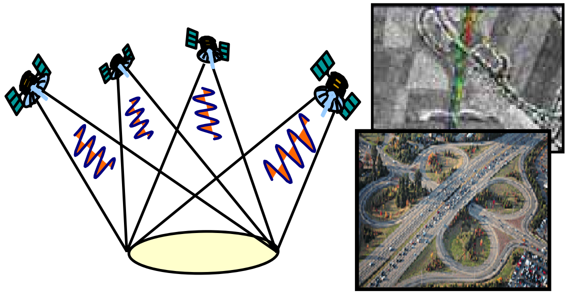

Frequent Monitoring

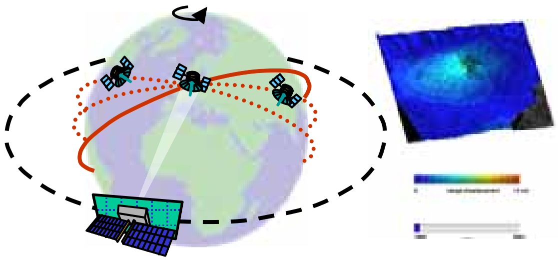

Wide Swath Imaging

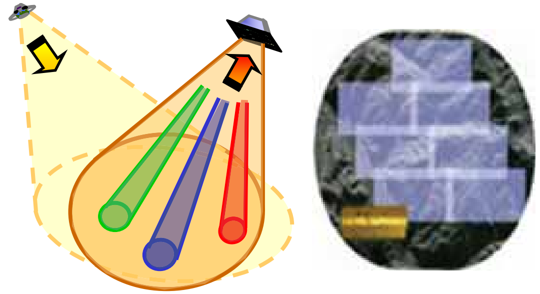

Resolution Enhancement

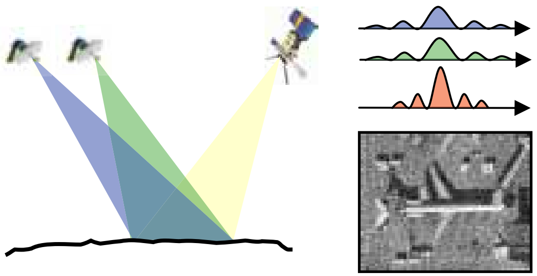

SAR Tomography

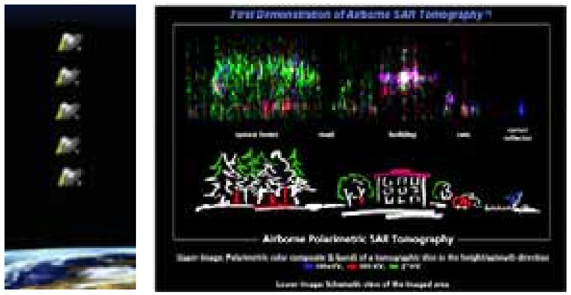

…

Interference Suppression

Silent Operation

Increased Radiom. Sensitivity

Double Differential InSAR

…

Geostationary Illuminator / LEO Receivers

Basic Idea:
- constant illumination by geostationary transmitter
- signal reception by multiple low-cost receivers

Receivers:
- passive (receive only)
- low power, small antennas
- low-cost micro-satellites
- low earth orbit

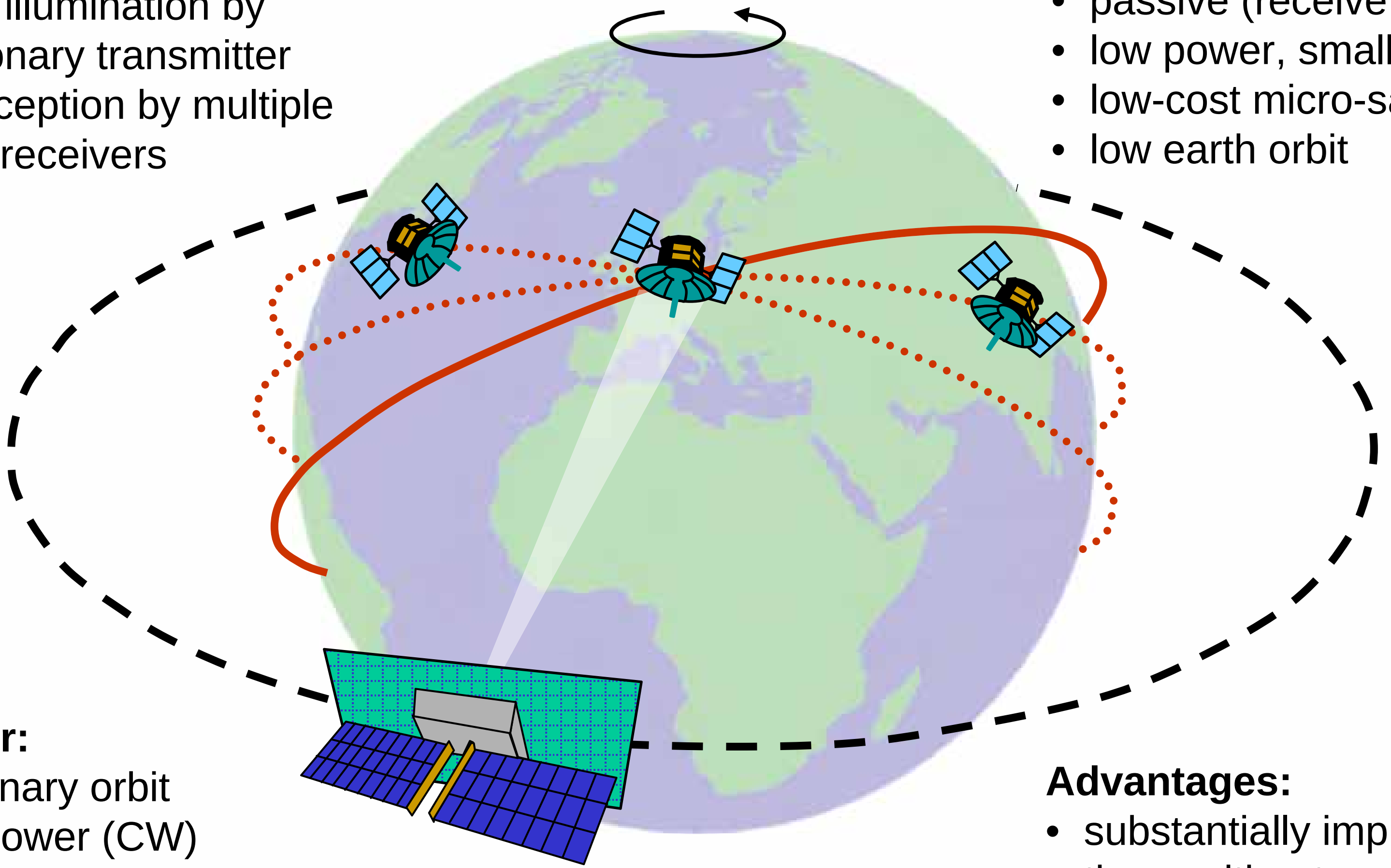

Illuminator:
- geostationary orbit
- high Tx power (CW)
- large antenna area
- optional: steerable antenna

Advantages:
- substantially improved revisit times without cost explosion
- multiple missions may share one illuminator

Microwaves and Radar Institute
gerhard.krieger@dlr.de

Bistatic SAR Systems: Basic Definitions

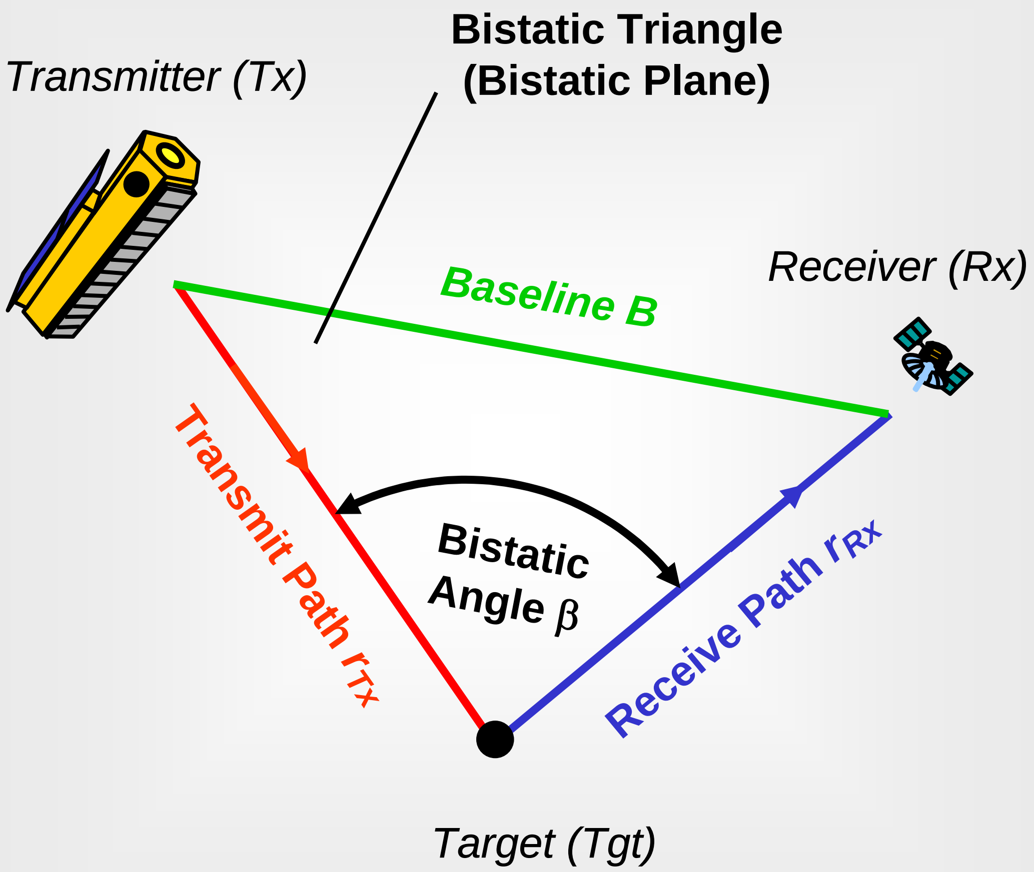

Bistatic Range:

$$r = r_{Tx} + r_{Rx}$$

→ for a given range r the target is located on an **ellipsoid** with semi major axis

$$a = \frac{r_{Tx} + r_{Rx}}{2}$$

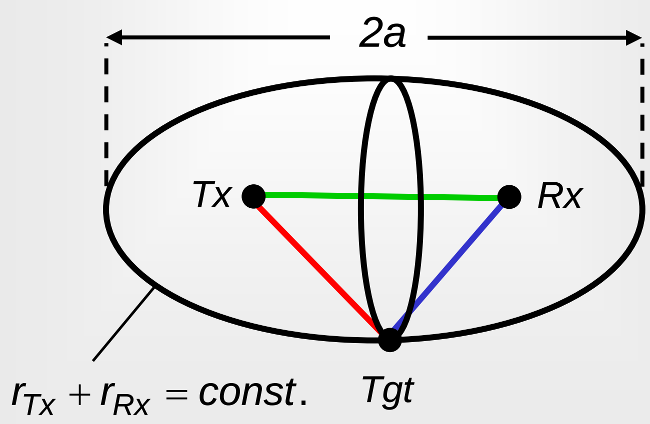

Microwaves and Radar Institute
gerhard.krieger@dlr.de

Iso-Range Contours

Tangent Plane:

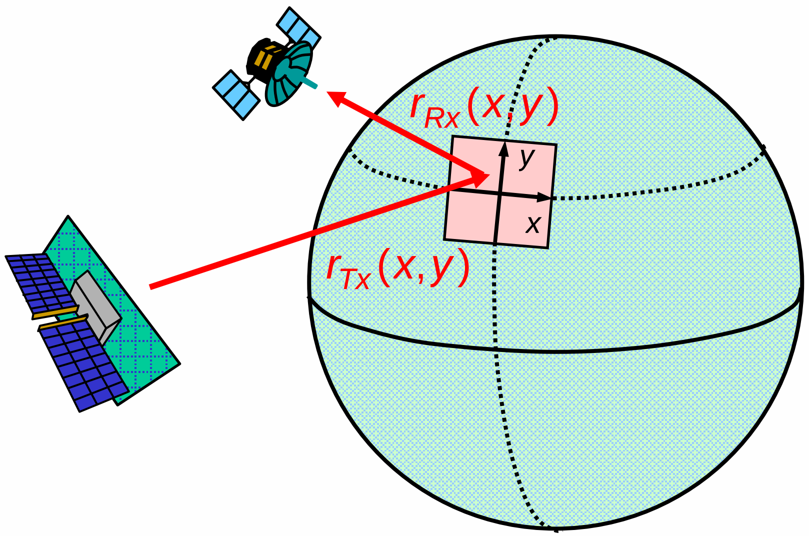

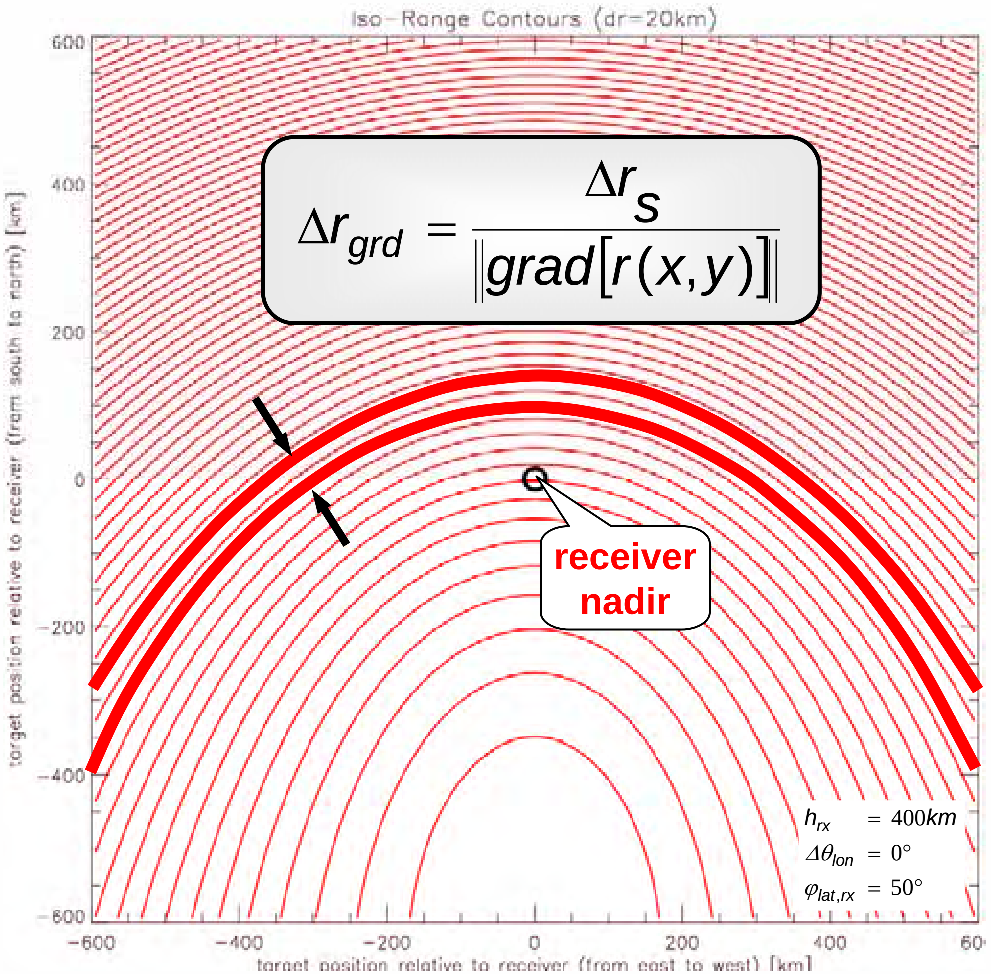

Iso-Range Contours:

$$\boxed{r(x,y) = r_{Tx}(x,y) + r_{Rx}(x,y) = const.}$$

(Intersection of Ellipsoid with Tangent Plane)

Ground Range Resolution

Slant Range Resolution:
(after Pulse Compression)

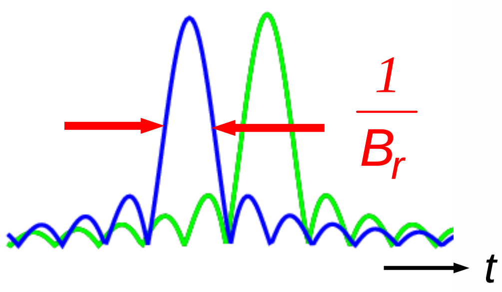

$$\Delta r_s = \frac{c_0}{B_r}$$

B_r : bandwidth of range chirp
c_0 : veolocity of light

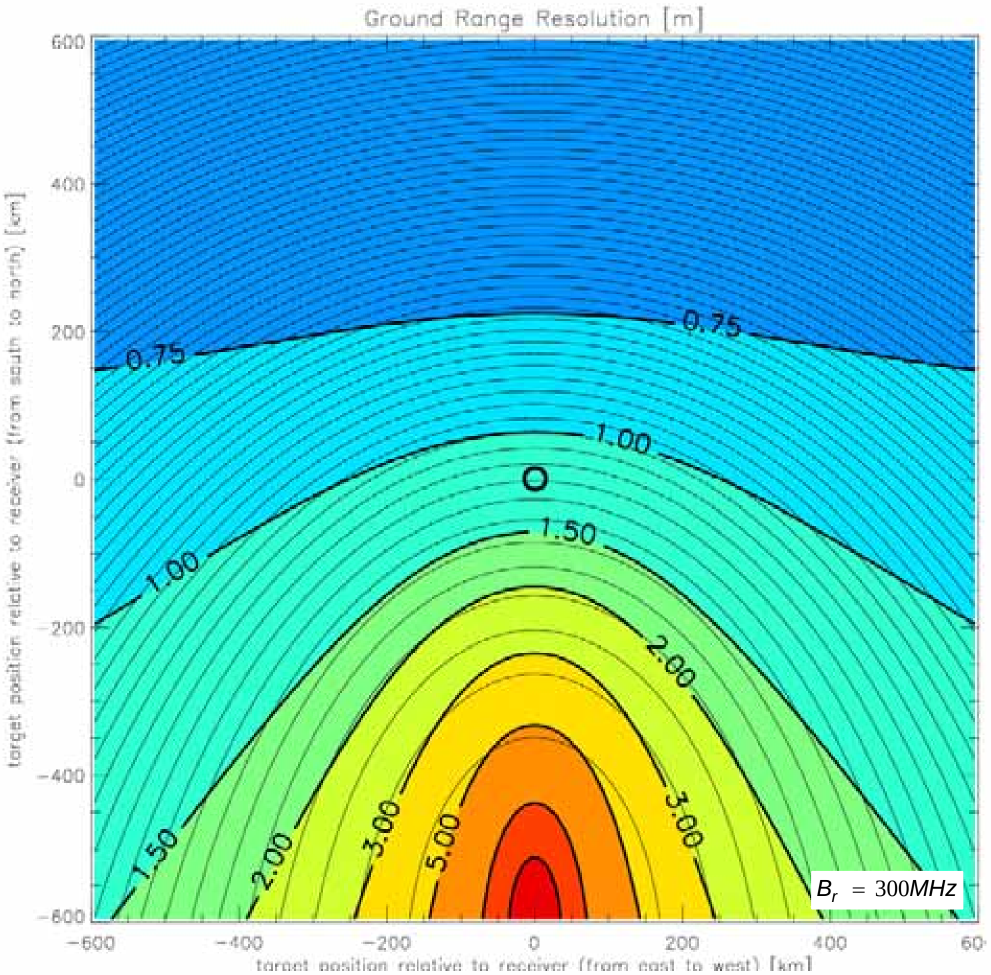

Ground Range Resolution:

$$\boxed{\Delta r_{grd} = \frac{1}{\left\| grad\left[r(x,y)\right]\right\|} \cdot \frac{c_0}{B_r}}$$

Microwaves and Radar Institute
gerhard.krieger@dlr.de

Ground Range Resolution

<u>*Special Case:*</u>

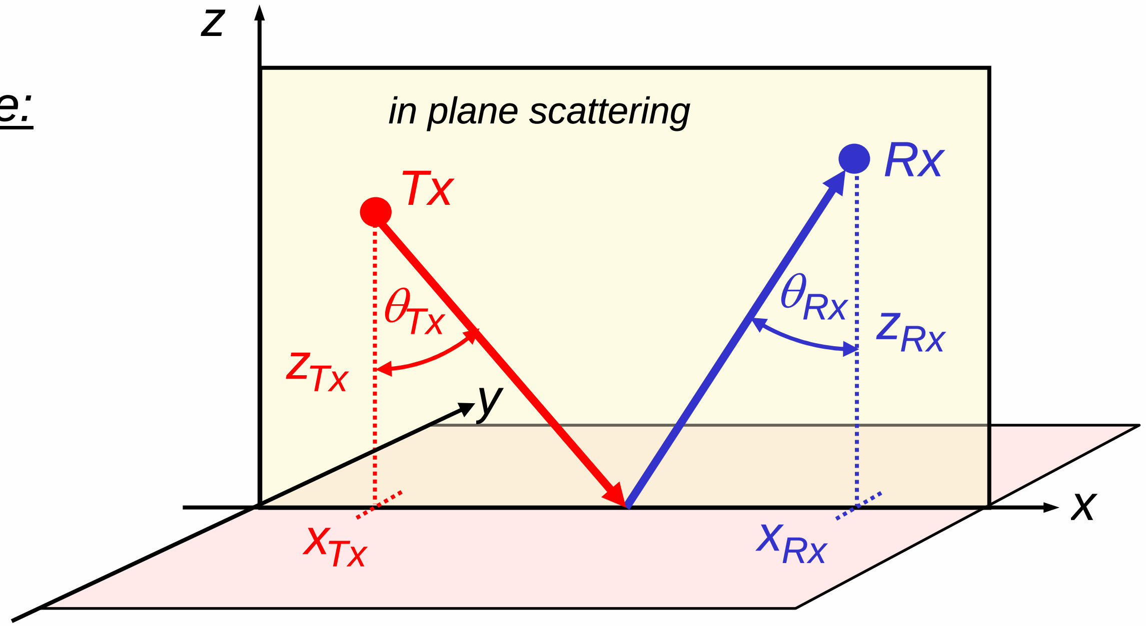

$$r(x,y) = \underbrace{\sqrt{(x-x_{Tx})^2 + z_{Tx}^2}}_{r_{Tx}(x,y)} + \underbrace{\sqrt{(x-x_{Rx})^2 + z_{Rx}^2}}_{r_{Rx}(x,y)} \longrightarrow \frac{\partial}{\partial x}[r(x,y)] = \underbrace{\frac{x-x_{Tx}}{\sqrt{(x-x_{Tx})^2 + z_{Tx}^2}}}_{\sin\theta_{Tx}} + \underbrace{\frac{x-x_{Rx}}{\sqrt{(x-x_{Rx})^2 + z_{Rx}^2}}}_{-\sin\theta_{Rx}}$$

$$\boxed{\Delta r_{grd} = \frac{c_0}{B_r\left|\sin\theta_{Tx} - \sin\theta_{Rx}\right|}}$$

Microwaves and Radar Institute
gerhard.krieger@dlr.de

Bistatic Iso-Doppler Contours

Doppler Frequencies:

$$f_{Dop} = \frac{-1}{\lambda}\left[\frac{\partial}{\partial t}(r_{Tx} + r_{Rx})\right] \approx$$

$$\approx \frac{-1}{\lambda}\left[\frac{\vec{v}_{Tx}\cdot\vec{r}_{Tx}}{\left\|\vec{r}_{Tx}\right\|} + \frac{\vec{v}_{Rx}\cdot\vec{r}_{Rx}}{\left\|\vec{r}_{Rx}\right\|}\right]$$

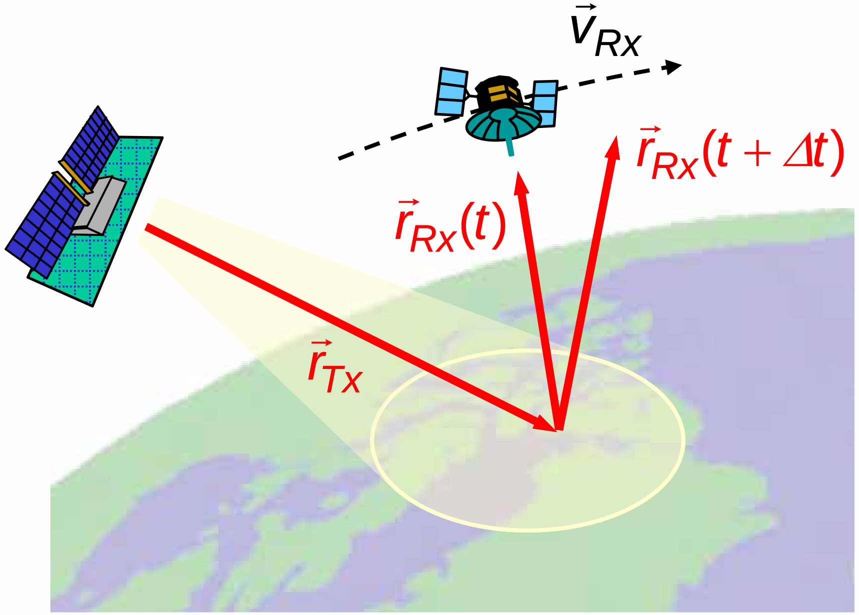

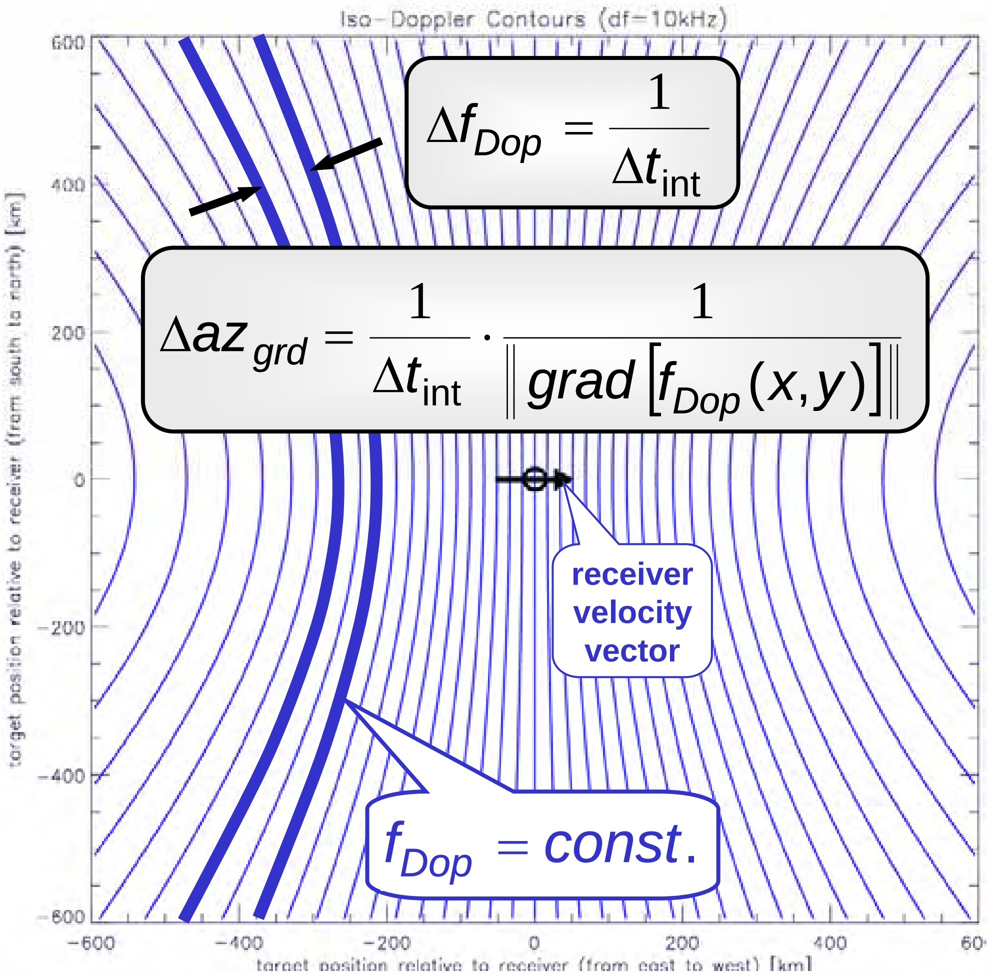

Resolution Cell: Area and Diameter

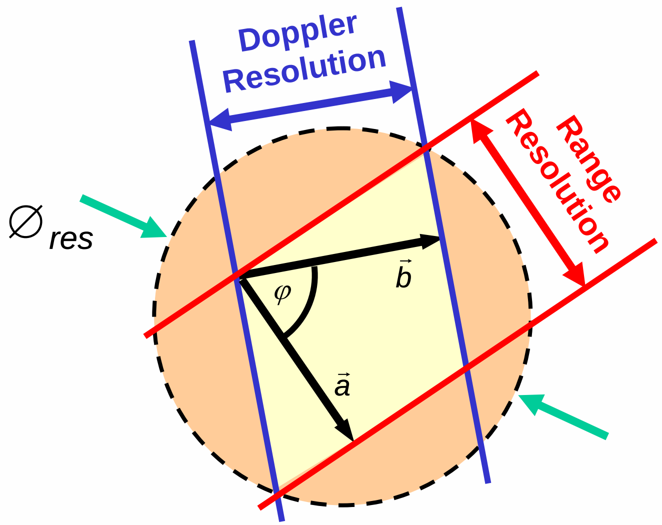

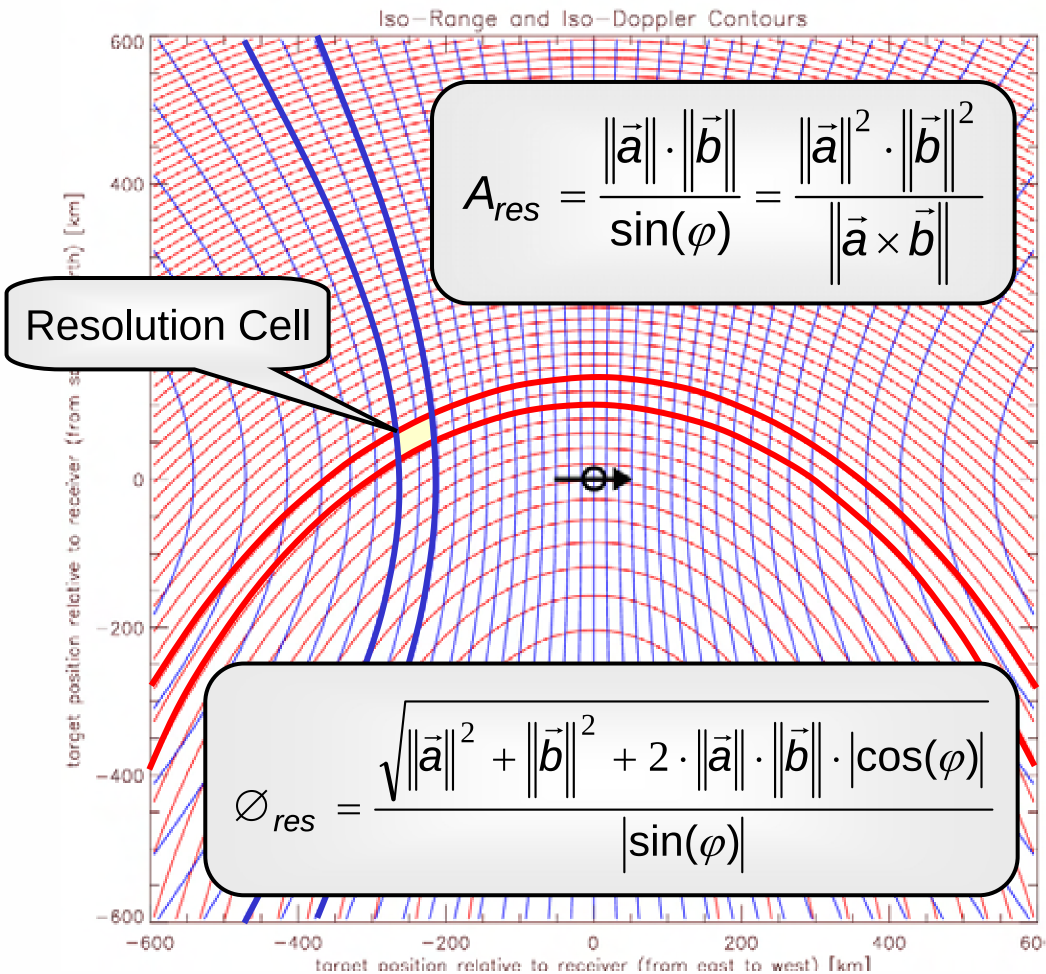

$$A_{res} = \frac{\|\vec{a}\| \cdot \|\vec{b}\|}{\sin(\varphi)} = \frac{\|\vec{a}\|^2 \cdot \|\vec{b}\|^2}{\|\vec{a} \times \vec{b}\|}$$

$$\varnothing_{res} = \frac{\sqrt{\|\vec{a}\|^2 + \|\vec{b}\|^2 + 2 \cdot \|\vec{a}\| \cdot \|\vec{b}\| \cdot |\cos(\varphi)|}}{|\sin(\varphi)|}$$

Range Resolution Vector:

$$\vec{a} = \frac{grad(r(x,y))}{\|grad(r(x,y))\|^2} \cdot \frac{c_0}{B_r}$$

Doppler Resolution Vector:

$$\vec{b} = \frac{grad(f_{Dop}(x,y))}{\|grad(f_{Dop}(x,y))\|^2} \cdot \frac{1}{t_{int}(x,y)}$$

Microwaves and Radar Institute
gerhard.krieger@dlr.de

Bistatic Radar Equation (1)

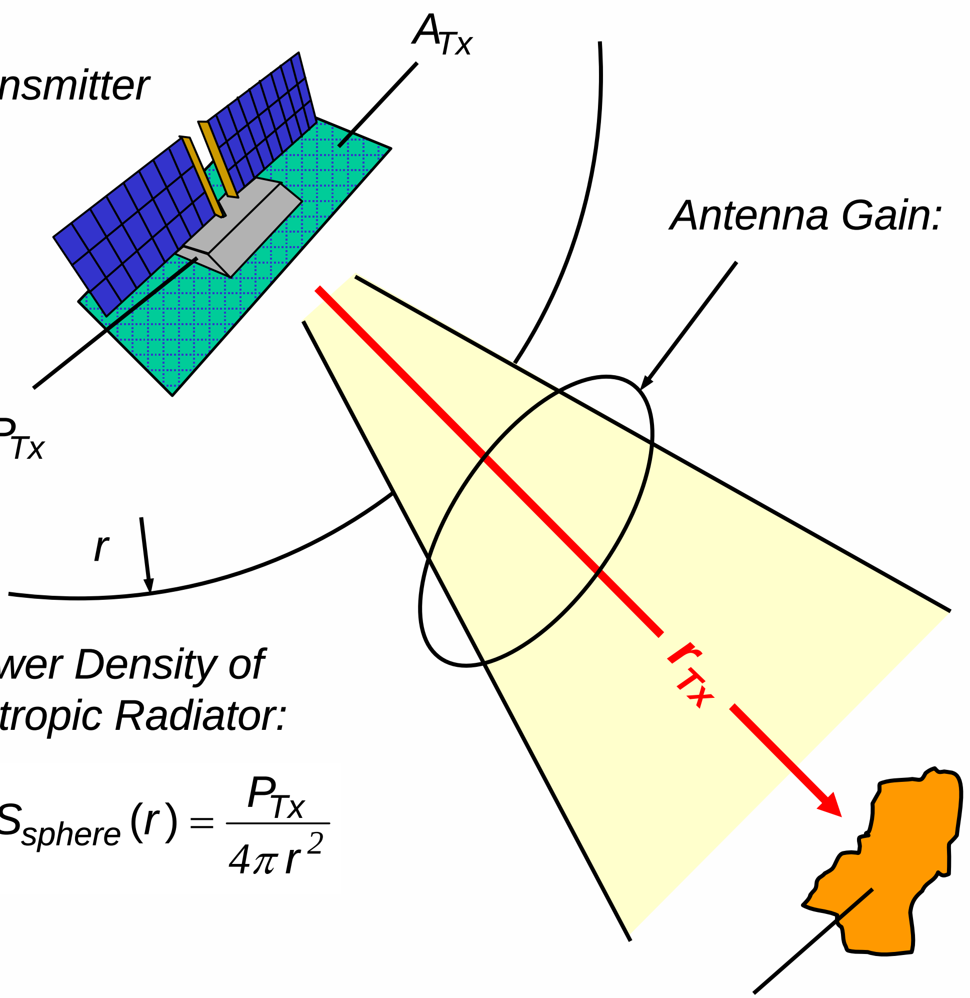

Antenna Gain: $G_{Tx} = \frac{4\pi A_{Tx}}{\lambda^2}$

Power Density of Isotropic Radiator:

$$S_{sphere}(r) = \frac{P_{Tx}}{4\pi r^2}$$

Power Density at Resolution Cell:

$$S_{rescell} = S_{sphere}(r_{Tx}) \cdot G_{Tx} = \frac{P_{Tx} G_{Tx}}{4\pi r_{Tx}^2}$$

Microwaves and Radar Institute
gerhard.krieger@dlr.de

Bistatic Scattering Coefficient

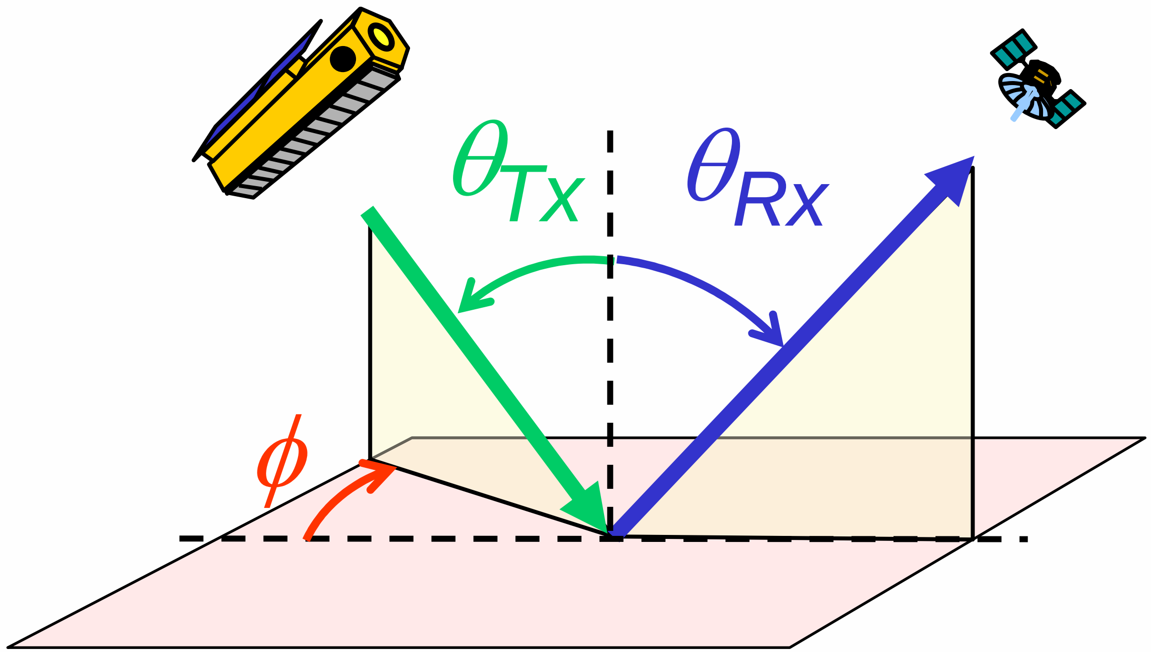

Bistatic scattering coefficient depends on:

- *Incident angle* θ_{Tx}
- *Scattering angle* θ_{Rx}
- *Out-of-plane angle* ϕ
- *Frequency*
- *Polarization*
- *Surface / Object*

Microwaves and Radar Institute
gerhard.krieger@dlr.de

Bistatic Scattering Coefficient: Example

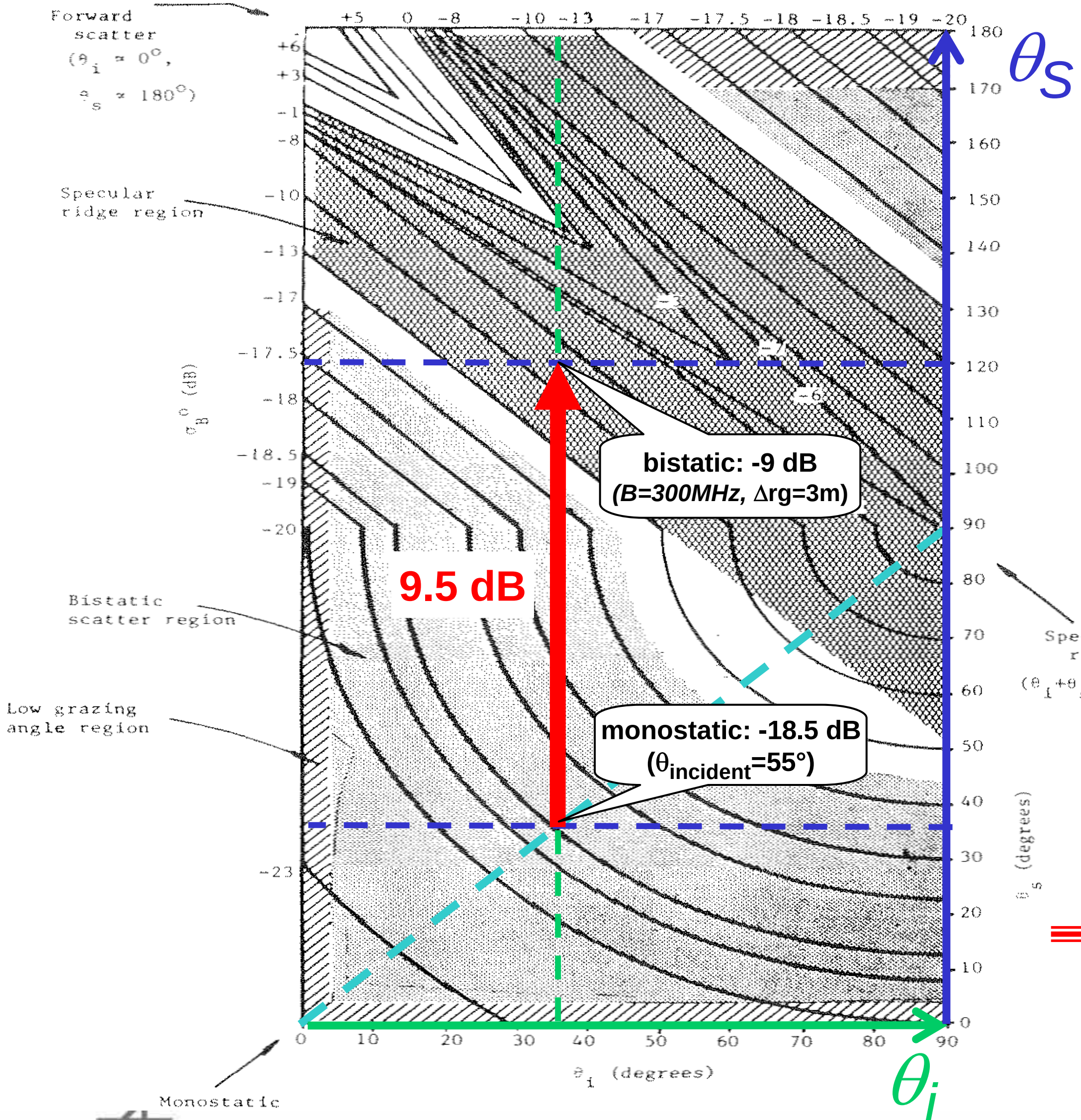

Data from Domville (1967)

- X-Band scattering for rural land
- vertical polarization (VV)
- only in-plane scattering
- see also Willis, 1991

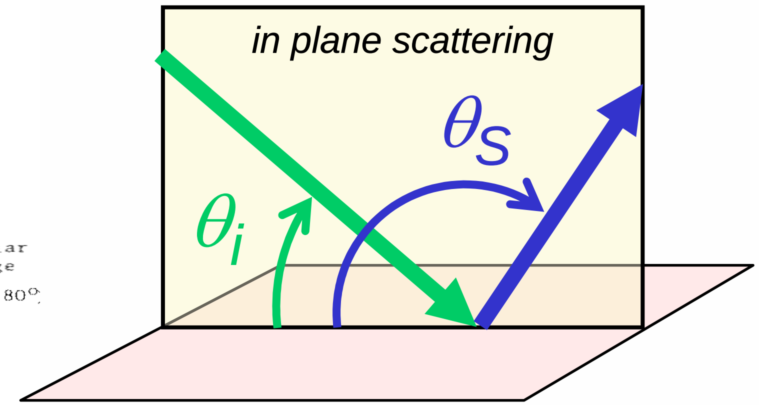

⇒ ***Forward scattering may increase the radar cross section by 10 dB and more***

Microwaves and Radar Institute
gerhard.krieger@dlr.de

Bistatic Radar Equation (2)

Power at Receiver: $$P_{Rx} = \frac{P_{Tx} G_{Tx}}{4\pi\, r_{Tx}^{\;2}} \cdot A_{res} \sigma_B^0 \cdot \frac{A_{Rx}}{4\pi\, r_{Rx}^{\;2}}$$

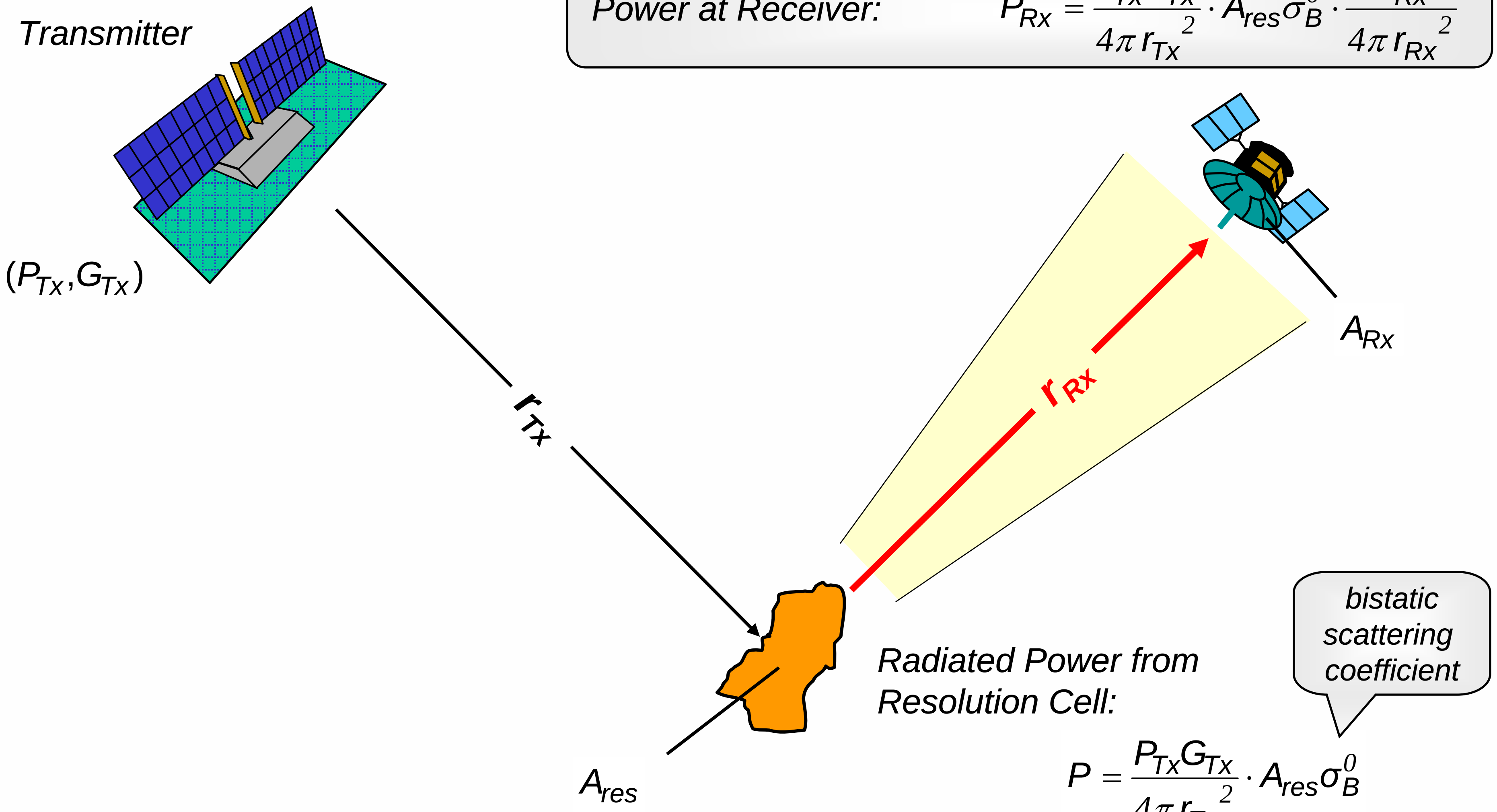

Radiated Power from Resolution Cell:

$$P = \frac{P_{Tx} G_{Tx}}{4\pi\, r_{Tx}^{\;2}} \cdot A_{res} \sigma_B^0$$

Microwaves and Radar Institute
gerhard.krieger@dlr.de

Signal to Noise Ratio

Single Pulse SNR:

$$SNR_1 = \frac{\frac{P_{Tx}G_{Tx}}{4\pi r_{Tx}^2} \cdot A_{res}\sigma_B^0 \cdot \frac{A_{Rx}}{4\pi r_{Rx}^2}}{kT_sB_nFL}$$

power at receiver

thermal noise & losses

Independent Samples:

$$n_{rg} = B_r \cdot \tau_P \approx B_n \cdot \tau_P = B_n \cdot \frac{P_{avg}}{P_{Tx} \cdot PRF}$$

$$n_{az} = t_{\text{int}} \cdot PRF$$

SNR after Coherent Integration:

$$SNR_n = n_{rg} \cdot n_{az} \cdot SNR_1 = \frac{P_{avg}G_{Tx}}{4\pi r_{Tx}^2} \cdot A_{res}\sigma_B^0 \cdot \frac{A_{Rx}}{4\pi r_{Rx}^2} \cdot \frac{t_{\text{int}}}{kT_sFL}$$

usually $A_{res} \sim \frac{1}{t_{\text{int}}}$

→ SNR independent of azimuth resolution

r_{Tx}	Distance from transmitter to scene
r_{Rx}	Distance from receiver to scene
k	Boltzmann's constant ($1.3805\ 10^{-23}$ Ws/K)
T_s	Receiving system noise temperature
B_r (B_n)	Range Chirp (Receiver) Bandwidth
F	System Noise Figure
L	Losses
τ_P	Pulse length
PRF	Pulse repetition frequency
P_{avg} (P_{Tx})	Average (Peak) transmit power
G_{Tx}	Gain of transmit antenna
A_{Rx}	Effective aperture of receive antenna
A_{res}	Size of resolution cell (1 look)
t_{int}	Coherent integration time

Microwaves and Radar Institute
gerhard.krieger@dlr.de

Noise Equivalent Sigma Zero (NESZ)

- The Noise Equivalent Sigma Zero (NESZ) measures the ***sensitivity*** of a given SAR
- The NESZ corresponds to the bistatic scattering coefficient for which the SNR is equal to one

$$SNR = \frac{P_{avg} G_{Tx} A_{Rx} \cdot A_{res} \cdot t_{\mathrm{int}}}{(4\pi)^2 r_{Tx}^2 r_{Rx}^2 k T_s F L} \cdot \sigma_B^0 \overset{!}{=} 1 \quad (0\ \mathrm{dB})$$

$$\longrightarrow \boxed{NESZ = \sigma_B^0 (SNR = 1) = \frac{(4\pi)^2 r_{Tx}^2 r_{Rx}^2 k T_s F L}{P_{avg} G_{Tx} A_{Rx} \cdot A_{res} \cdot t_{\mathrm{int}}}}$$

- Lower NESZ values are better
- For spaceborne SAR, typical values of the NESZ are in the order of -20 dB
- The SNR is given by: $SNR = \sigma_B^0 - NESZ \qquad [dB]$

Microwaves and Radar Institute
gerhard.krieger@dlr.de

NESZ Example: Geostationary Illuminator

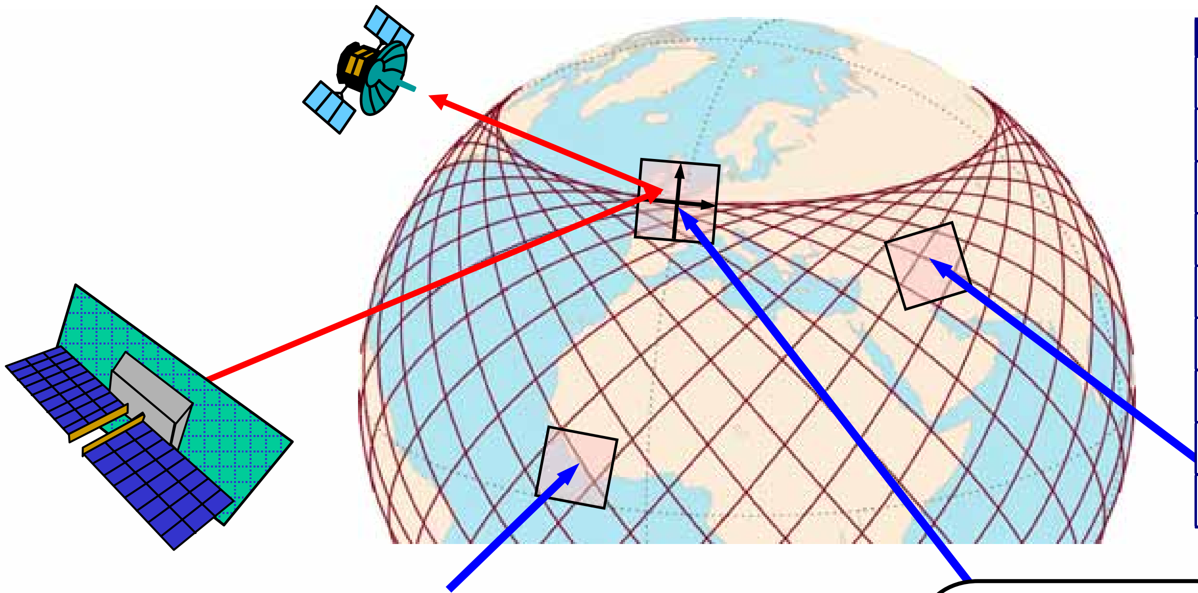

Wavelength	3.1 cm
Max. Bandwidth	300 MHz
Average Transmit Power	1000 W
Antenna Size Tx	100 m^2
Antenna Size Rx	6 m^2
Noise Figure + Losses	5 dB
Receiver Altitude	400 km
Ground Resolution	3 m
Max. Res. Cell Diameter	6 m

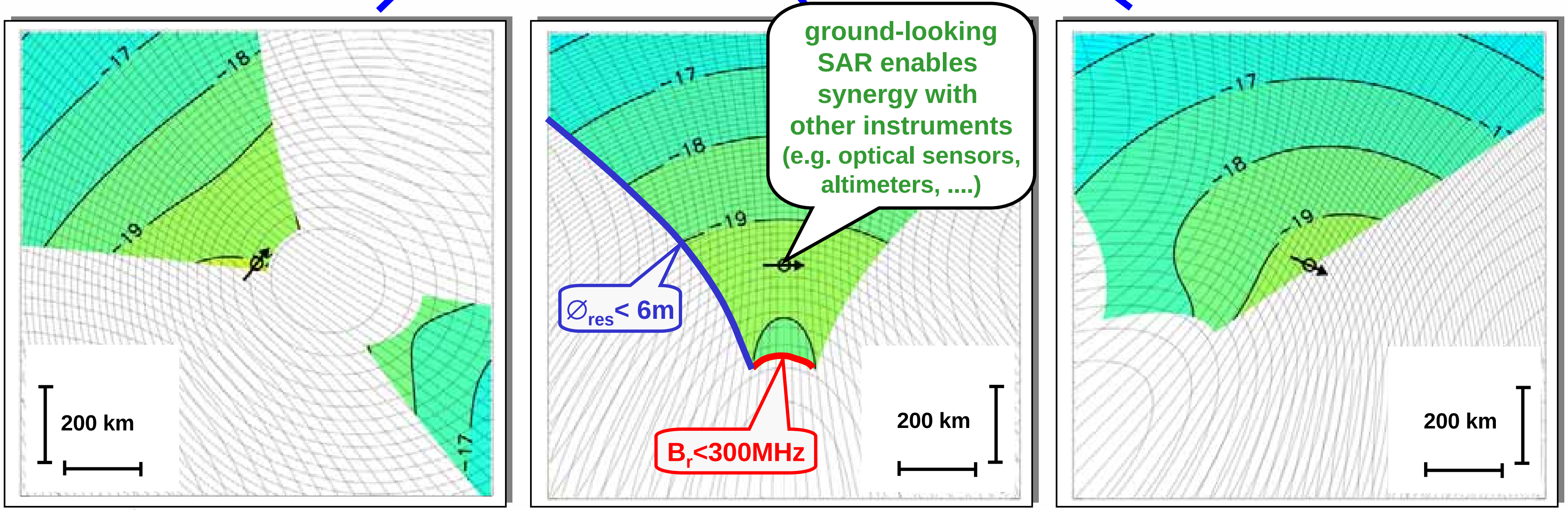

Microwaves and Radar Institute
gerhard.krieger@dlr.de

Digital Beamforming in Passive Receivers

Digital beamforming on receive makes effective use of the total signal energy in the large illuminated footprint:

- ⇒ **mapping of a *wide swath or multiple spots***
  (in spite of extended antennas in elevation)
- ⇒ ***very long synthetic apertures***
  (also with long receiver apertures)
  - – ***high azimuth resolution***
  - – ***more independent looks***
  - – ***improved sensitivity***
- ⇒ **interference suppression**
- ⇒ **ambiguity reduction**
- ⇒ **multiple phase center MTI**

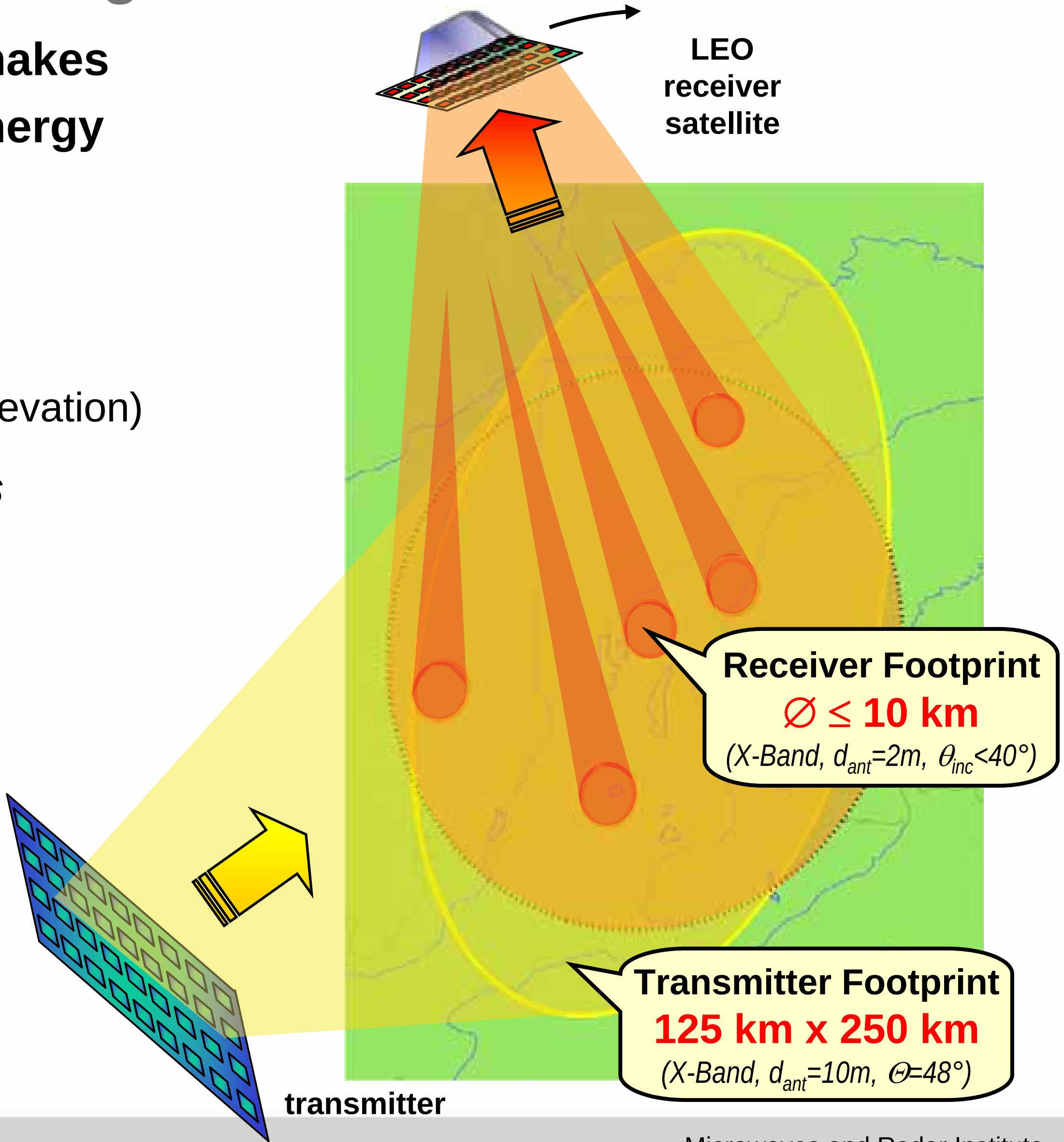

Microwaves and Radar Institute
gerhard.krieger@dlr.de

Digital Beamforming on Receive

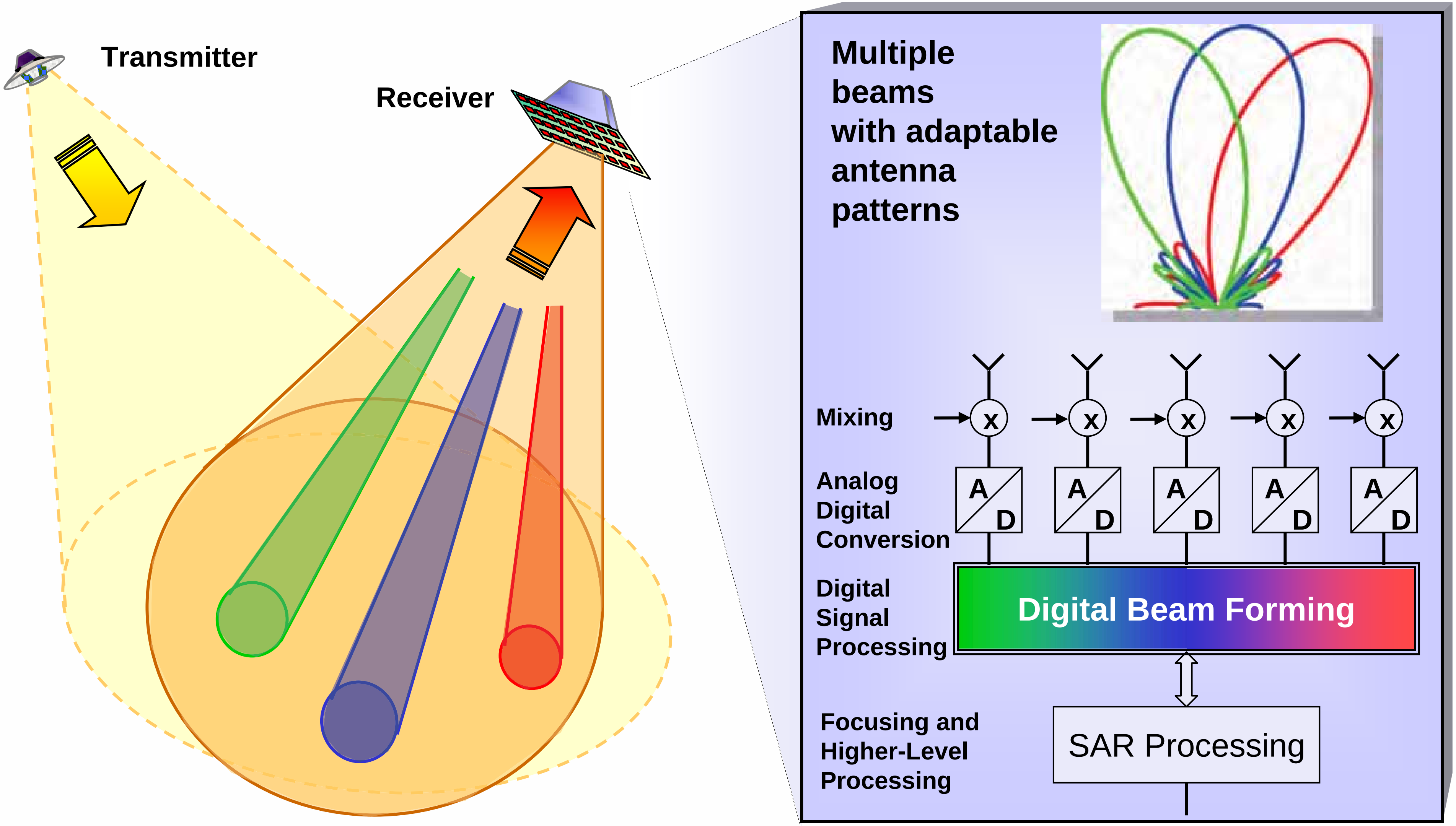

Microwaves and Radar Institute
gerhard.krieger@dlr.de

Parasitic SAR with Communication Satellite

Basic Idea:
- illumination by a transmitter of opportunity
- sufficient SNR is provided by very long coherent integration time and moderate resolution

Receivers:
- passive, low-cost mini- or micro-satellites
- e.g. geosynchronous orbit for long integration time (Prati et al., 1998)

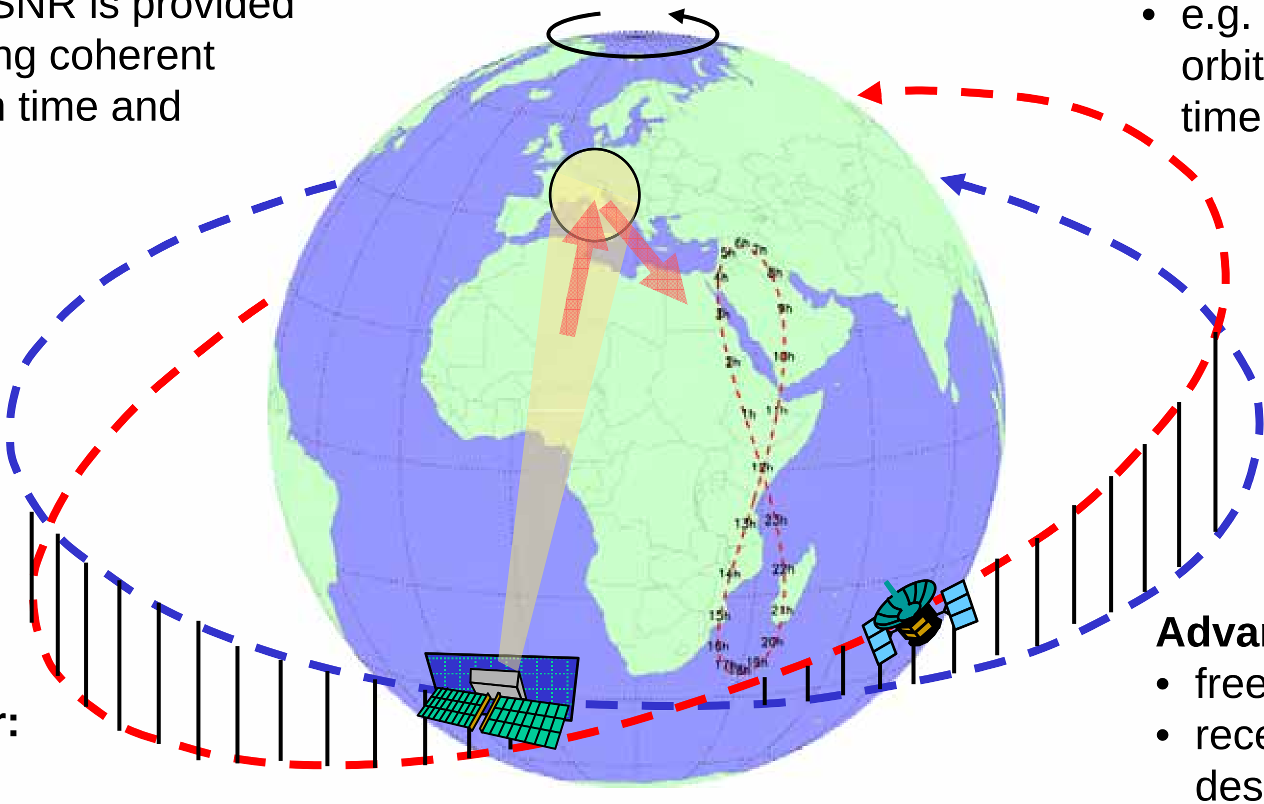

Illuminator:
- e.g. digital communication satellite
- geostationary orbit

Advantages:
- free transmitter
- receiving part can be designed using commercial DAB- or TV-SAT components

Microwaves and Radar Institute
gerhard.krieger@dlr.de

Performance of a Parasitic SAR with Communication Satellite and Geosynchronous Receiver

Power Budget Example (cf. Prati, Rocca, Giancola, Monti Guarnieri,1998):

Geostationary Illuminator & Geosynchronous Receiver			
Power Density on Ground $$P_{ground} = \frac{P_{Tx}G_{Tx}}{4\pi r_{Tx}^2 B_{Tx}}$$	Effective Irradiated Power (P_{Tx} G_{Tx})	57 dBW	-171.1 dB [W/m²/Hz]
	Transmit Range	36000 km	
	Transmit Bandwidth	4 MHz	
Power at Receiver Satellite $$P_{rec} = \frac{P_{ground}B_{Rx}}{4\pi r_{Rx}^2} \cdot A_{Rx} \cdot A_{res}\sigma_0$$	Receiver Bandwidth	4 MHz	-232.5 dB [W]
	Receive Range	37000 km	
	Receiver Antenna Area	20 m²	
	Ground Resolution	100 m x 100 m	
	Sigma	-18 dB m²/m²	
SNR $$SNR = \frac{P_{rec}}{kTFB} = \frac{P_{rec}}{kTF} \cdot t_{\text{int}}$$	Receiver Noise Figure + Losses	7 dB	**7.1 dB** (NESZ: -25.1 dB)
	Receiver Temperature	290 K	
	Integration Time	5 h	

Microwaves and Radar Institute
gerhard.krieger@dlr.de

Multistatic SAR System Concepts

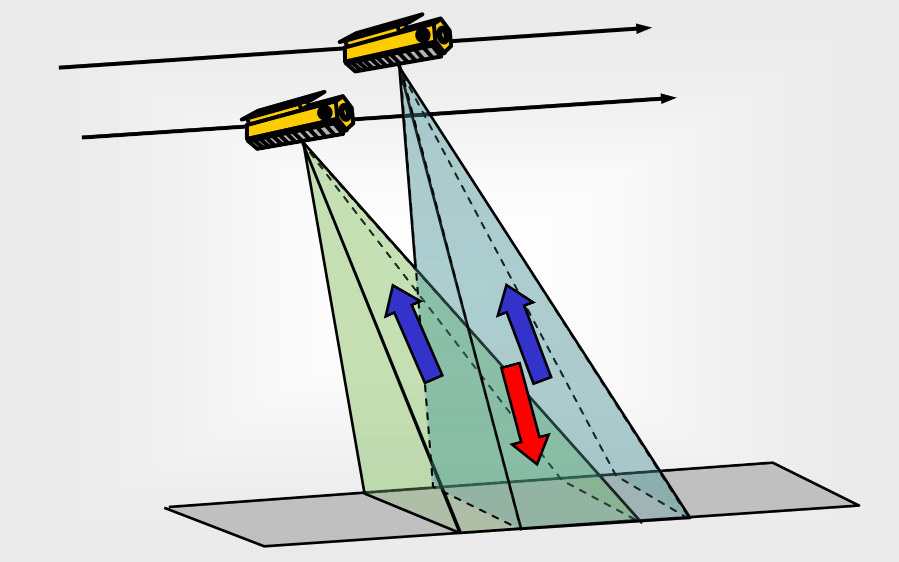

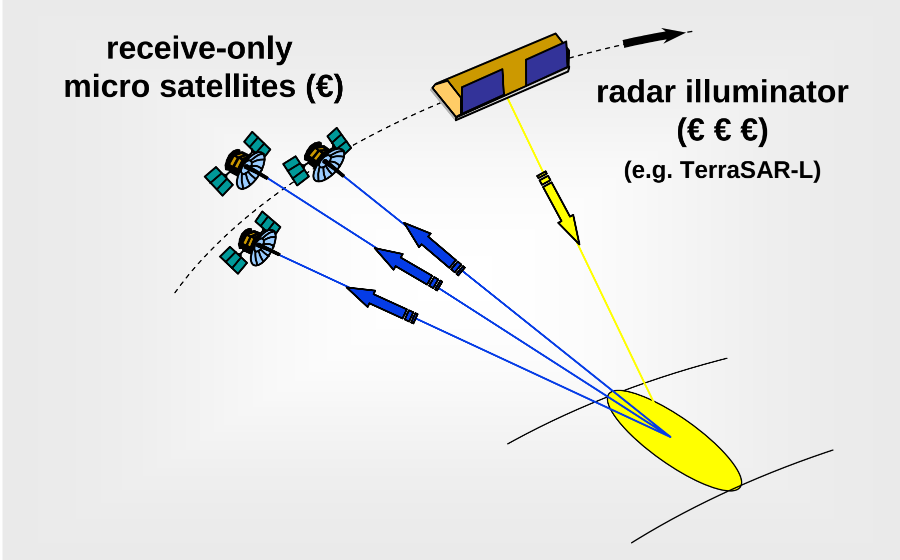

Combination of multiple receiver signals enables:

- *cross-track interferometry for cost efficient acquisition of high quality global DEMs*
- *along-track interferometry (e.g. oceanography) & moving target indication*
- *increased geometric resolution by super-resolution techniques in azimuth and range*
- *retrieval of vegetation and volume parameters by polarimetric interferometry*
- *real 3-D imaging of semitransparent volume scatterers by SAR tomography*
- *ambiguity reduction and high resolution wide swath SAR imaging*
- *improved classification (e.g. joint evaluation of multiple mono- and bistatic RCS)*
- *…*

Microwaves and Radar Institute
gerhard.krieger@dlr.de

Basic Principle of Cross-Track Interferometry

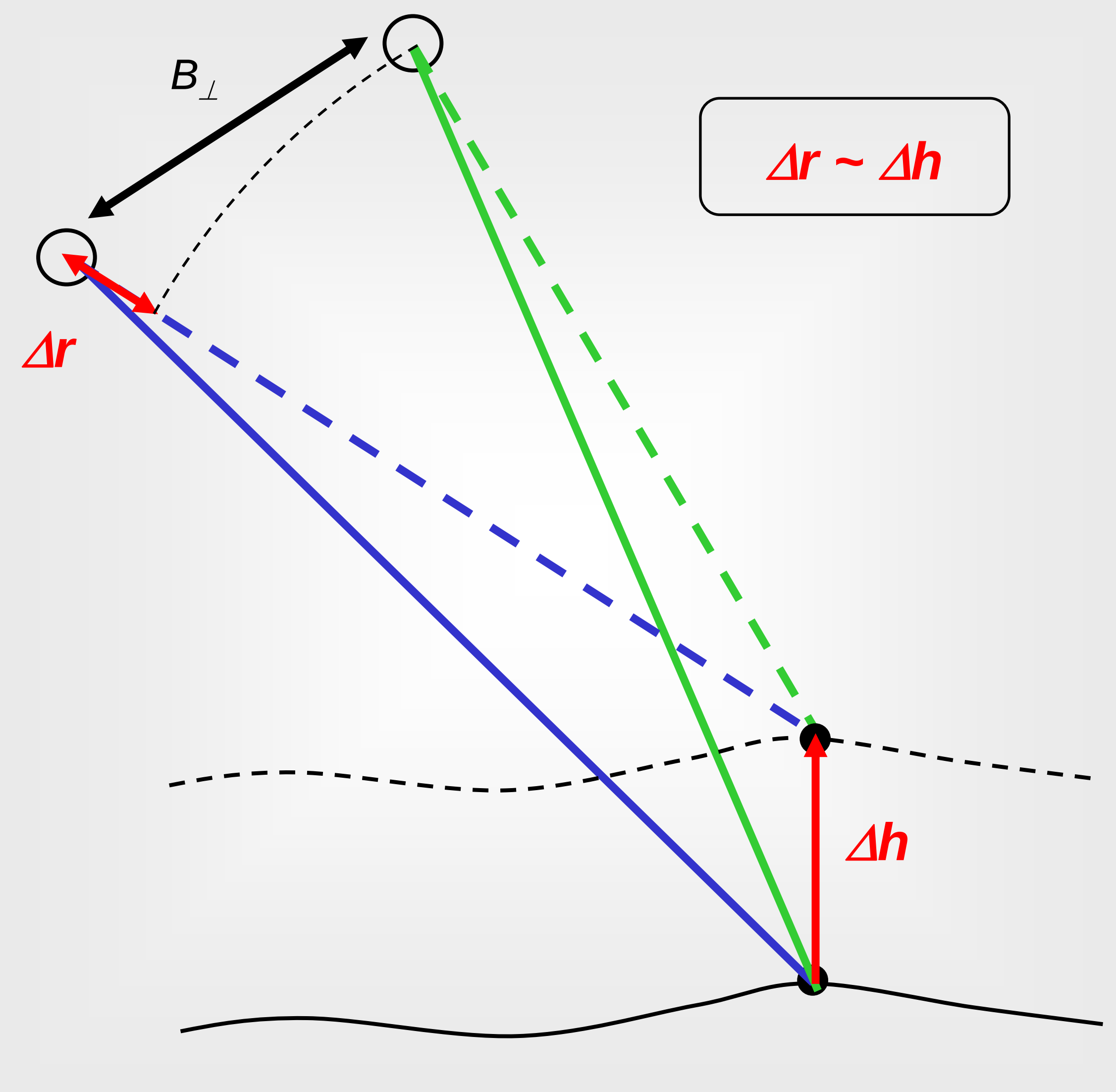

single-pass:

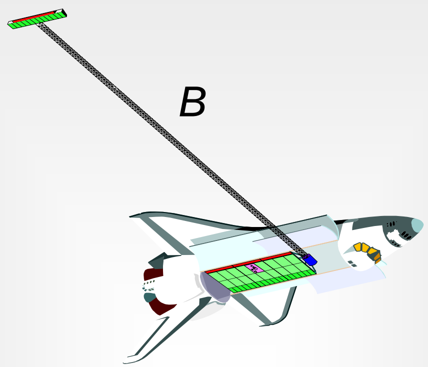

repeat-pass:

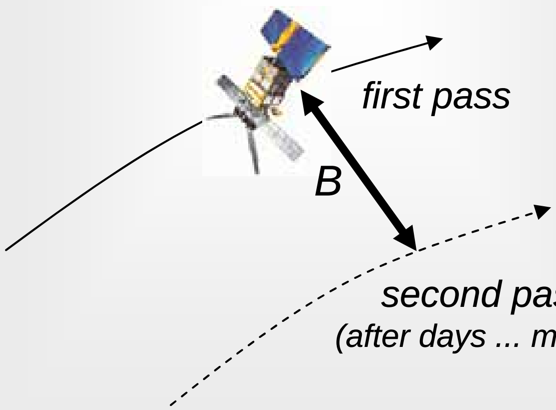

Microwaves and Radar Institute
gerhard.krieger@dlr.de

Single-Pass Cross-Track Interferometry

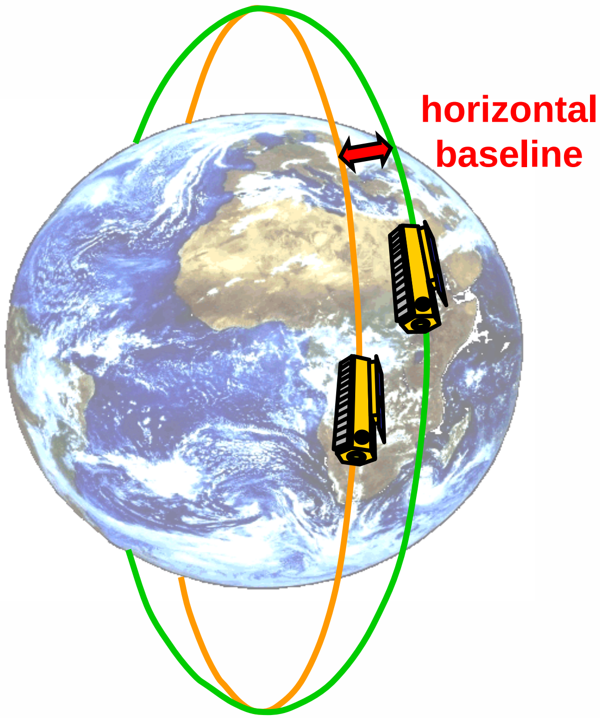

Digital Elevation Model (DEM)
from SRTM Mission

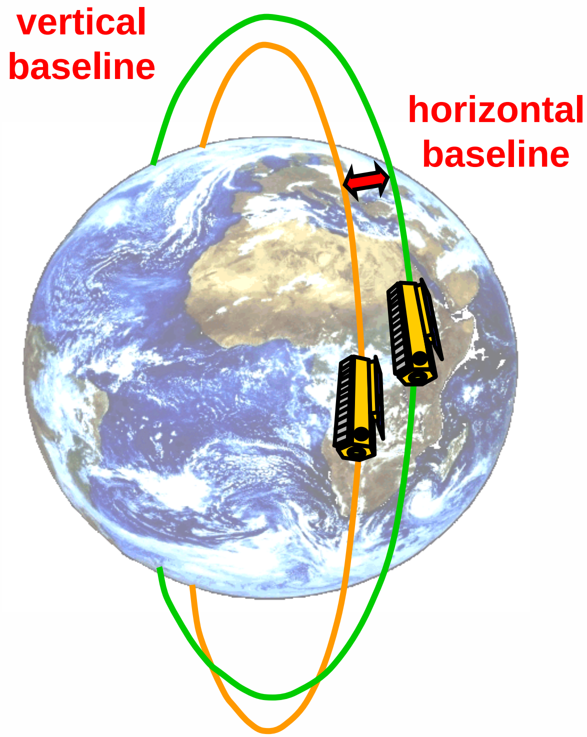

Single-Pass Cross-Track Interferometry with Multiple Satellites:

- → ***no temporal decorrelation*** *(as opposed to repeat-pass interferometry)*
- → ***no atmospheric distortions*** *(as opposed to repeat-pass interferometry)*
- → ***large interferometric baselines*** *(as opposed to e.g. SRTM)*

Microwaves and Radar Institute
gerhard.krieger@dlr.de

Relative Movement in Satellite Clusters

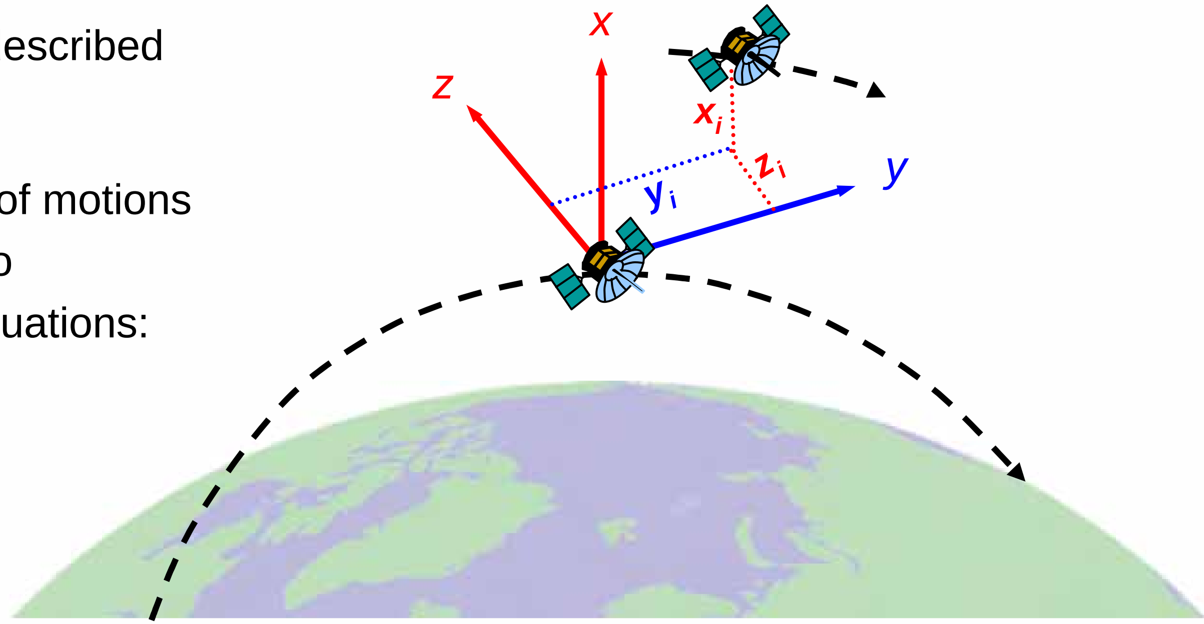

- Relative satellite movement is described in a ***rotating reference frame***

- ***Linearization*** of the equations of motions in a circular Kepler orbit leads to Clohessy-Wiltshire (or Hill's) Equations:

$$
\begin{aligned}
\ddot{x} - 2n\dot{y} - 3n^2 x &= 0 \\
\ddot{y} + 2n\dot{x} &= 0 \\
\ddot{z} + n^2 z &= 0
\end{aligned}
$$

with $n = \sqrt{\dfrac{GM_\oplus}{a_{sat}^3}}$

- Solution to Clohessy-Wiltshire Equations :

with $T_0 = 2\pi\sqrt{\dfrac{a_{sat}^3}{GM_\oplus}}$

$$
\begin{aligned}
x_i(t) &= A_i \sin\left(\frac{2\pi}{T_0} t + \alpha_i\right) \\
y_i(t) &= 2A_i \cos\left(\frac{2\pi}{T_0} t + \alpha_i\right) + \Delta y_i \\
z_i(t) &= B_i \sin\left(\frac{2\pi}{T_0} t + \beta_i\right)
\end{aligned}
$$

vertical cross-track baseline

along-track displacement

horizontal cross-track baseline

Microwaves and Radar Institute
gerhard.krieger@dlr.de

2-SAT Pendulum

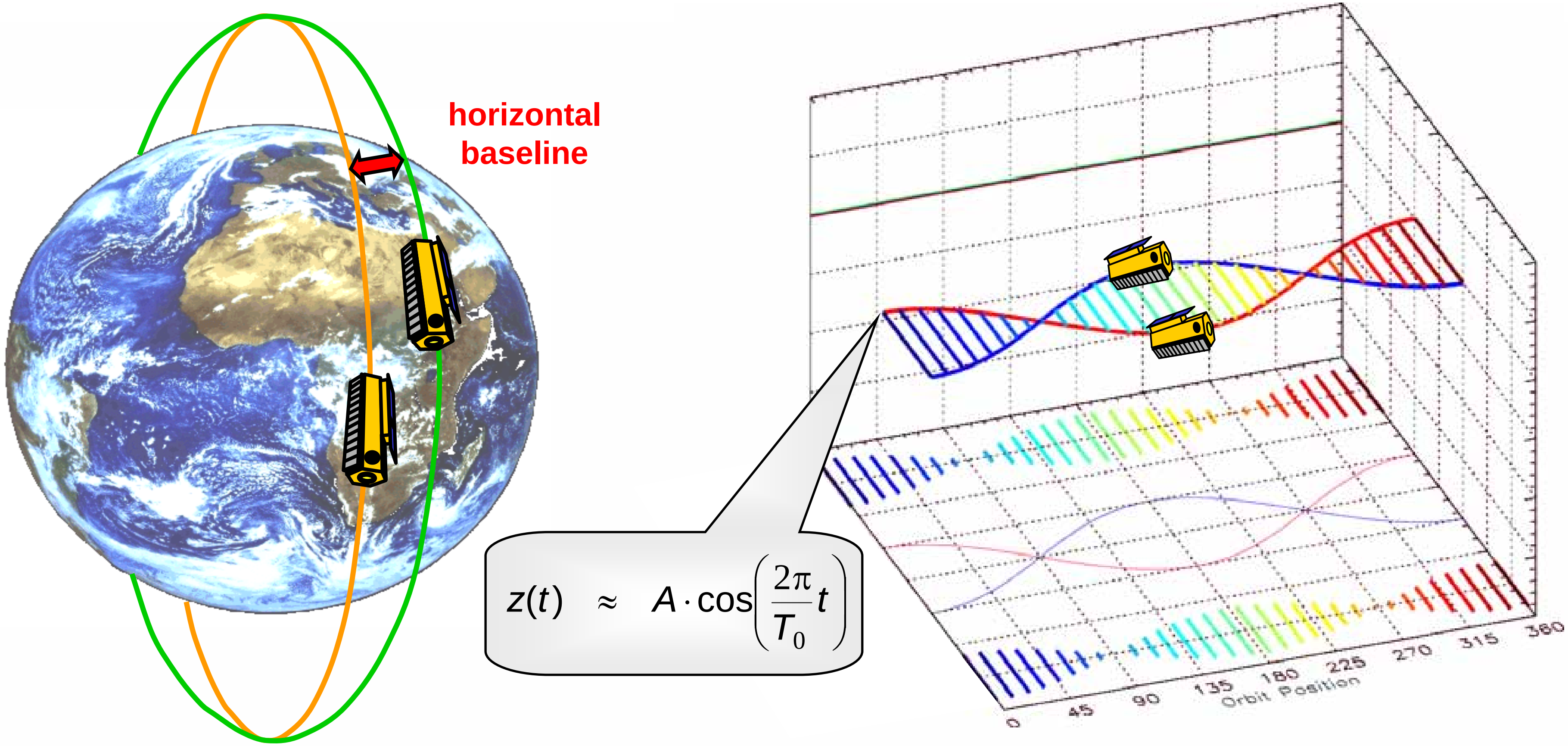

2-SAT Pendulum (Hartl 1989, Zebker, 1992)

- *horizontal cross-track separation at equator by different ascending nodes*
- *requires along-track displacement to avoid satellite collision at orbit crossing*
- *insufficient baselines for polar regions*

HELIX Formation

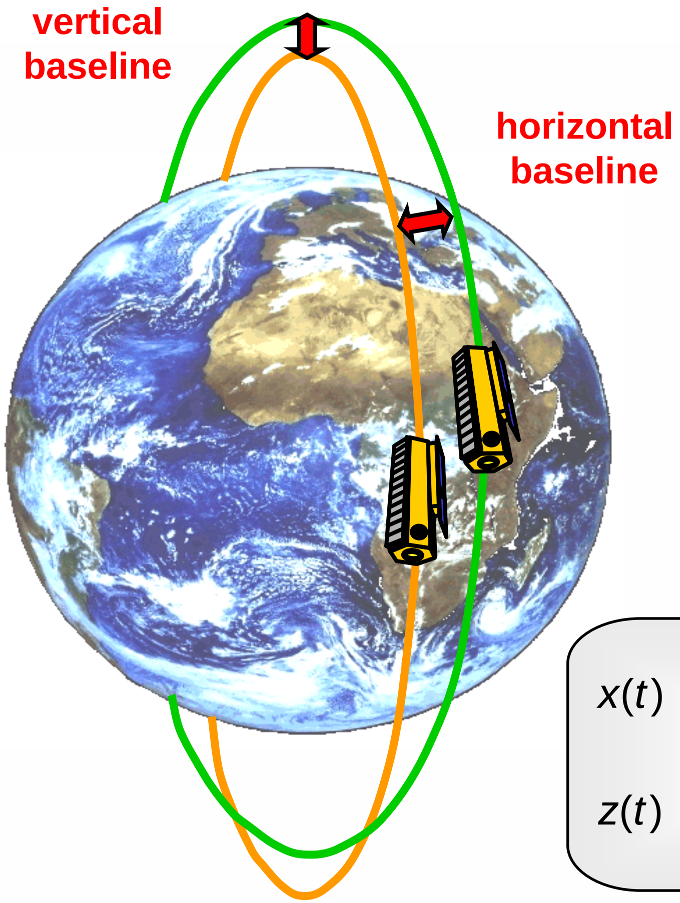

$$x(t) \approx A \cdot \sin\left(\frac{2\pi}{T_0}t\right)$$

$$z(t) \approx B \cdot \cos\left(\frac{2\pi}{T_0}t\right)$$

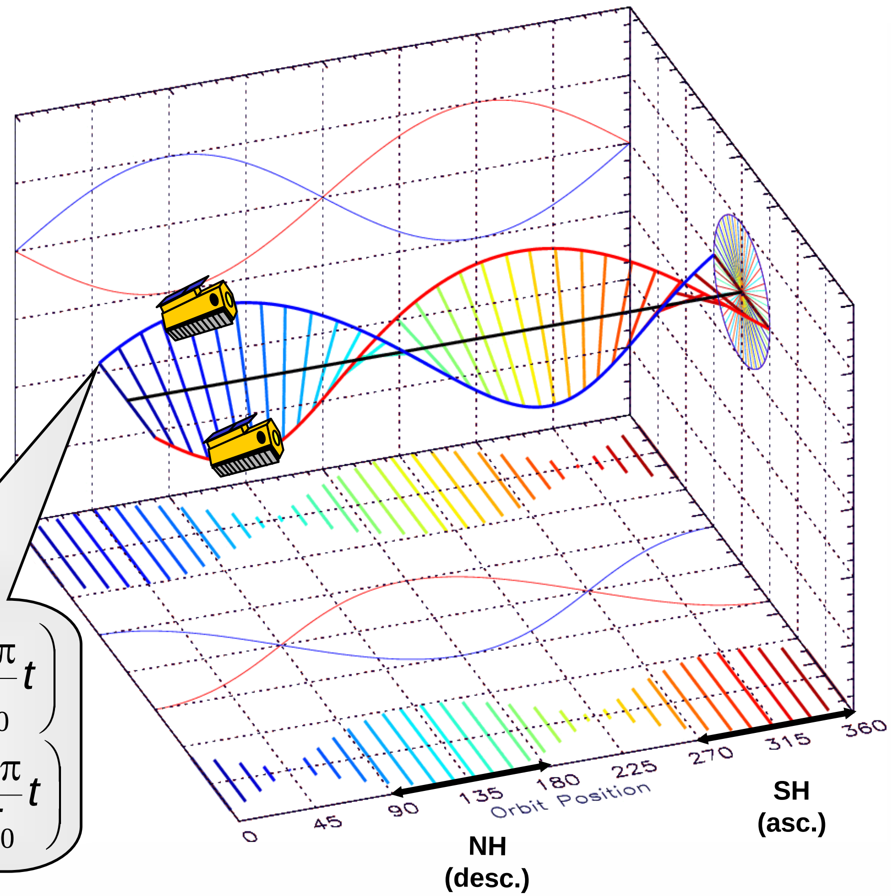

HELIX satellite formation enables safe operation

- *horizontal cross-track separation at equator by different ascending nodes*
- *vertical (radial) separation at poles by orbits with different eccentricity vectors (periodic motion of libration has to be compensated by regular manoeuvres)*

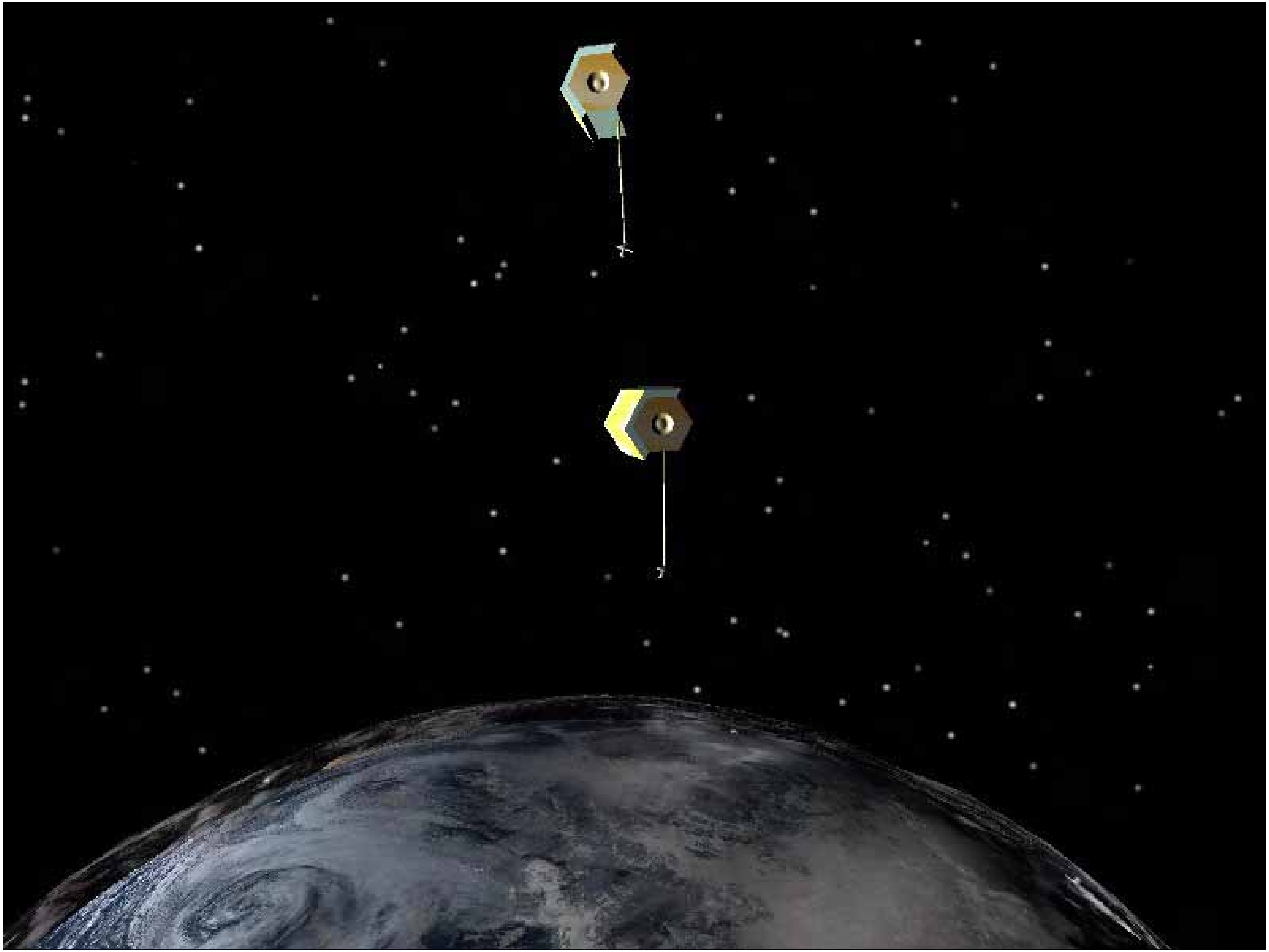

Interferometric Cartwheel

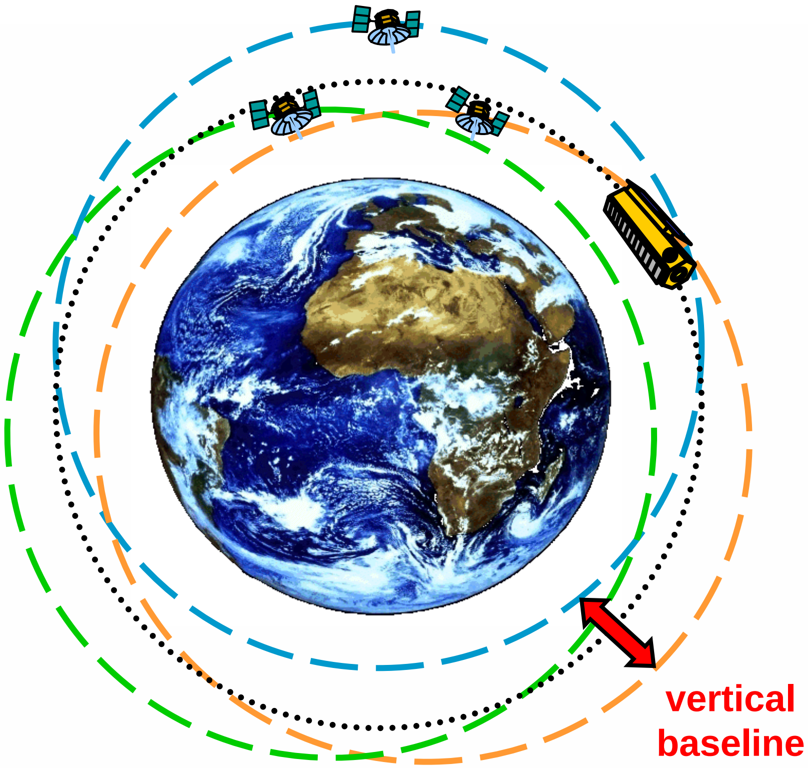

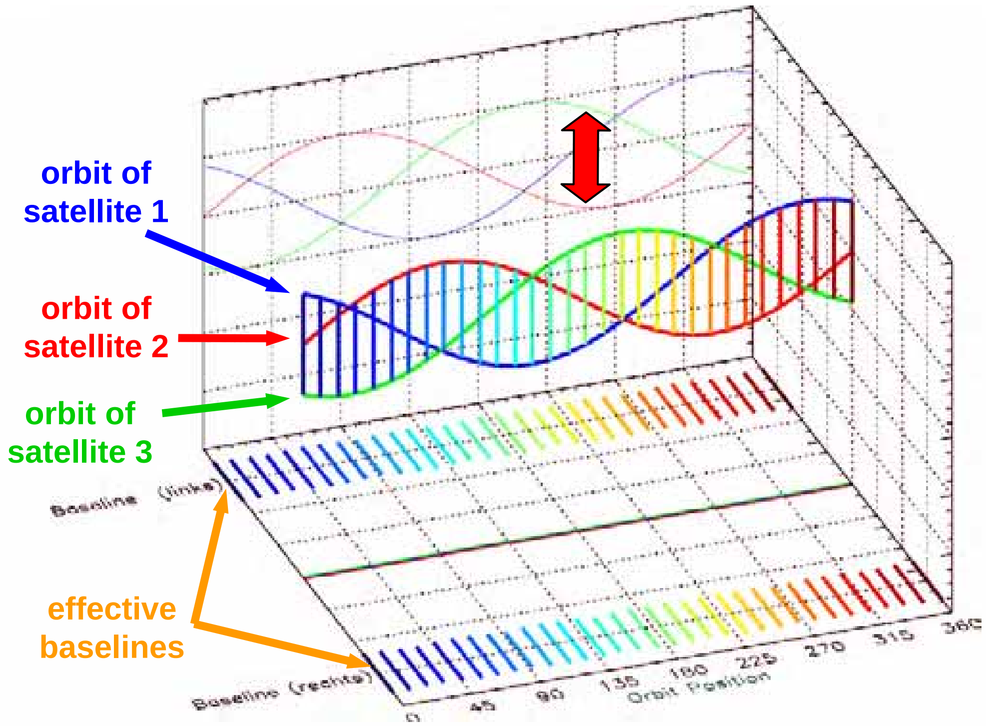

Interferometric Cartwheel (Massonnet, 1998)

- *all satellites share the same orbital plane*
- *arguments of apogee differ by 120º for a Cartwheel with 3 satellites*
- *provides a stable vertical baseline for all orbit positions*
- *relative movement of the receiver satellites can be approximated by an ellipse*

Interferometric Performance Analysis

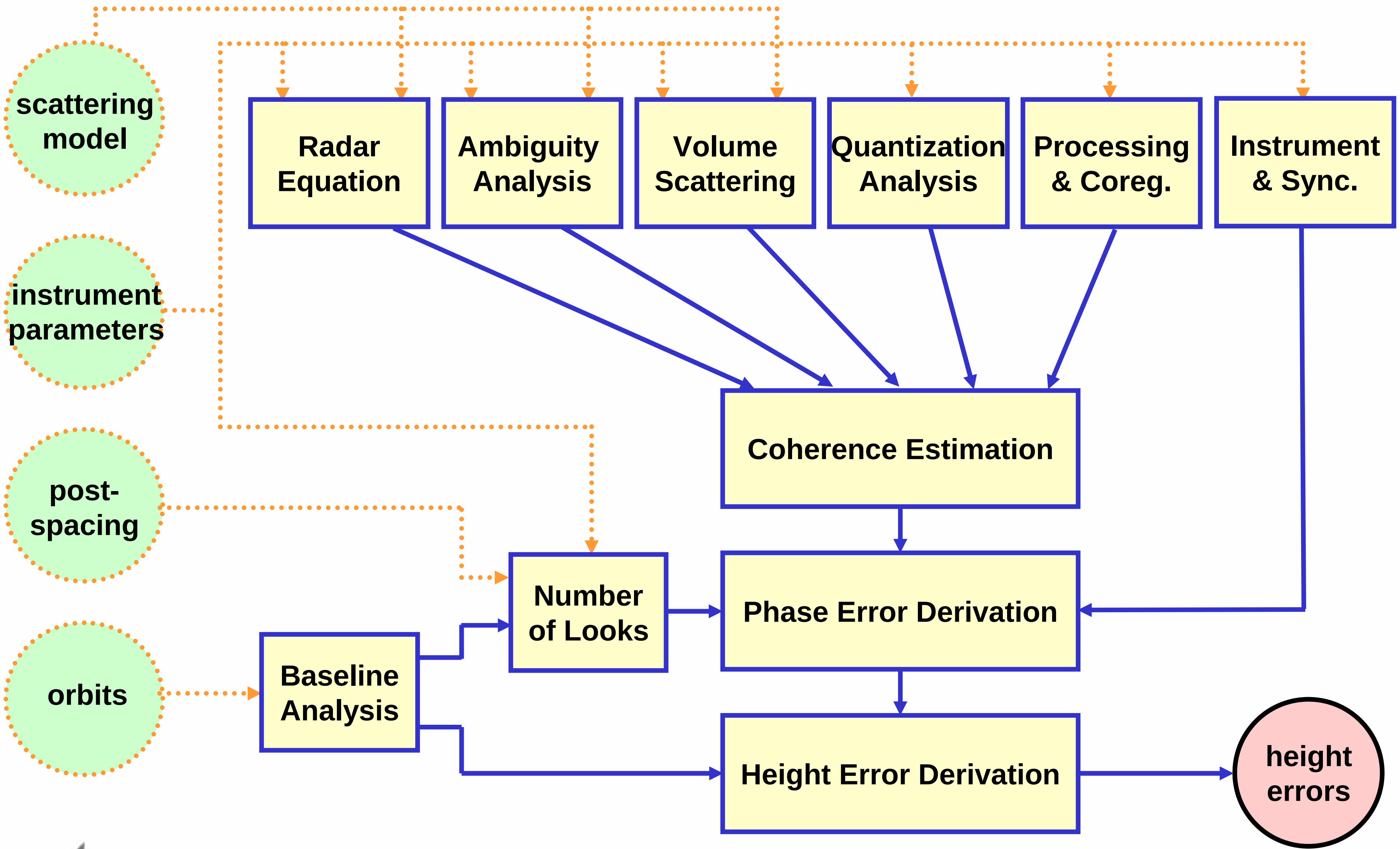

Coherence Estimation

$$\gamma_{tot} = \gamma_{SNR} \cdot \gamma_{quant} \cdot \gamma_{amb} \cdot \gamma_{geo} \cdot \gamma_{az} \cdot \gamma_{vol} \cdot \gamma_{temp} \cdot \gamma_{proc}$$

System Noise (radar equation)

Ambiguities $\gamma_{amb} \approx \frac{1}{1+RASR} \cdot \frac{1}{1+AASR}$

Volume Decorrelation

Processing & Coregistration Errors $\gamma_{proc} = 0.97$

Quantization Noise (4 bit) $\gamma_{quant} = 0.99$

Baseline Decorrelation $\gamma_{geo} = 1$ (range filtering)

Doppler Decorrelation $\gamma_{az} = 1$ (azimuth filtering)

Temporal Decorrelation $\gamma_{temp} = 1$

Microwaves and Radar Institute
gerhard.krieger@dlr.de

Computation of Coherence Loss from Limited SNR

Computation of Noise Equivalent Sigma Zero:

$$NESZ = \frac{4^4 \pi^3 r^3 v \sin(\theta_{inc}) k T B_{rg} F L}{P_{Tx} G_{Tx} G_{Rx} \lambda^3 c_0 \tau_p PRF}$$

Derivation of Single Channel SNR:

$$SNR[dB] = \sigma_0[dB] - NESZ[dB]$$

Derivation of Coherence:

$$\gamma_{SNR} = \frac{1}{\sqrt{1+SNR_1^{-1}} \cdot \sqrt{1+SNR_2^{-1}}}$$

r	: slant range
v	: satellite velocity
θ_{inc}	: incident angle
k	: Boltzman constant
T	: system temperature (290K)
B_{rg}	: chirp bandwidth
F	: system noise figure
L	: losses
P_{Tx}	: peak transmit power
G_{Tx}	: gain of transmit antenna
G_{Rx}	: gain of receive antenna
λ	: wavelength
c_0	: velocity of light
τ_p	: pulse duration
PRF	: pulse repetition frequency
σ_0	: backscatter coefficient

Noise Equivalent Sigma Zero (Example)

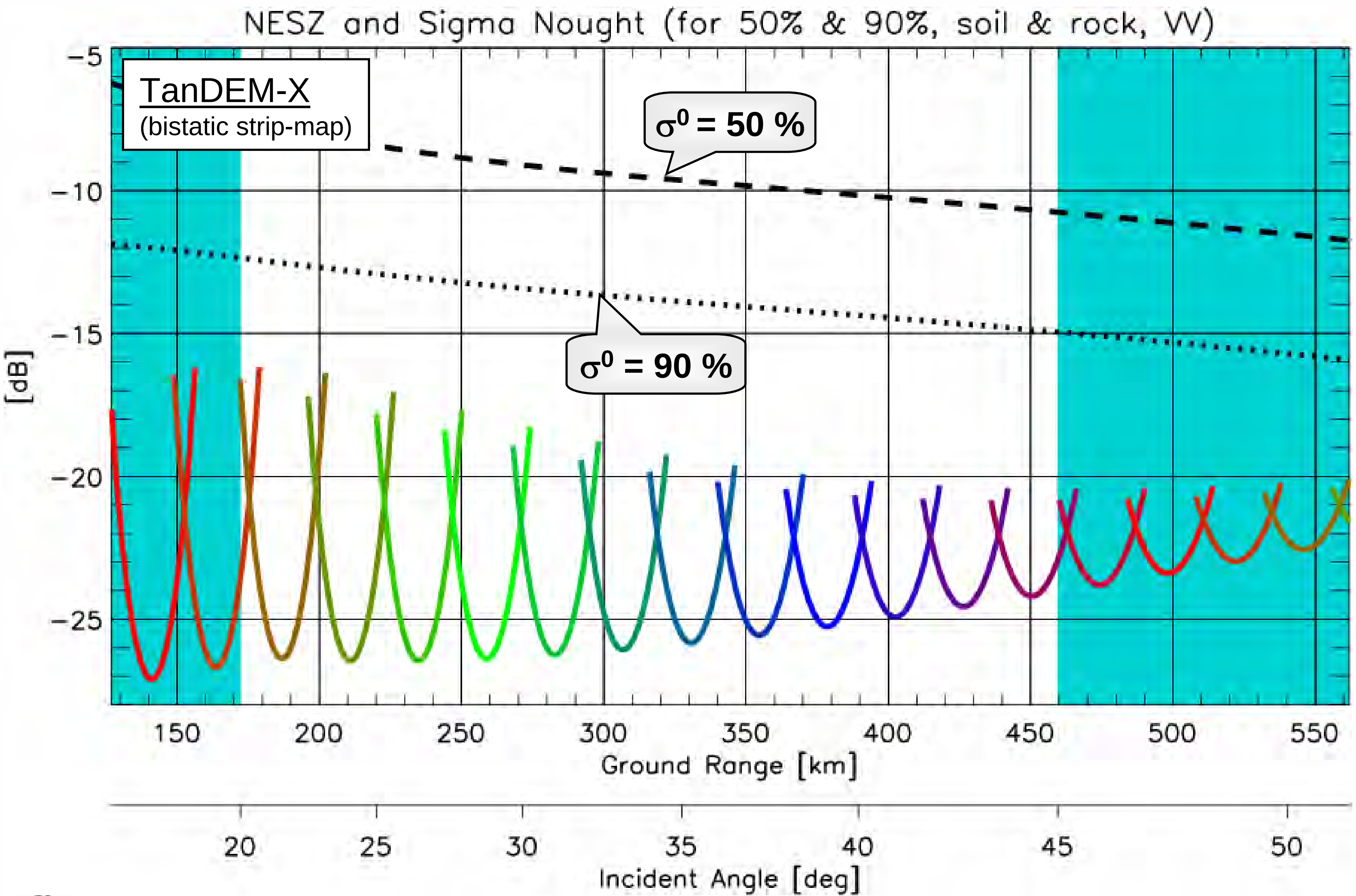

Microwaves and Radar Institute
gerhard.krieger@dlr.de

Total Coherence (Example)

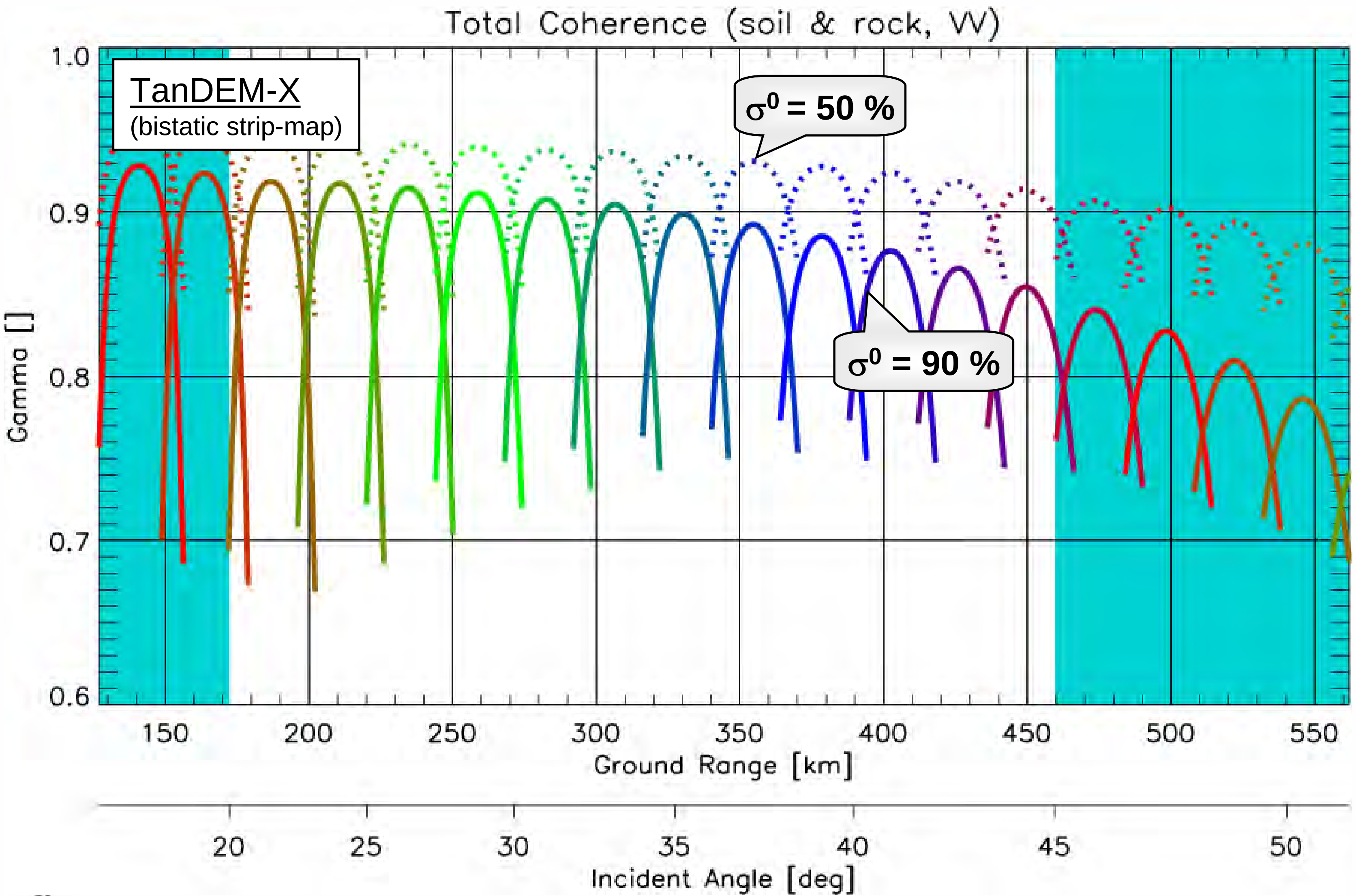

Microwaves and Radar Institute
gerhard.krieger@dlr.de

Derivation of Interferometric Phase Errors

Phase Error PDF:

$$p_\varphi(\varphi) = \frac{\Gamma\left(n+\frac{1}{2}\right)\left(1-\gamma^2\right)^n \gamma\cos\varphi}{2\sqrt{\pi}\,\Gamma(n)\left(1-\gamma^2\cos^2\varphi\right)^{n+\frac{1}{2}}} + \frac{\left(1-n^2\right)^n}{2\pi} F\left(n,1;\tfrac{1}{2};\gamma^2\cos^2\varphi\right)$$

(cf. Lee et al., 1994)

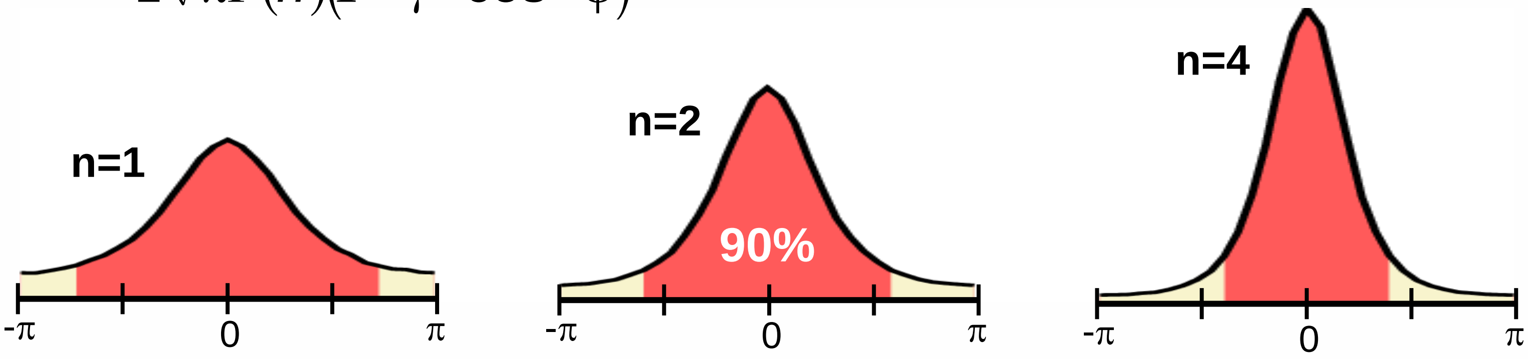

Standard Deviation:

$$\sigma_\varphi = \sqrt{\int_{-\pi}^{\pi} \varphi^2 p_\varphi(\varphi)\cdot d\varphi}$$

90 Percentile:

$$\Delta\varphi^{90\%}: \int_{-\Delta\varphi^{90\%}}^{\Delta\varphi^{90\%}} p_\varphi(\varphi)\cdot d\varphi = 0.9$$

Microwaves and Radar Institute
gerhard.krieger@dlr.de

Interferometric Phase Errors

Standard Deviation

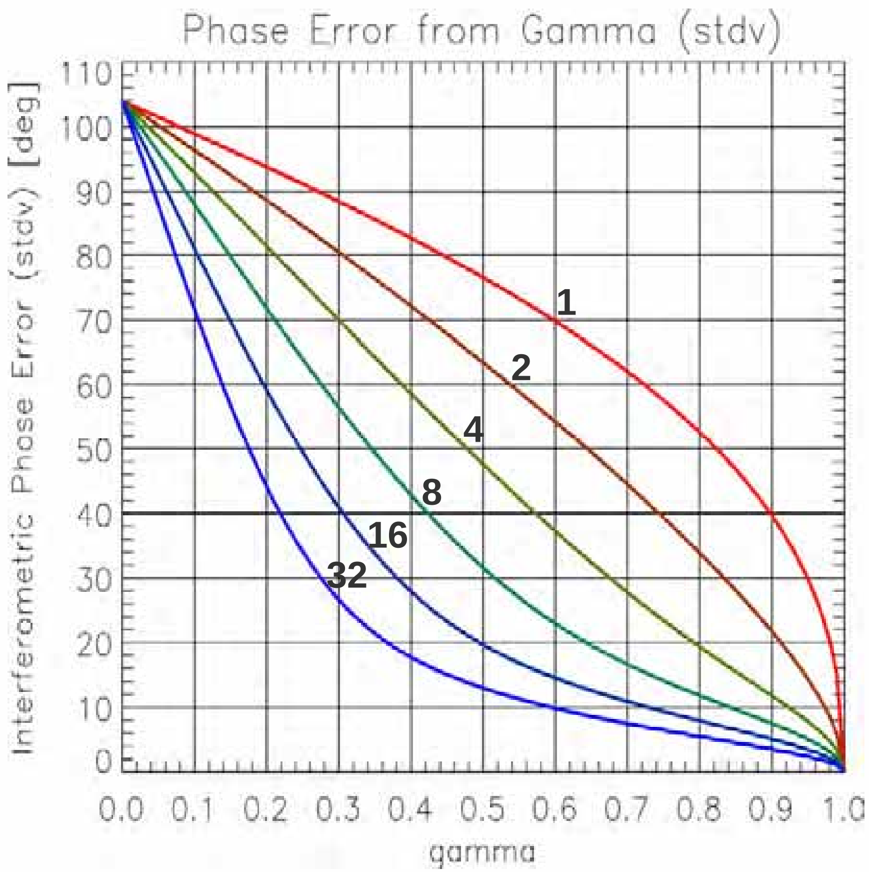

90 Percentile

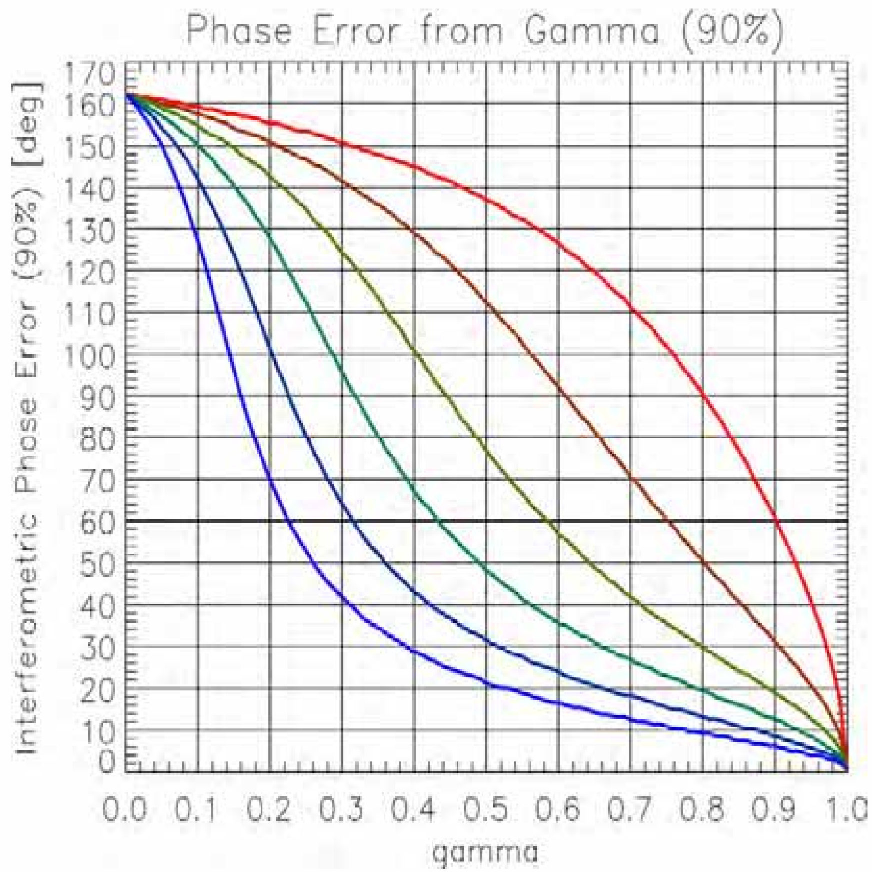

Independent Looks

Ground Range Resolution

(with range filtering)

$$\Delta rg = \frac{c_0}{2B_{rg}\sin(\theta_{inc}-\alpha)}\cdot\frac{B_{\perp,crit}}{B_{\perp,crit}-B_\perp}$$

with critical baseline

$$B_{\perp,crit} = \frac{2B_{rg}\lambda r\tan(\theta_i-\alpha)}{c_0}$$

and

c_0	:	velocity of light
B_{rg}	:	chirp bandwidth
λ	:	wavelength
r	:	slant range
θ_i	:	incident angle
α	:	local slope
$B_\perp$	:	effective baseline

Azimuth Resolution

(with azimuth filtering)

$$\Delta az = \frac{v_{grd}}{B_{proc}-\Delta f} \quad \text{with} \quad \Delta f = \left|f_{Dop,1}-f_{Dop,2}\right|$$

with Doppler Centroid approximation

$$f_{Dop,i} = \frac{1}{\lambda}\left[\frac{\mathbf{v}_{Tx}\cdot\mathbf{p}_{Tx}}{\|\mathbf{p}_{Tx}\|}+\frac{\mathbf{v}_{Rx,i}\cdot\mathbf{p}_{Rx,i}}{\|\mathbf{p}_{Rx,i}\|}\right]$$

and

v_{grd}	:	satellite velocity on ground
B_{proc}	:	processed bandwidth ($B = 2266 Hz$)
Δf	:	relative shift of Doppler Centroids
λ	:	wavelength
$\mathbf{v}_{\{Tx,Rx\}}$	:	velocity vector (transmitter/receiver)
$\mathbf{p}_{\{Tx,Rx\}}$	:	vector from satellite to scene center

$$N_{looks} = \frac{\Delta x}{\Delta rg}\cdot\frac{\Delta y}{\Delta az}$$

with independent post spacing Δx and Δy

Microwaves and Radar Institute
gerhard.krieger@dlr.de

Multilook Interferometric Phase Errors (Example)

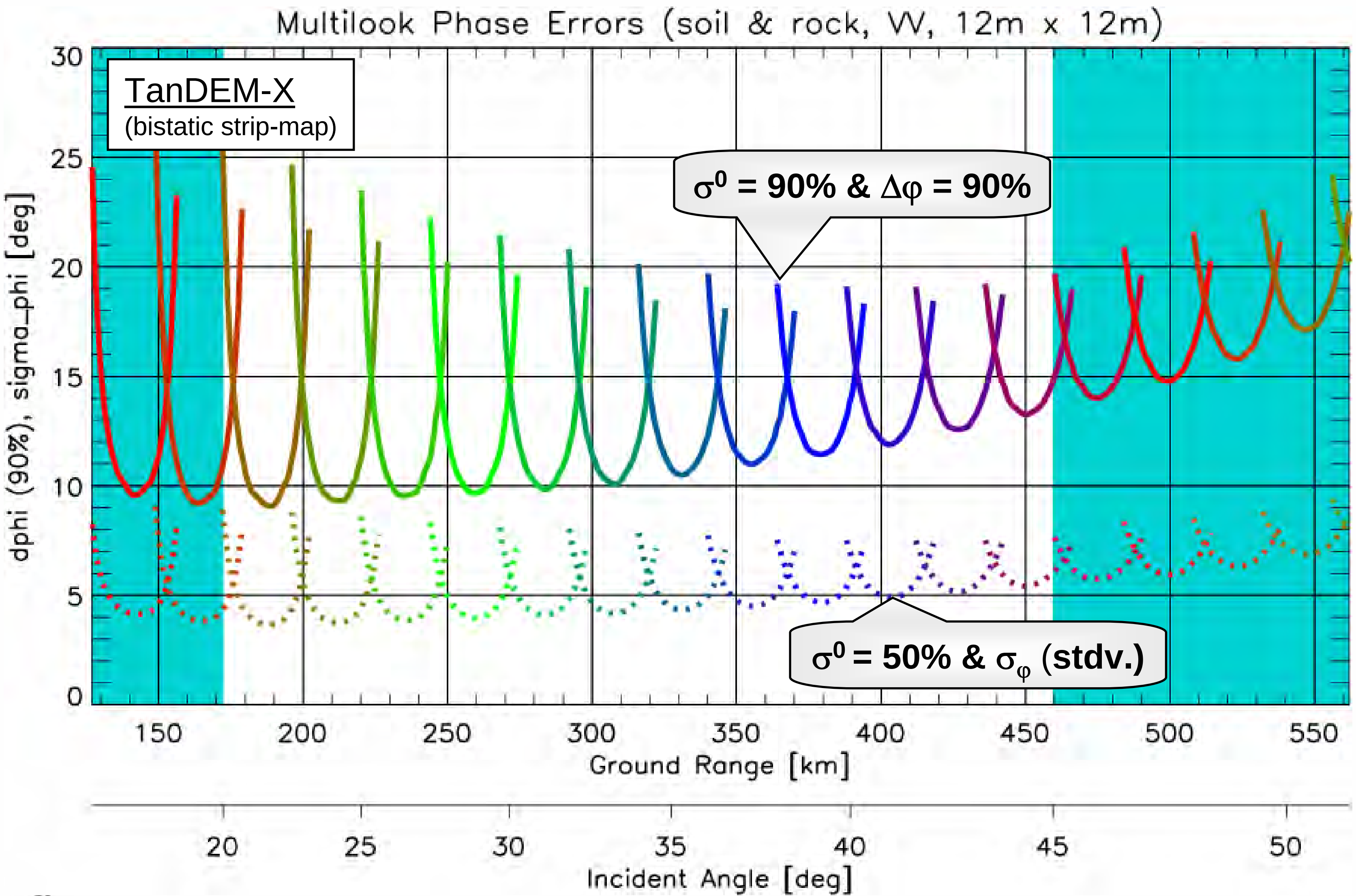

Derivation of Relative Height Errors

Standard deviation of height errors:

$$\sigma_h = \frac{\lambda r \sin(\theta_i)}{2\pi B_\perp} \cdot \sigma_\varphi \qquad \text{(flat terrain)}$$

HRTI-3 requires point-to-point height errors at 90% confidence levels:

$$\Delta h_{\mathrm{HRTI}} \approx \frac{\lambda r \sin(\theta_i)}{2\pi B_\perp} \cdot \varphi_{90\,\%} \cdot \sqrt{2}$$

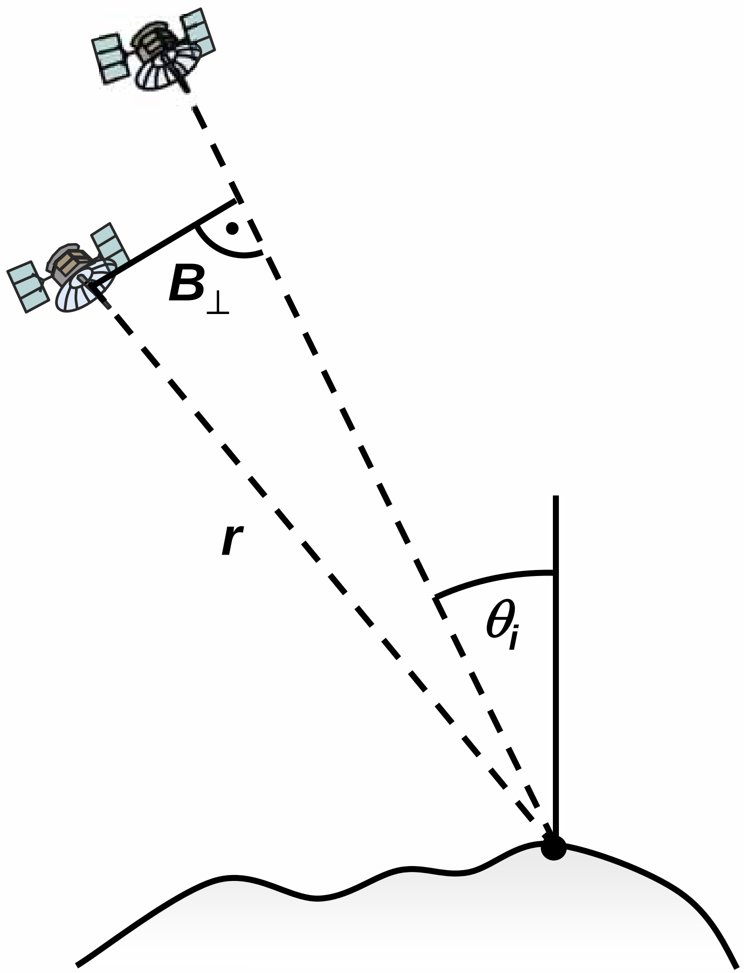

Microwaves and Radar Institute
gerhard.krieger@dlr.de

Relative Height Errors (Example)

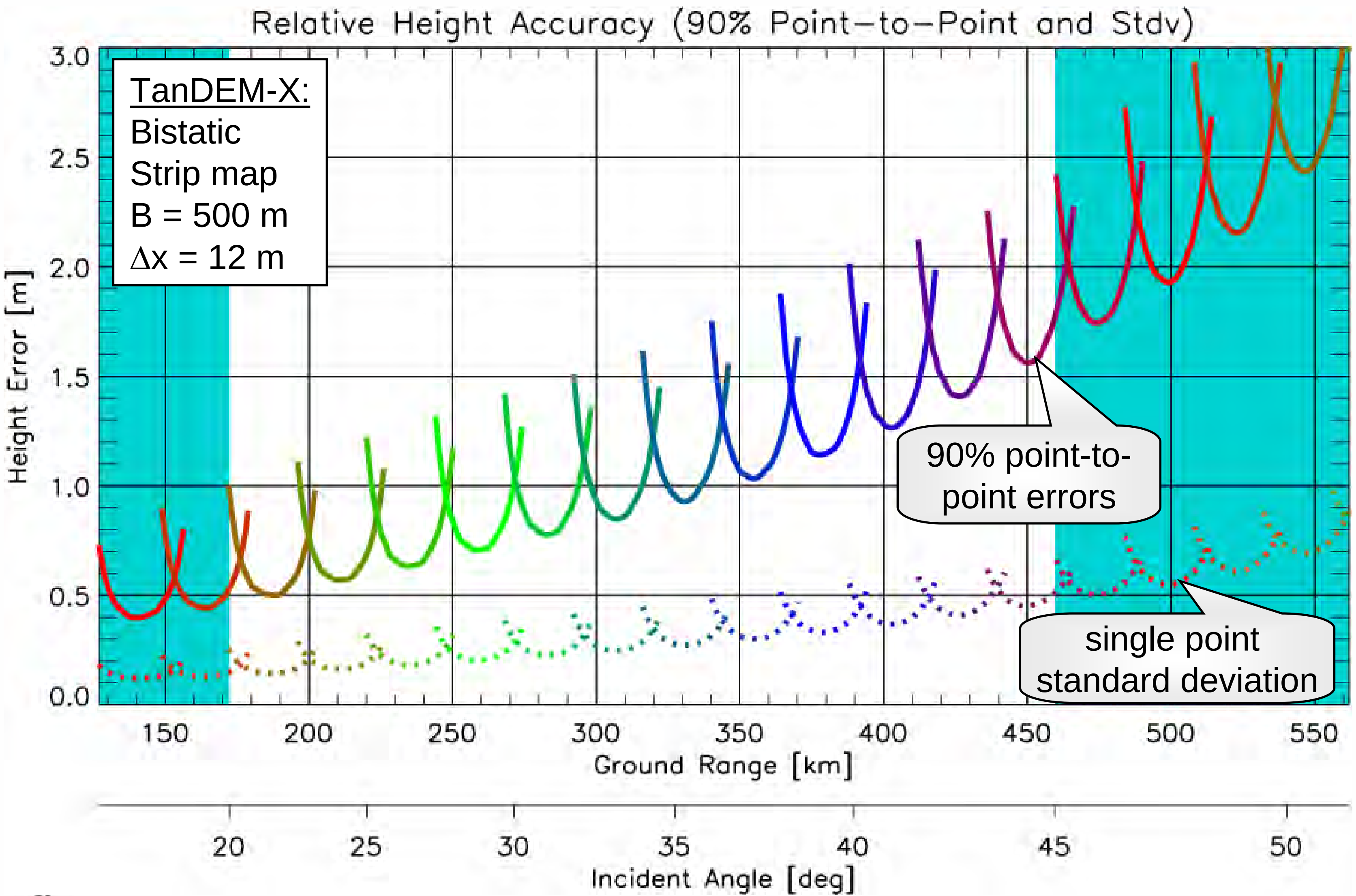

gerhard.krieger@dlr.de

Relative Height Errors (Example)

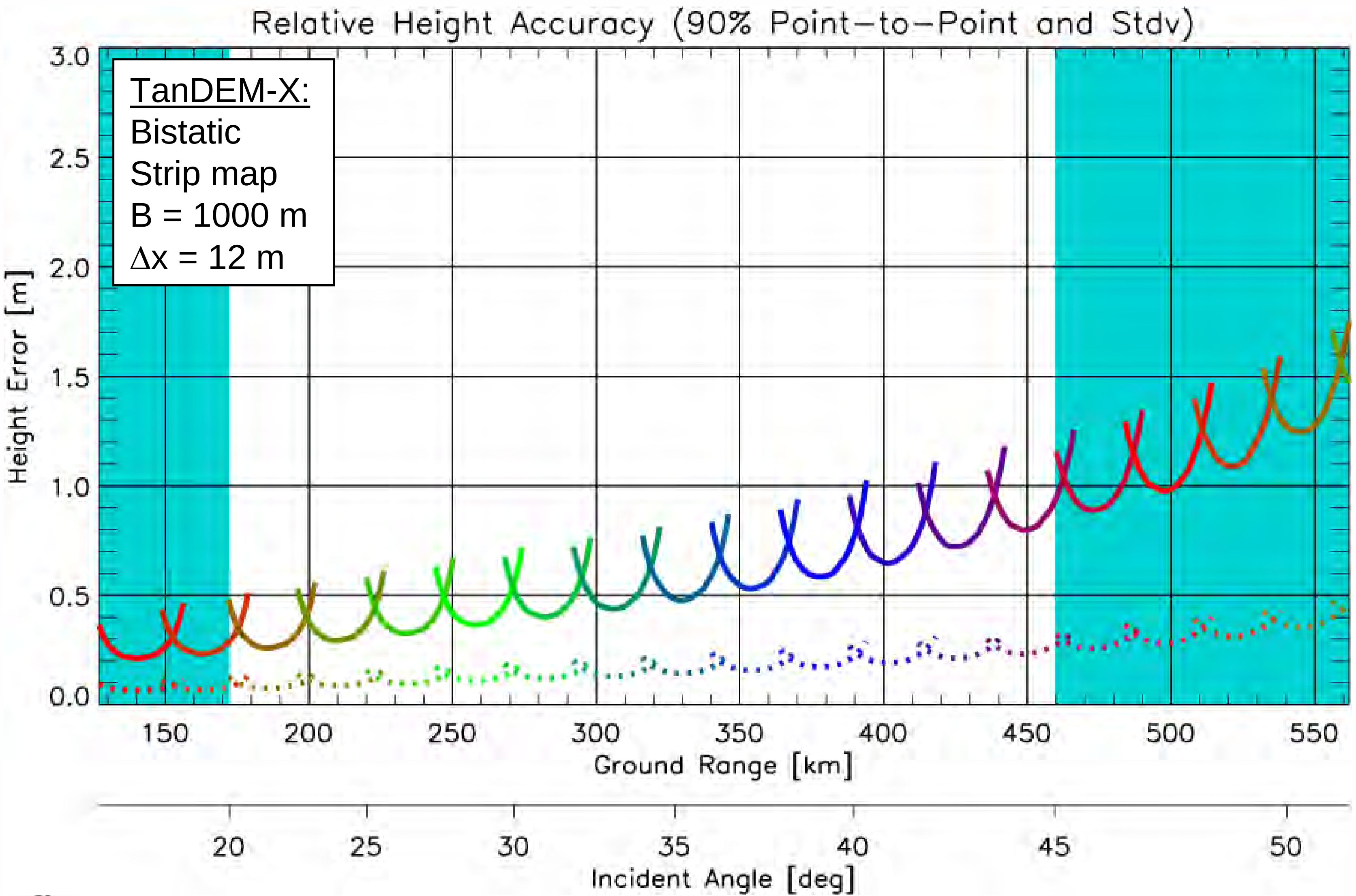

Relative Height Errors (Example)

TanDEM-X enables large baselines which allow for ultra high resolution DEMs with height accuracies in the sub-meter range, but …

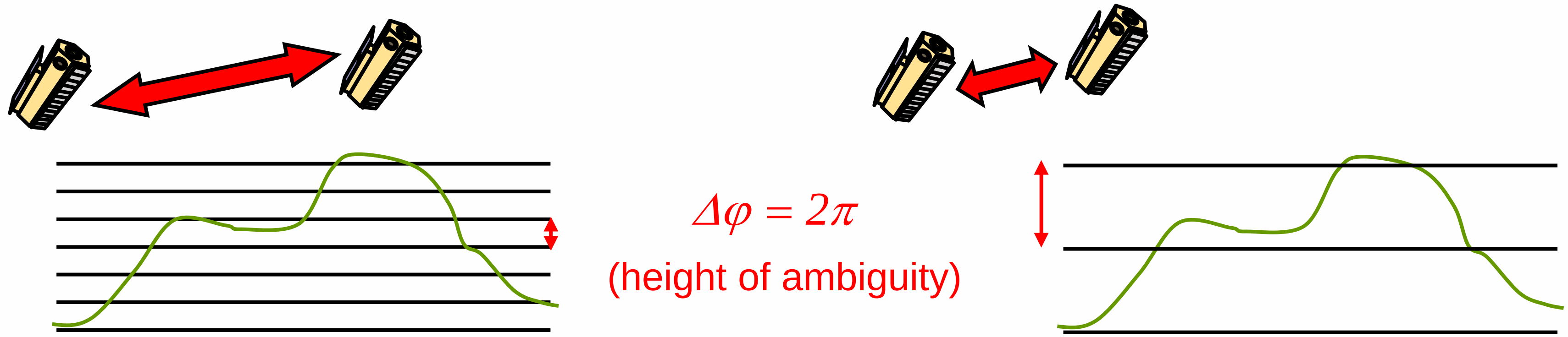

Compromise on Accuracy for Global DEM

- use reduced baselines
- additional acquisitions for difficult terrain

→ acquisition scenario for global DEM

Multi-Baseline Data Acquisitions

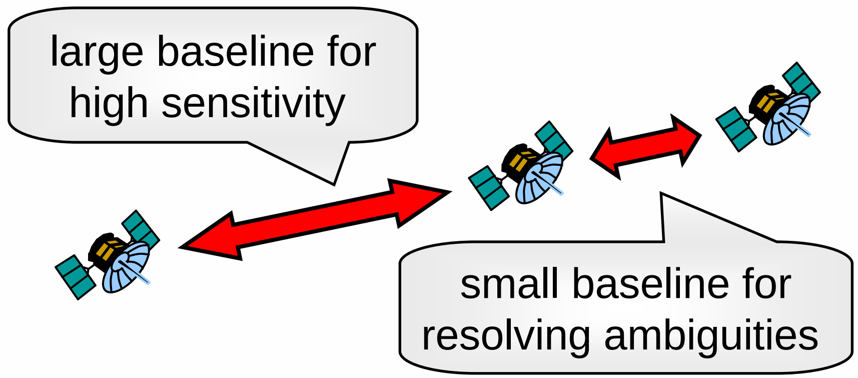

Microwaves and Radar Institute
gerhard.krieger@dlr.de

Multi-Baseline Data Acquisitions (Example)

Trinodal Pendulum

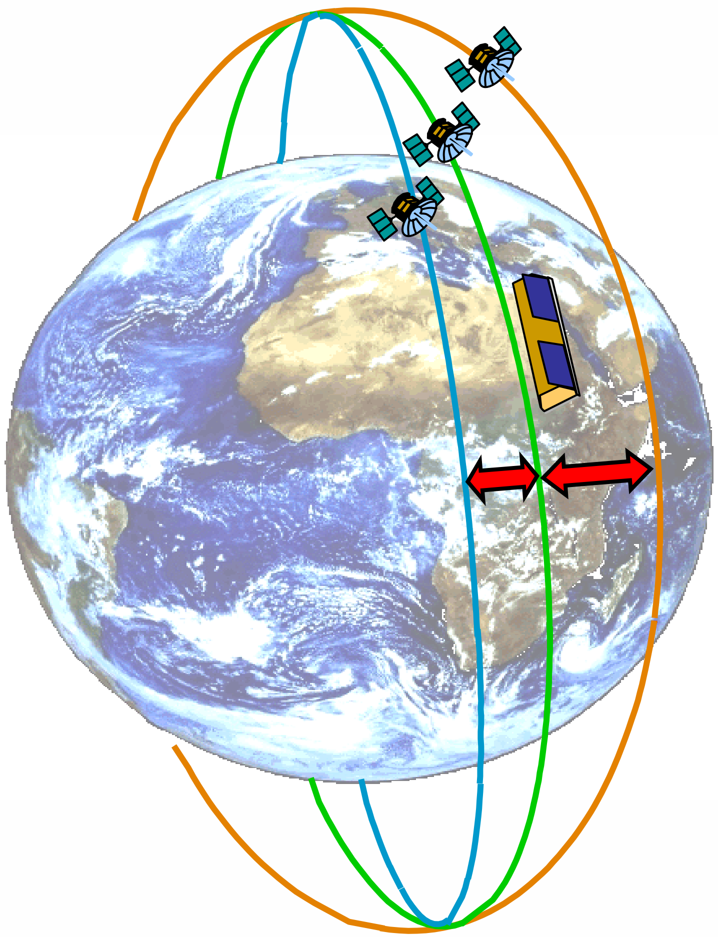

→ ***multiple baselines with fixed baseline ratio in one pass***

Performance Example (TerraSAR-L)

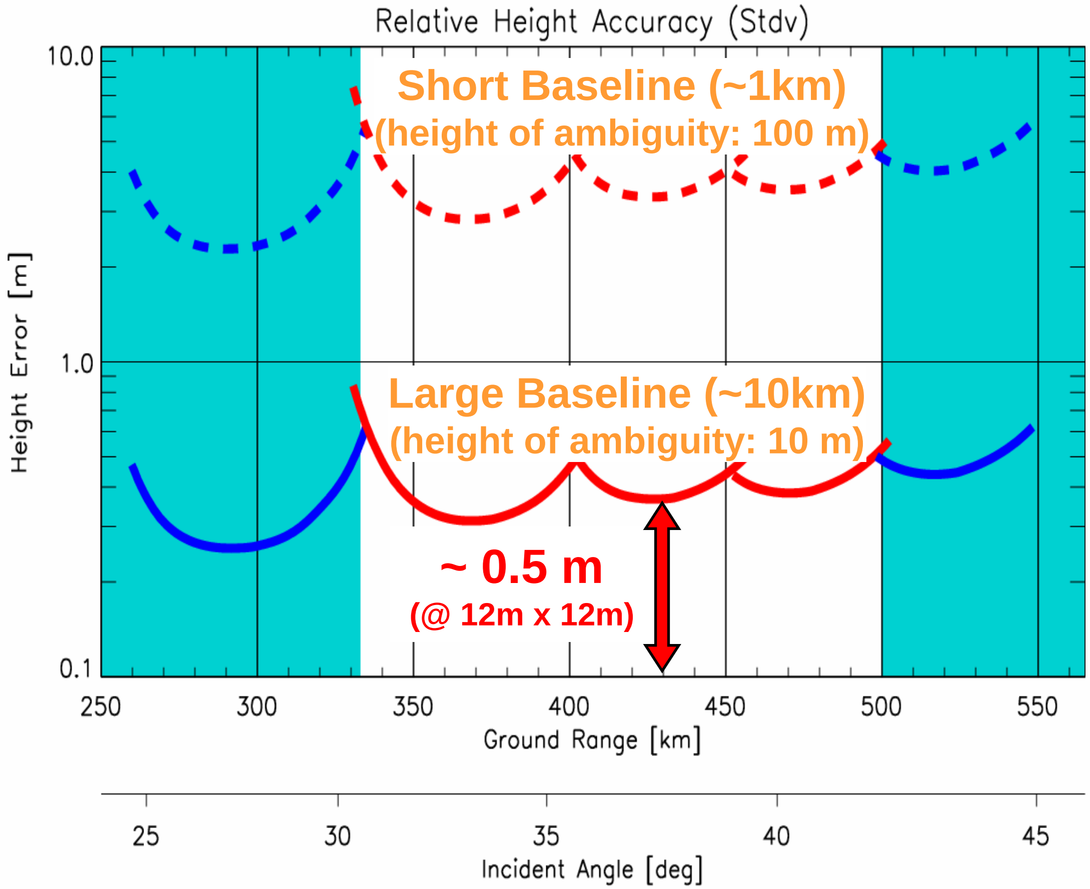

Large Baseline → Excellent Height Accuracy
Small Baseline → Easy Phase Unwrapping

Microwaves and Radar Institute
gerhard.krieger@dlr.de

Polarimetric SAR Interferometry

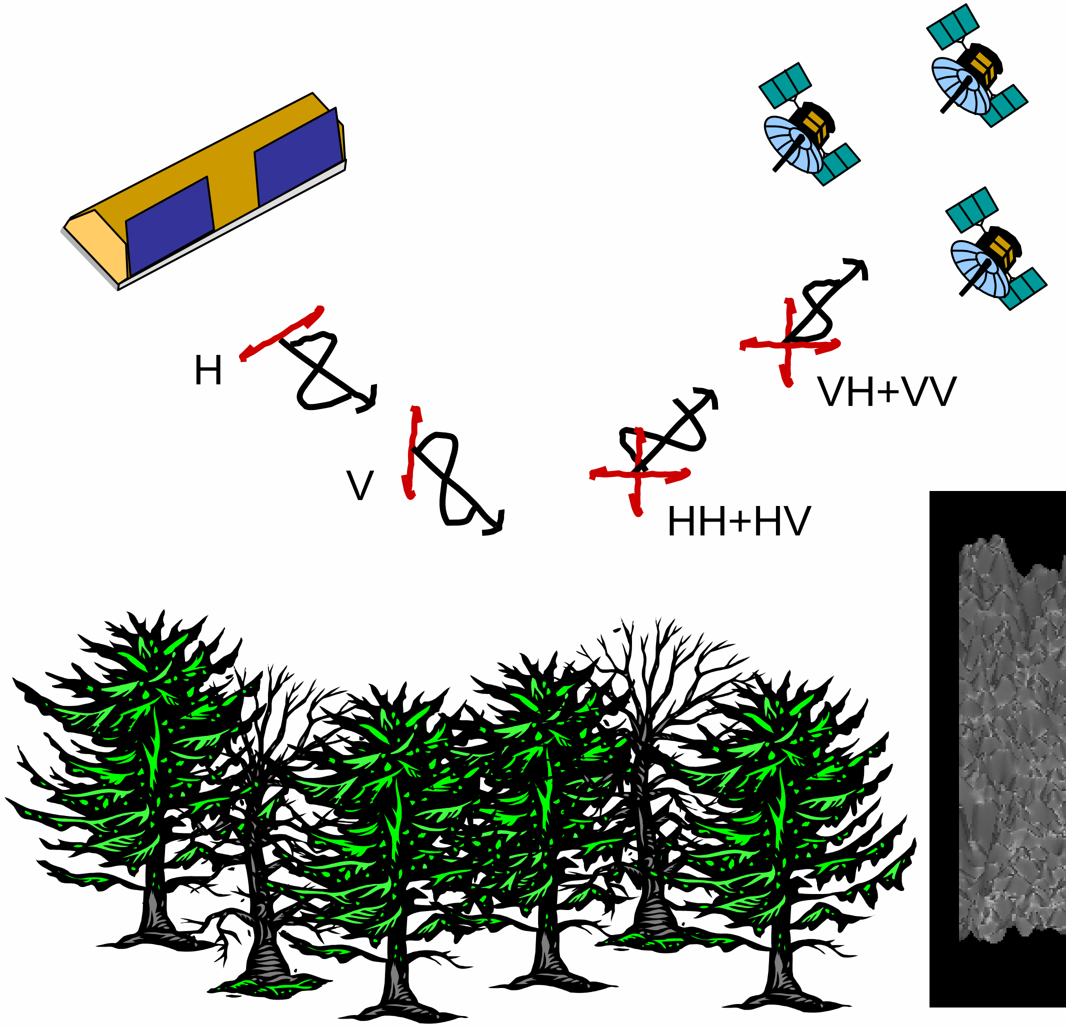

Inversion of Coherent Scattering Model

(e.g. Random Volume + Ground)

$h_V, \sigma, \phi_0, m_{1-3}$

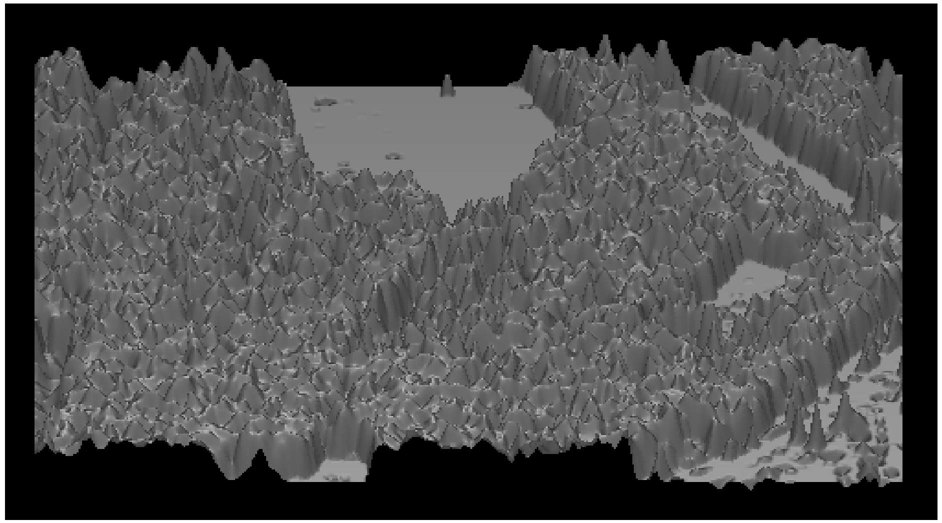

(from K. Papathanassiou & S. Cloude, 2001)

PolInSAR L-Band Performance Example

Monostatic Repeat Pass System ***(γ_{temp} = 0.5)***	***Multistatic Single Pass System*** ***(γ_{temp} = 1.0, but smaller Rx antennas)***
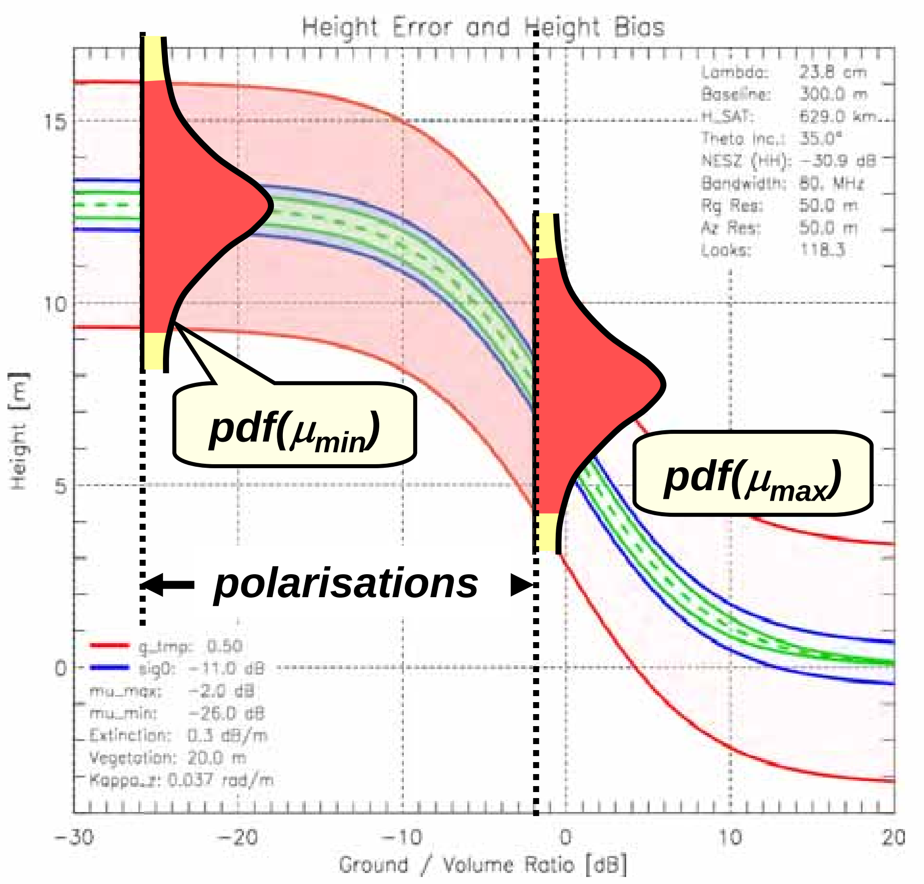	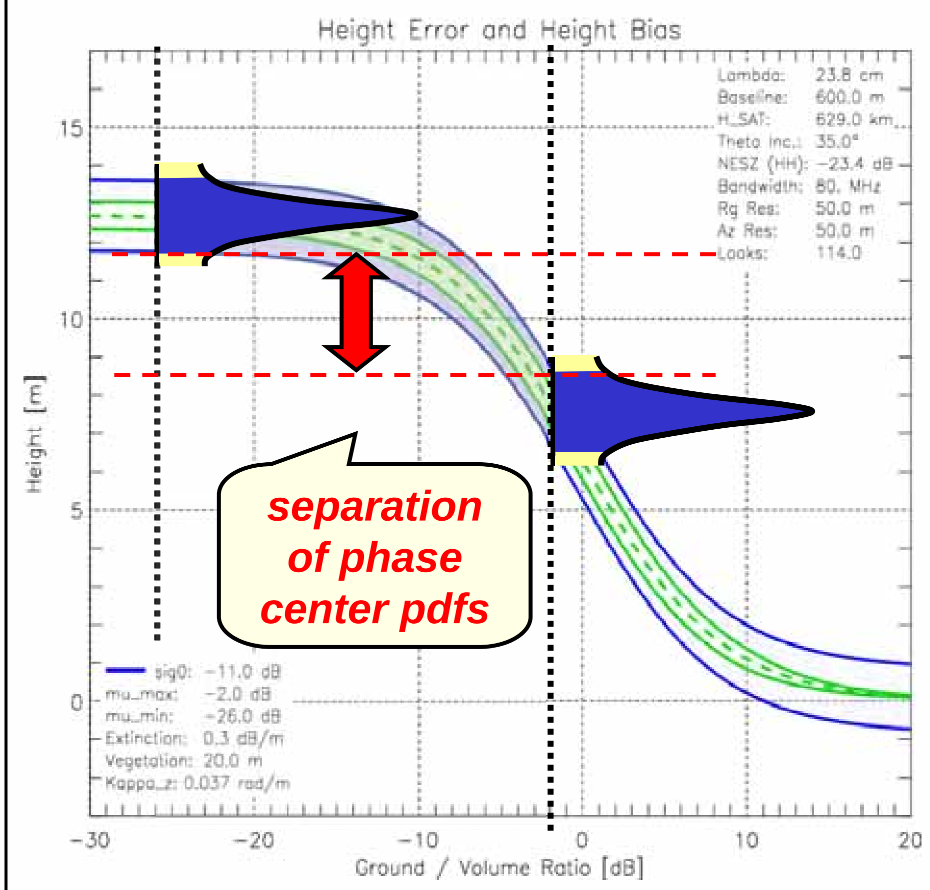
→ Poor Inversion Accuracy	***→ Good Inversion Accuracy***

Microwaves and Radar Institute
gerhard.krieger@dlr.de

PolInSAR L-Band Performance Example

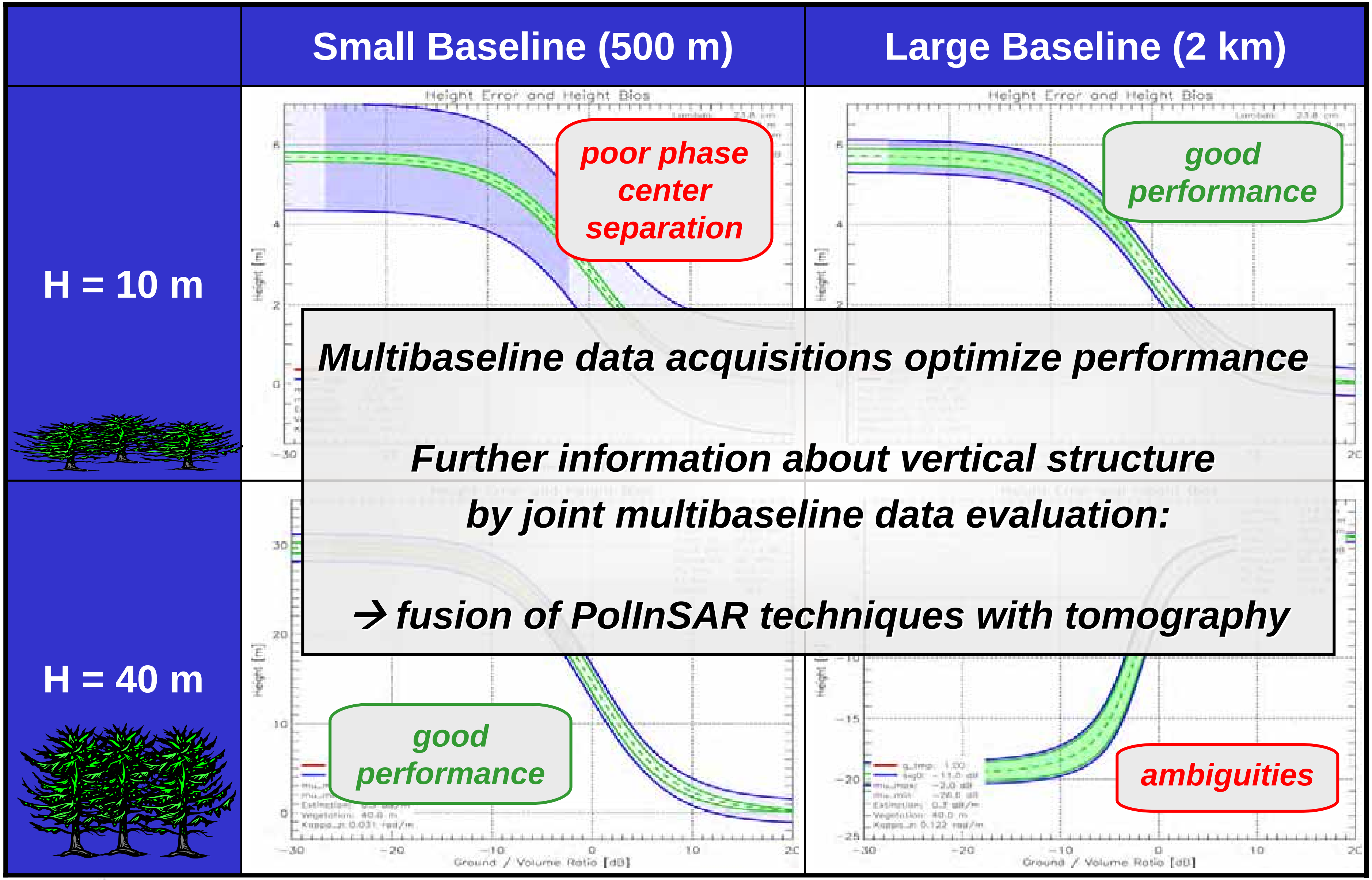

Multibaseline data acquisitions optimize performance

Further information about vertical structure by joint multibaseline data evaluation:

→ fusion of PolInSAR techniques with tomography

Microwaves and Radar Institute
gerhard.krieger@dlr.de

Tomography with Micro-Satellite Array

Basic Idea: Cluster of receiver satellites to form an additional aperture in elevation

- allows real three-dimensional imaging, i.e. a geometric resolution in height direction
- avoids the intrinsic height ambiguity in conventional SAR imaging
- accurate modeling and retrieval of vegetation parameters
- not affected by layover or foreshortening effects
- cross-track distance between the satellites defines the height ambiguity value for tomographic processing
- total tomographic baseline defines the height resolution

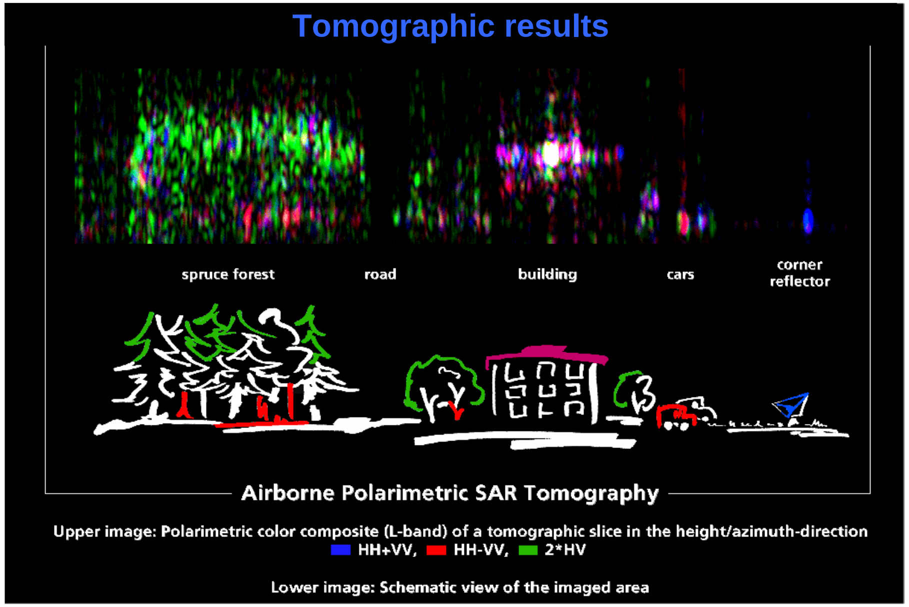

(from A. Reigber & A. Moreira, 1999)

Microwaves and Radar Institute
gerhard.krieger@dlr.de

Tomography with Semi-Active Micro-Satellite Array

Fundamental relations:

- height resolution:

$$\Delta h \approx \frac{\lambda \cdot r_0 \cdot \sin\theta_{inc}}{L \cdot \cos\theta_{look}}$$

- required sampling:

$$d < \frac{\lambda \cdot r_0 \cdot \sin\theta_{inc}}{h_v \cdot \cos\theta_{look}}$$

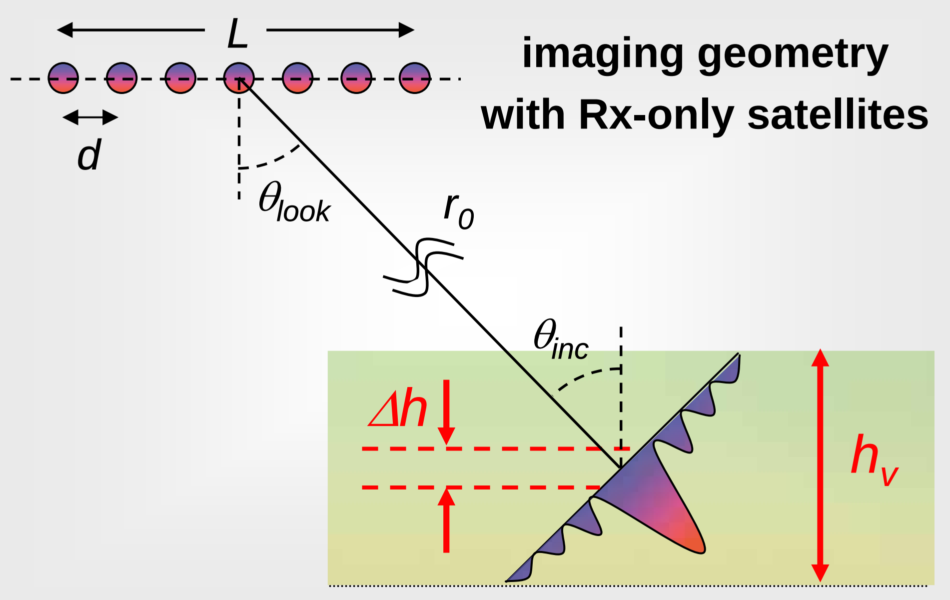

Example:

λ	0.23 m
r_0	700 km
θ_{inc}	30°
θ_{look}	30°
L	20 km
d	2 km

$\Delta h = 3$ m

$h_v < 30$ m

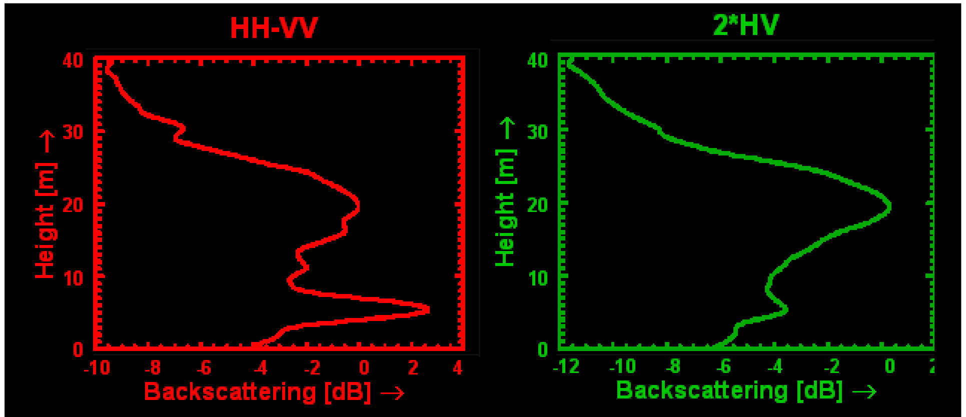

Examples of intensity profiles in the height direction

Microwaves and Radar Institute
gerhard.krieger@dlr.de

Multistatic SAR Imaging

- improved detection, segmentation, and classification in SAR images
- separation of different scattering mechanisms (e.g. coherent from non-coherent components)
- radargrammetry and multi-shadow evaluations
- speckle reduction without resolution degradation
- multibaseline coherence analyses
- acquisition of bi- and multistatic Doppler spectra (e.g. multiple ocean wave spectra)
- downward looking receivers (fusion with other sensors)

Extended Observation Space

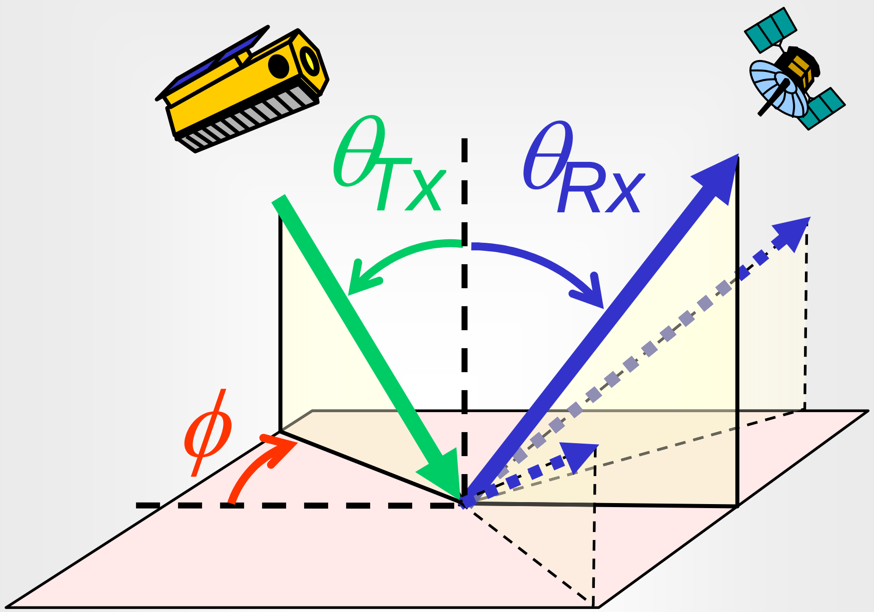

Multiple
- *Scattering angles* θ_{Rx}
- *Out-of-plane angles* ϕ
- *Doppler frequencies*

+ polarimetry (e.g. $\sigma_{HV} \neq \sigma_{VH}$*)*

Microwaves and Radar Institute
gerhard.krieger@dlr.de

Multistatic Scattering Coefficients: Example

Bistatic Airborne Radar Experiment:
(February 2003, Nimes, France)

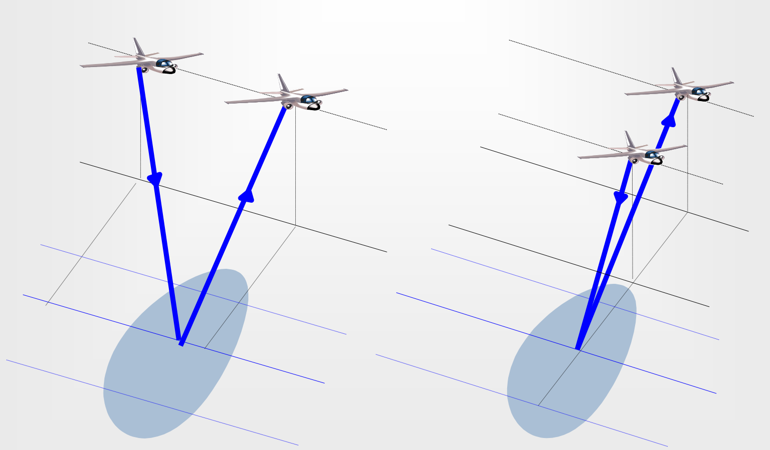

Color composite of
three bistatic images:

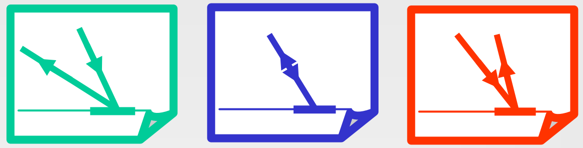

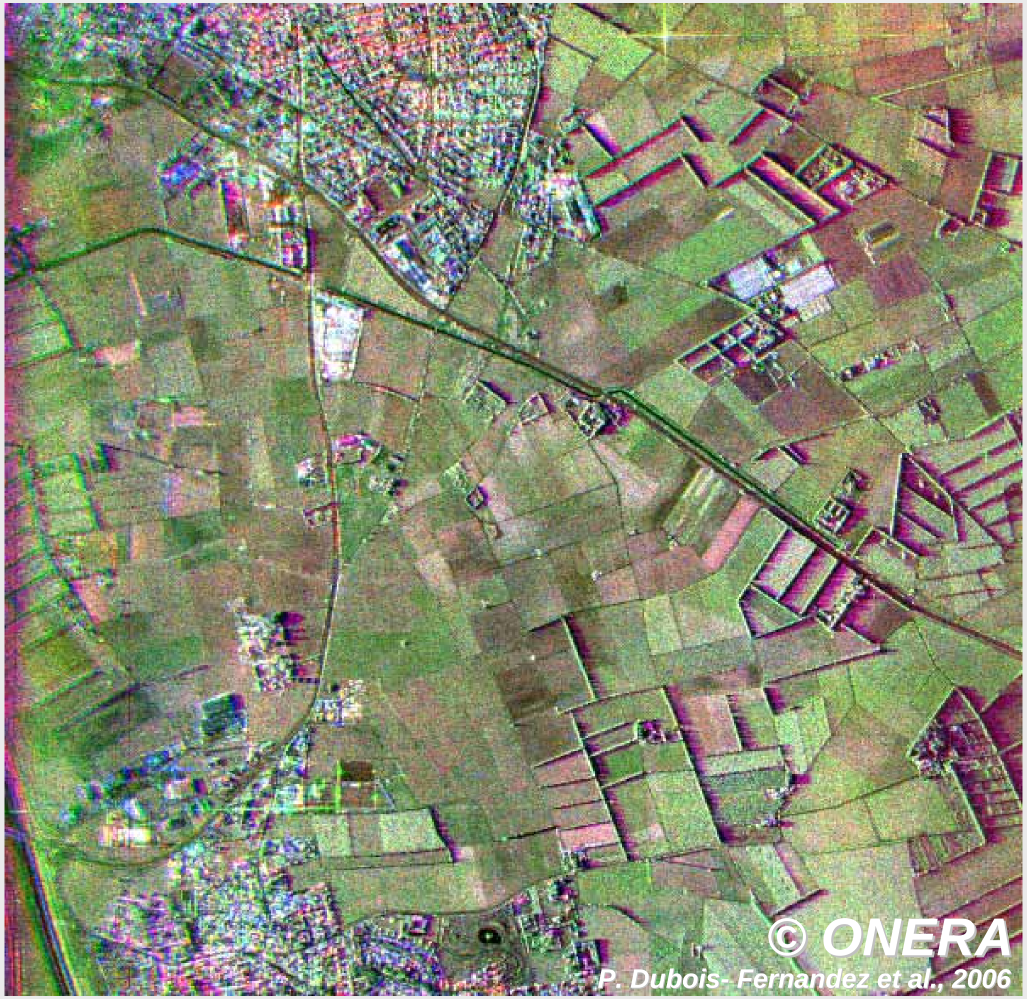

Along-Track Interferometry

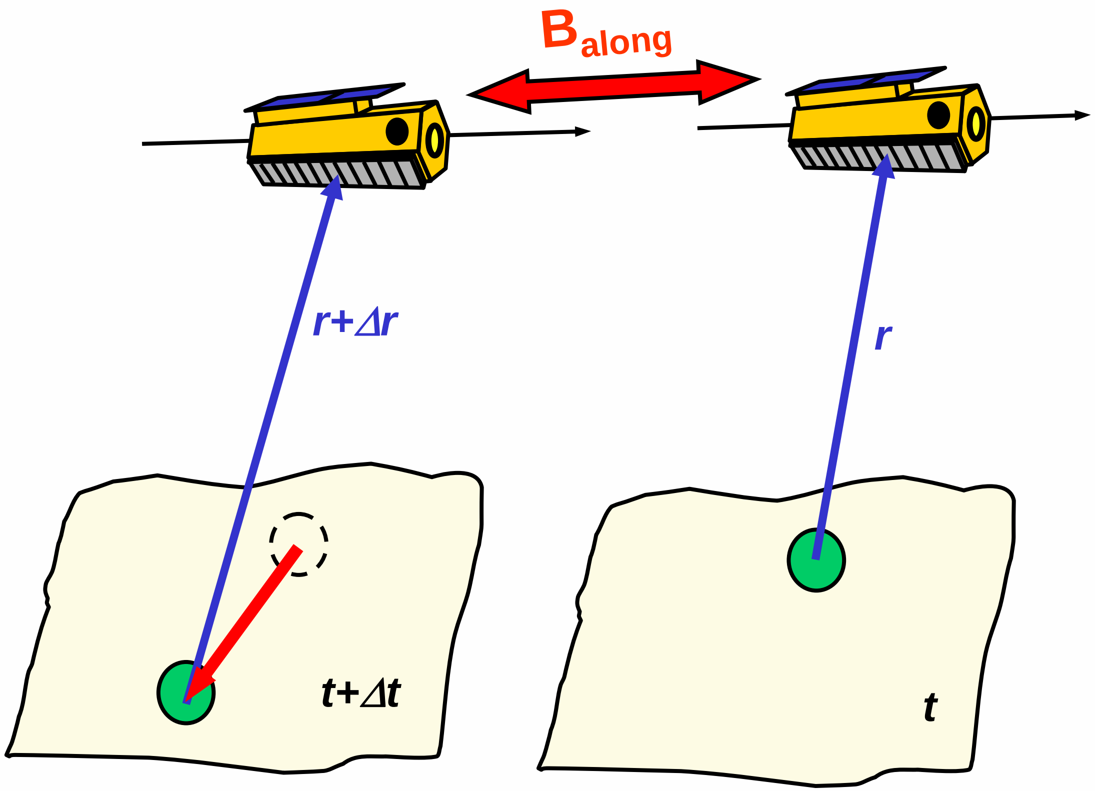

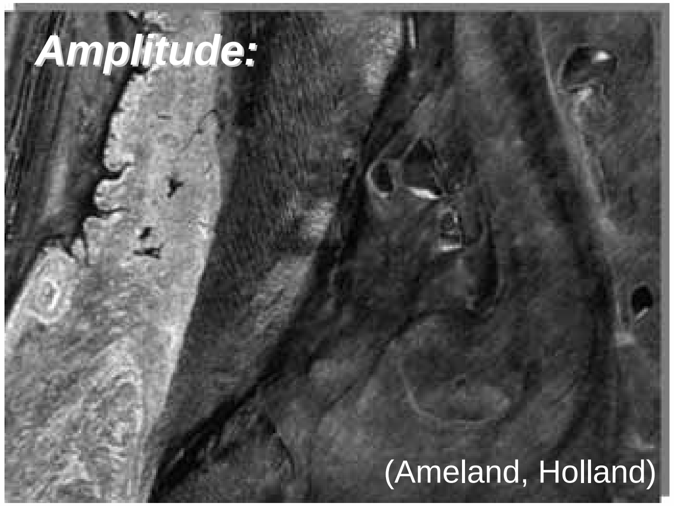

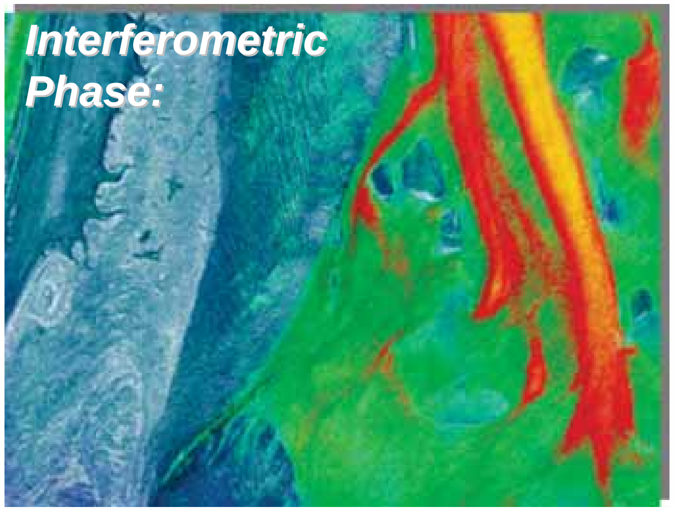

highly accurate measurements of the radial displacement between two radar observations separated by a short time lag

Microwaves and Radar Institute
gerhard.krieger@dlr.de

SAR Imaging with Four Phase Centres

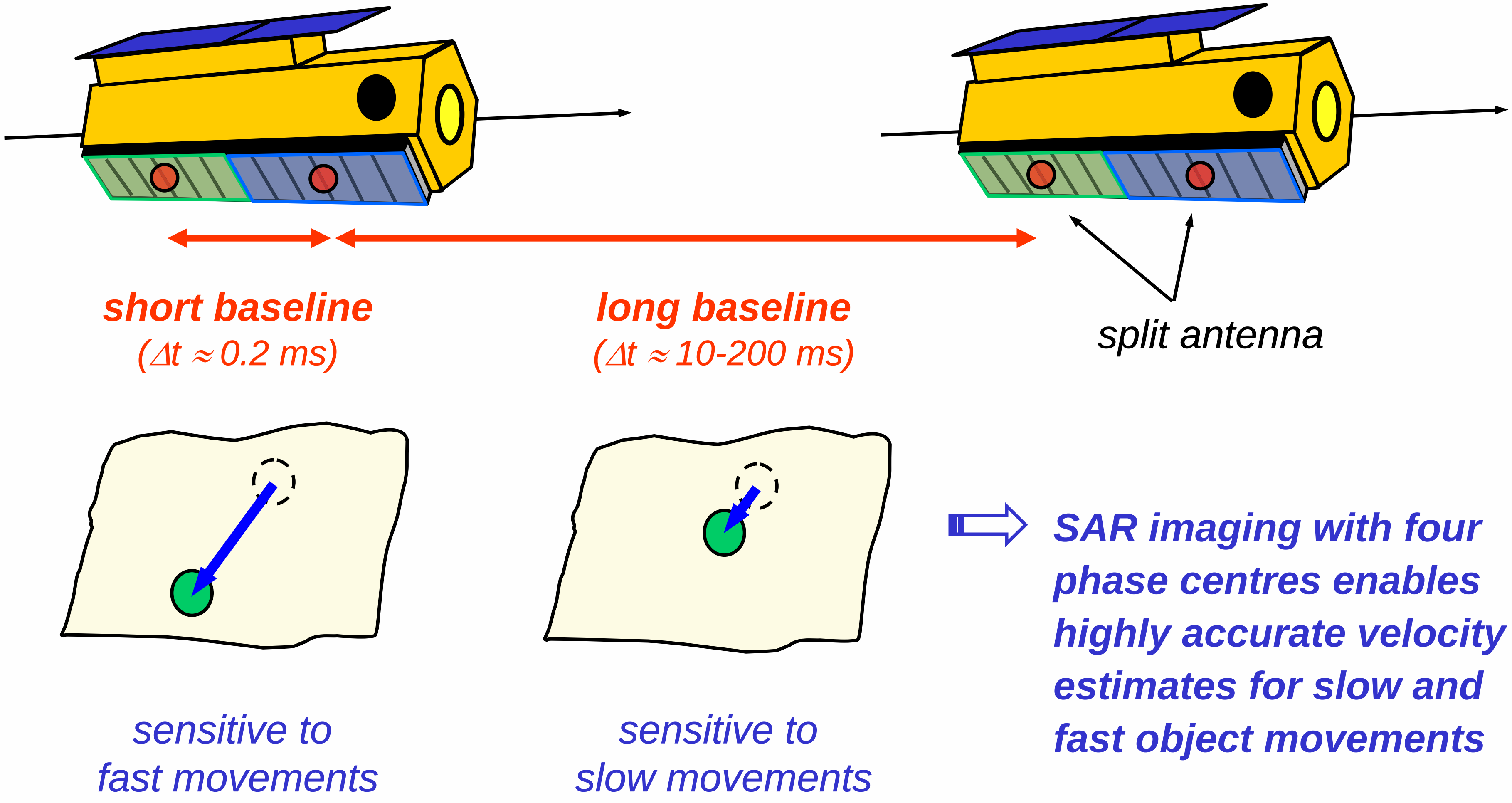

⇨ ***SAR imaging with four phase centres enables highly accurate velocity estimates for slow and fast object movements***

Microwaves and Radar Institute
gerhard.krieger@dlr.de

Applications of Along-Track Interferometry

Ocean Currents

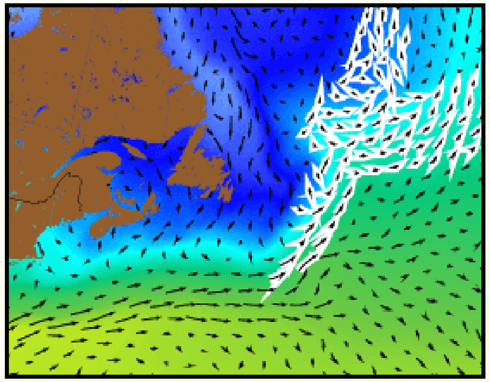

Coastal Surveillance

Ice Drift & Ice Flow

Traffic Monitoring

Microwaves and Radar Institute
gerhard.krieger@dlr.de

Multi-Baseline ATI and GMTI

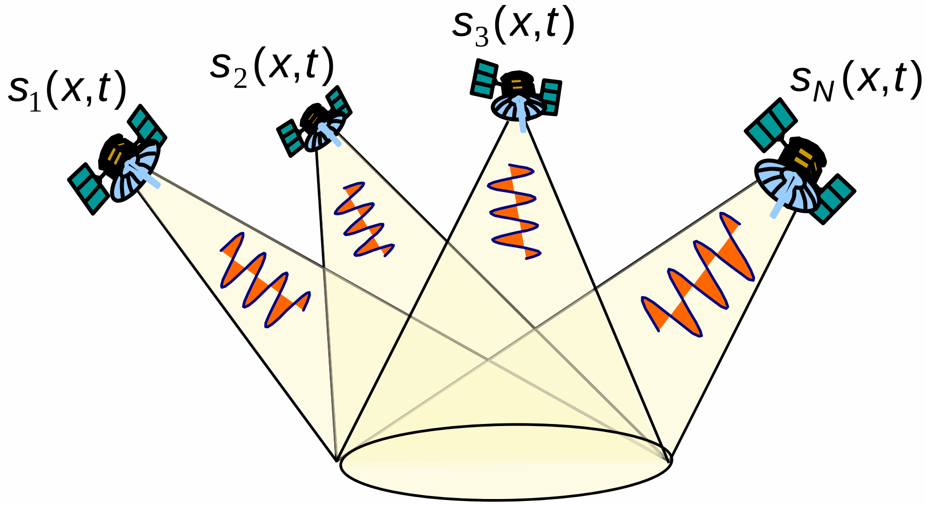

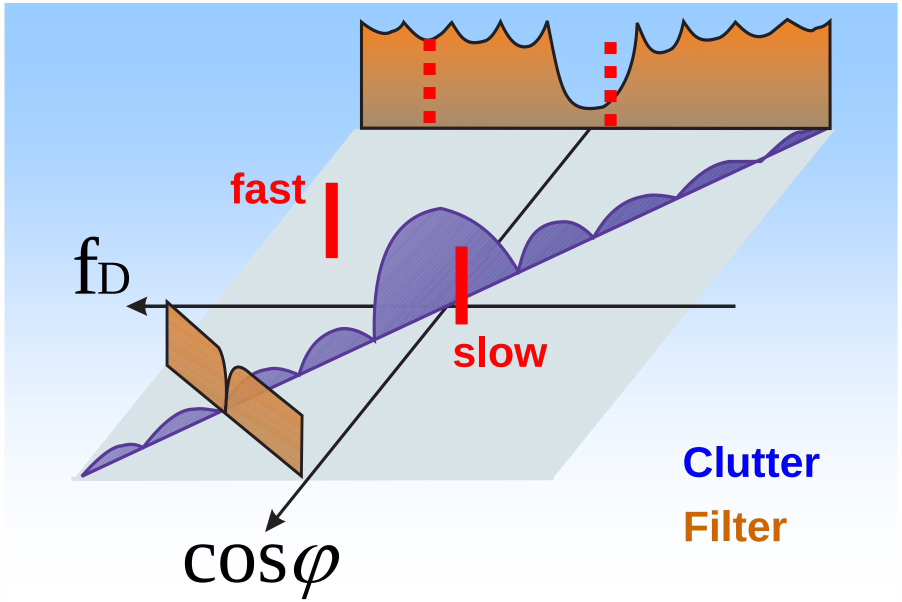

steep notch enables good clutter suppression

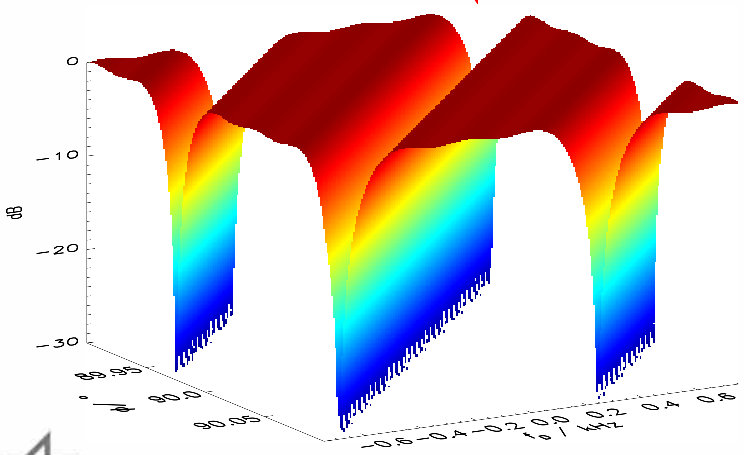

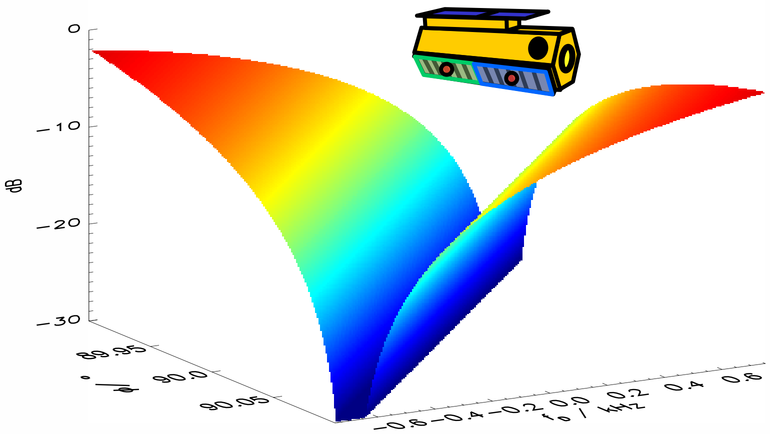

Microwaves and Radar Institute
gerhard.krieger@dlr.de

Ambiguity Reduction and Wide Swath Imaging

- single transmitter illuminates ***wide image swath***
- multiple receivers record scattered signal
- N receivers allow ***reduction of PRF*** by a factor of 1/N ***without*** raising ***azimuth ambiguities***:
  - increase of swath width by factor N at ***full azimuth resolution*** (as opposed to ScanSAR)
  - variability in optimum receiver displacement:

$$x_i - x_1 \approx \frac{2 \cdot v}{PRF}\left(\frac{i\text{-}1}{N} + k_i\right) \quad i \in \{1,2,\ldots,N-1\}, k_i \in Z$$

  - reconstruction possible for other displacements
  - performance can be optimized by PRF adaptation
  - requires stable oscillators or RF synchronization and accurate estimation of relative displacement
- major application: ***high resolution*** imaging of a ***wide image swath*** with ***small antennas*** (e.g. distributed L-Band SAR with multiple microsatellites)

Distributed aperture radar with multiple receivers

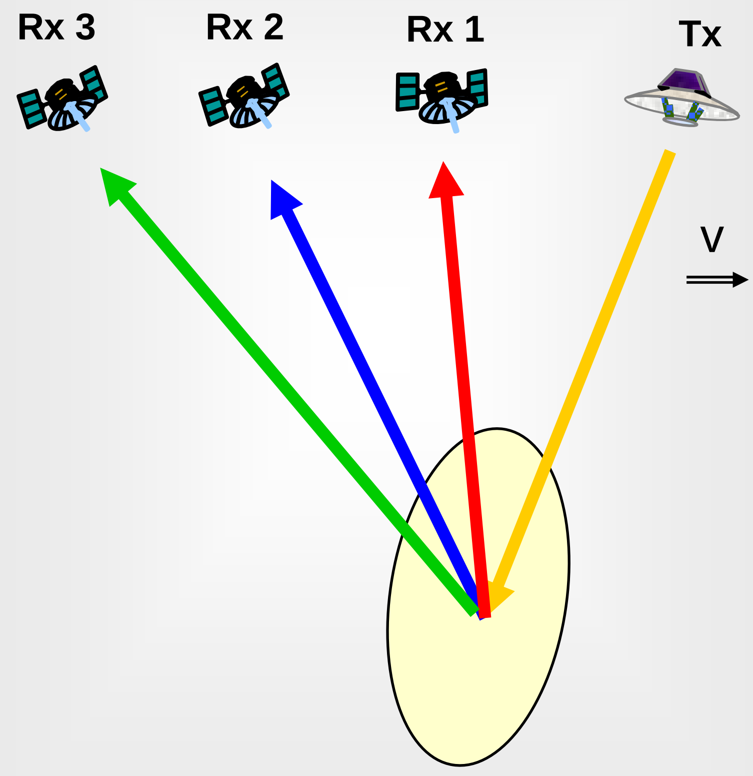

Microwaves and Radar Institute
gerhard.krieger@dlr.de

Multi-Channel Model for Sparse Array

Multiple Aperture Array:

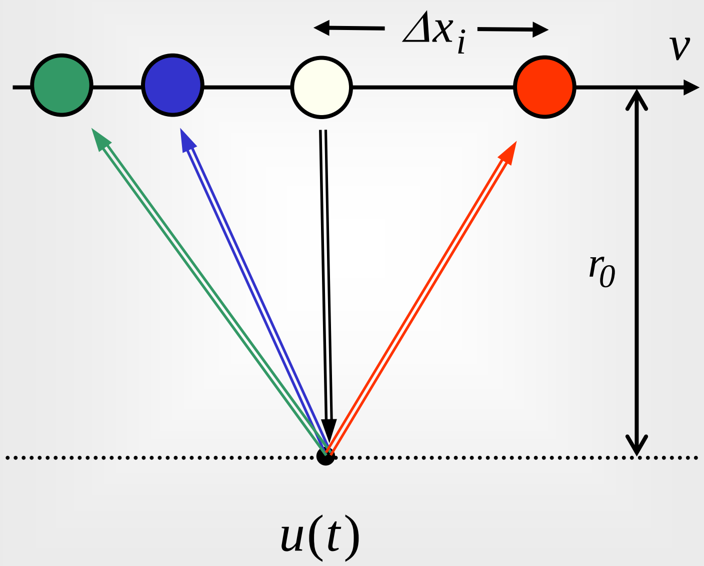

System Model:

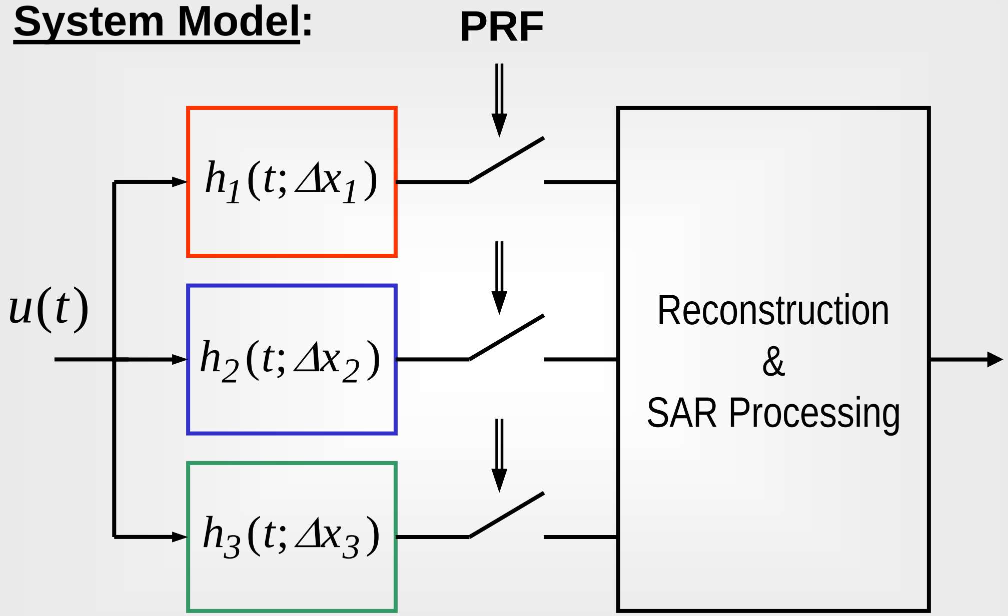

Bistatic Azimuth Impulse Response:

$$h_i(t;\Delta x_i) = A_{Tx}(vt)\cdot A_{Rx,i}(vt-\Delta x_i)\cdot \exp\left[-j\frac{2\pi}{\lambda}\left(\sqrt{r_0^2+(vt)^2}+\sqrt{r_0^2+(vt-\Delta x_i)^2}\right)\right]$$

Coherent Reconstruction

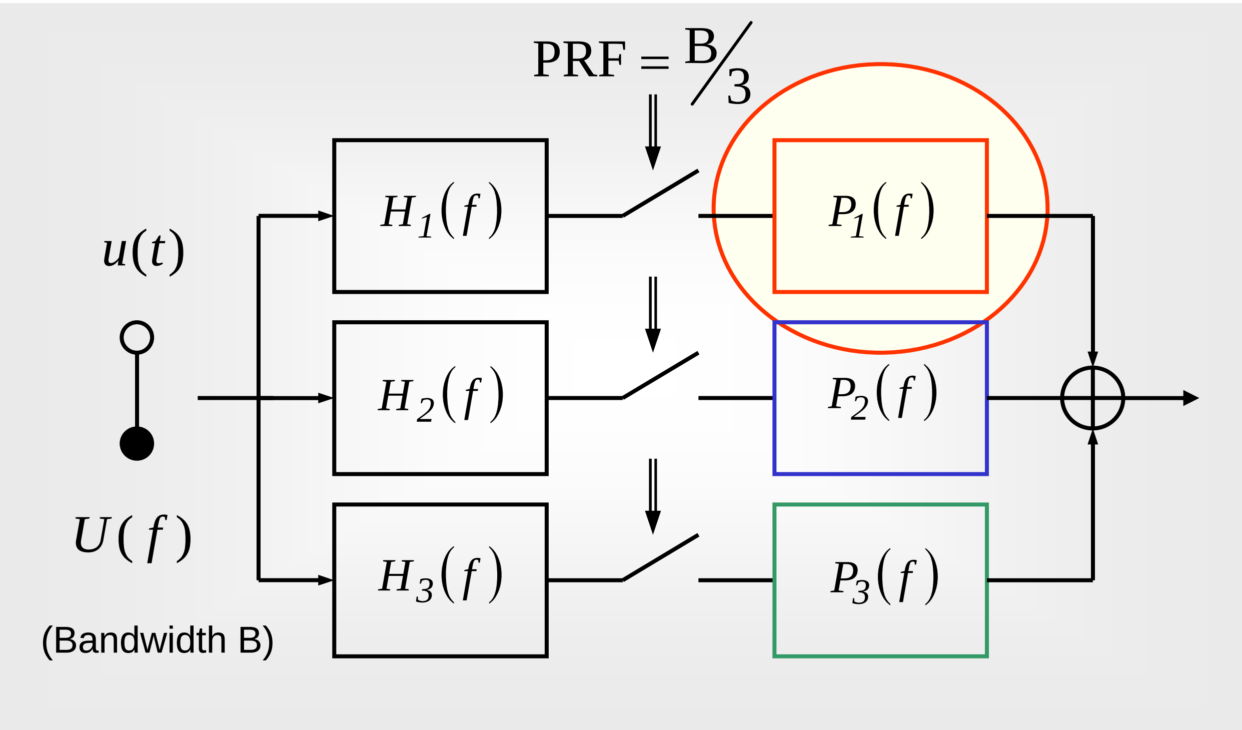

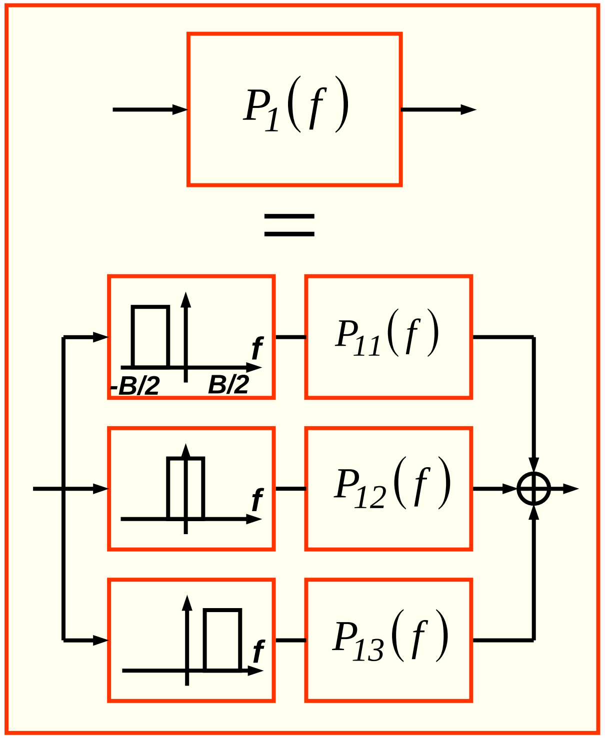

$$\mathbf{A(f)} = \begin{bmatrix} H_1(f) & H_2(f) & H_3(f) \\ H_1(f+B/3) & H_2(f+B/3) & H_3(f+B/3) \\ H_1(f+2B/3) & H_2(f+2B/3) & H_3(f+2B/3) \end{bmatrix} \longrightarrow \mathbf{A^{-1}(f)} = \begin{bmatrix} P_{11}(f) & P_{12}(f+B/3) & P_{13}(f+2B/3) \\ P_{21}(f) & P_{22}(f+B/3) & P_{23}(f+2B/3) \\ P_{31}(f) & P_{32}(f+B/3) & P_{33}(f+2B/3) \end{bmatrix}$$

(cf. A. Papoulis, 1977 & J.L. Brown, 1981)

Model with Quadratic Phase Approximation

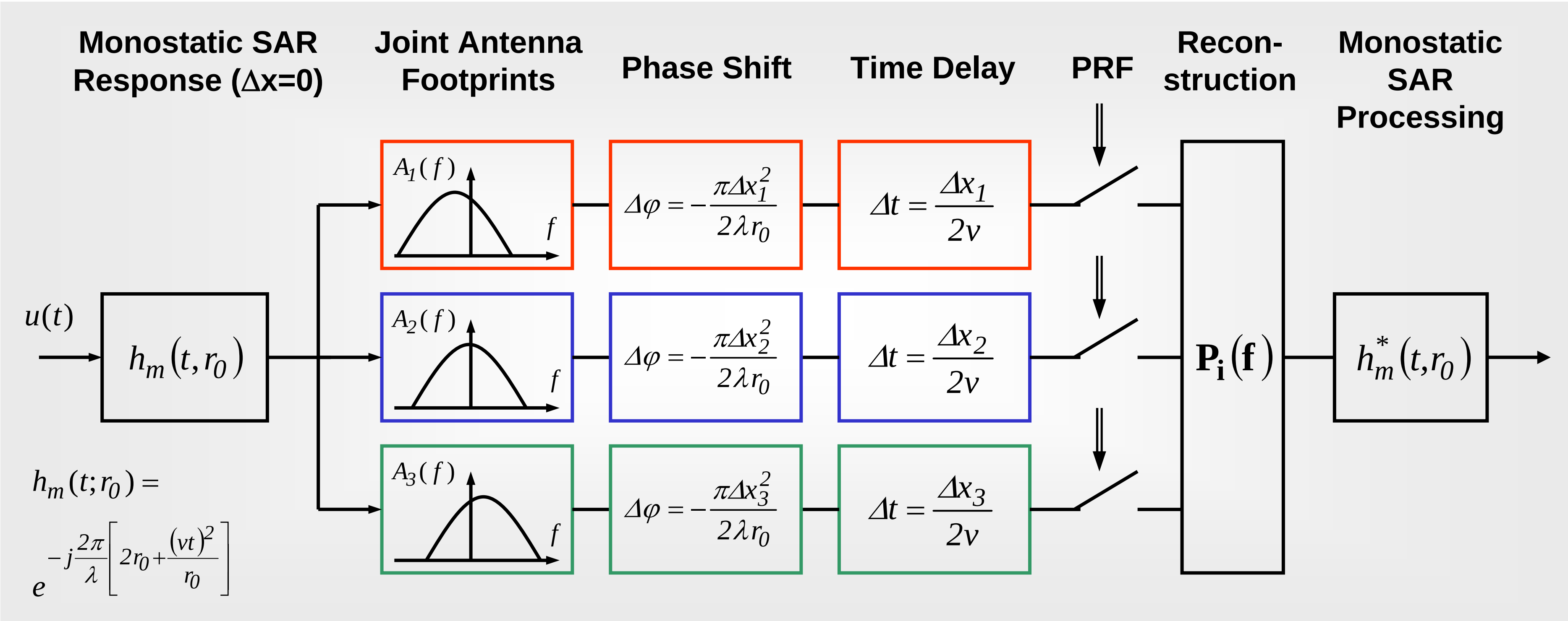

<u>Bistatic Azimuth Impulse Response:</u>

$$h_i(t;\Delta x_i) \cong A_{Tx}(vt) \cdot A_{Rx,i}(vt - \Delta x_i) \cdot \exp\left[-j\frac{4\pi}{\lambda} r_0 \left(1 + \frac{\Delta x_i^2}{8 r_0^2}\right)\right] \cdot \exp\left[-j\frac{2\pi}{\lambda} \frac{\left(vt - \frac{\Delta x_i}{2}\right)^2}{r_0}\right]$$

Microwaves and Radar Institute
gerhard.krieger@dlr.de

Sparse Array Reconstruction: Raw Data

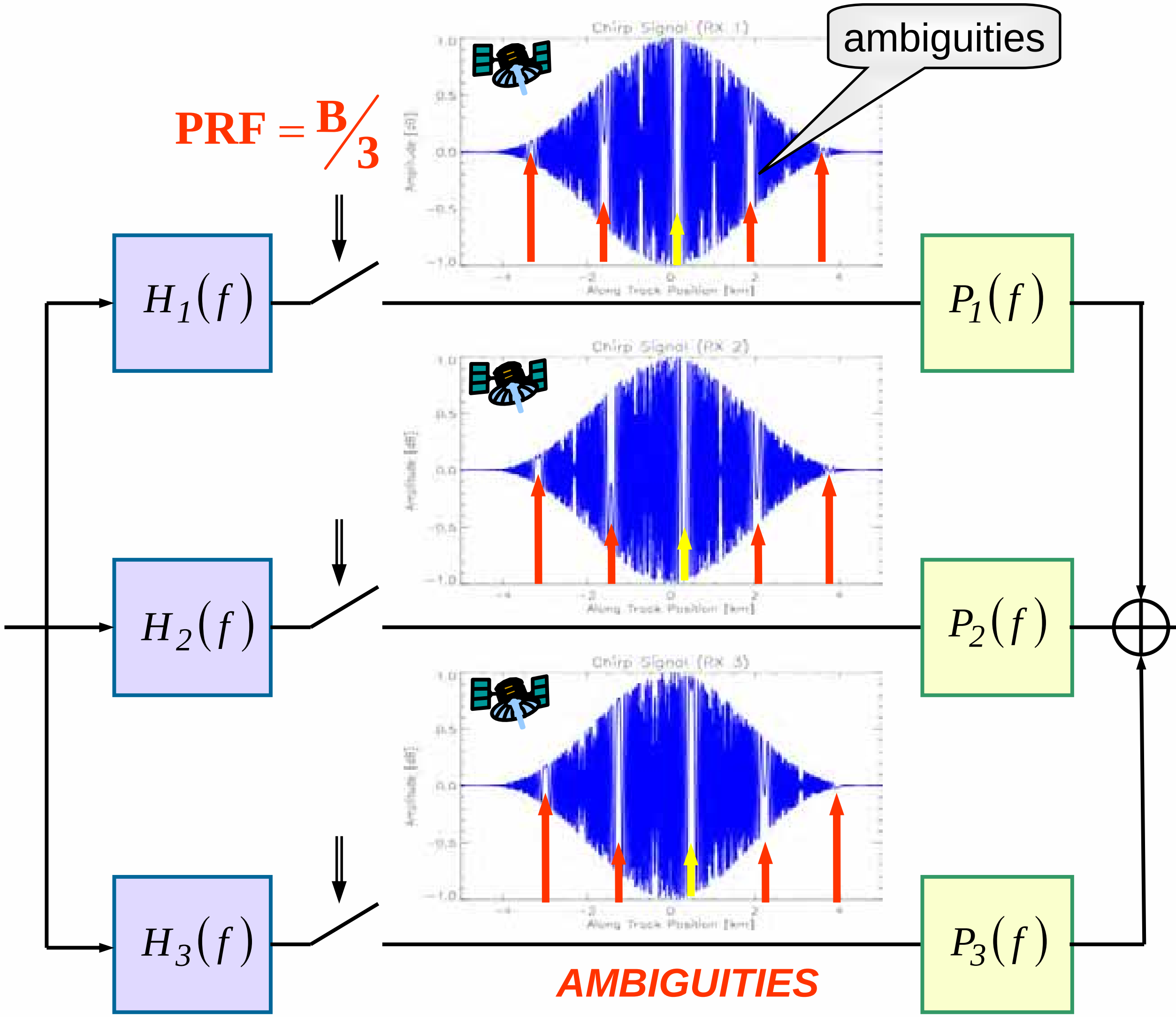

Simulation Parameters	
PRF	1167 Hz
Antenna Length (Tx)	4.8 m
Antenna Length (Rx)	4.8 m
Displacement (Rx1)	300.0 m
Displacement (Rx2)	614.0 m
Displacement (Rx3)	934.1 m
Processed Bandwidth	2600 Hz
Wavelength (X-Band)	3.1 cm
Antenna Pointing	±0.0°

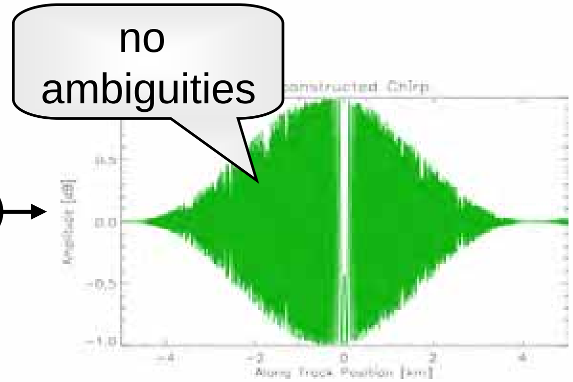

SIGNAL RECONSTRUCTION (SUPPRESESSED AMBIGUITIES)

Sparse Array Reconstruction: Focused Data

Simulation Parameters	
PRF	1167 Hz
Antenna Length (Tx)	4.8 m
Antenna Length (Rx)	4.8 m
Displacement (Rx1)	300.0 m
Displacement (Rx2)	614.0 m
Displacement (Rx3)	934.1 m
Processed Bandwidth	2600 Hz
Wavelength (X-Band)	3.1 cm
Antenna Pointing	±0.0°

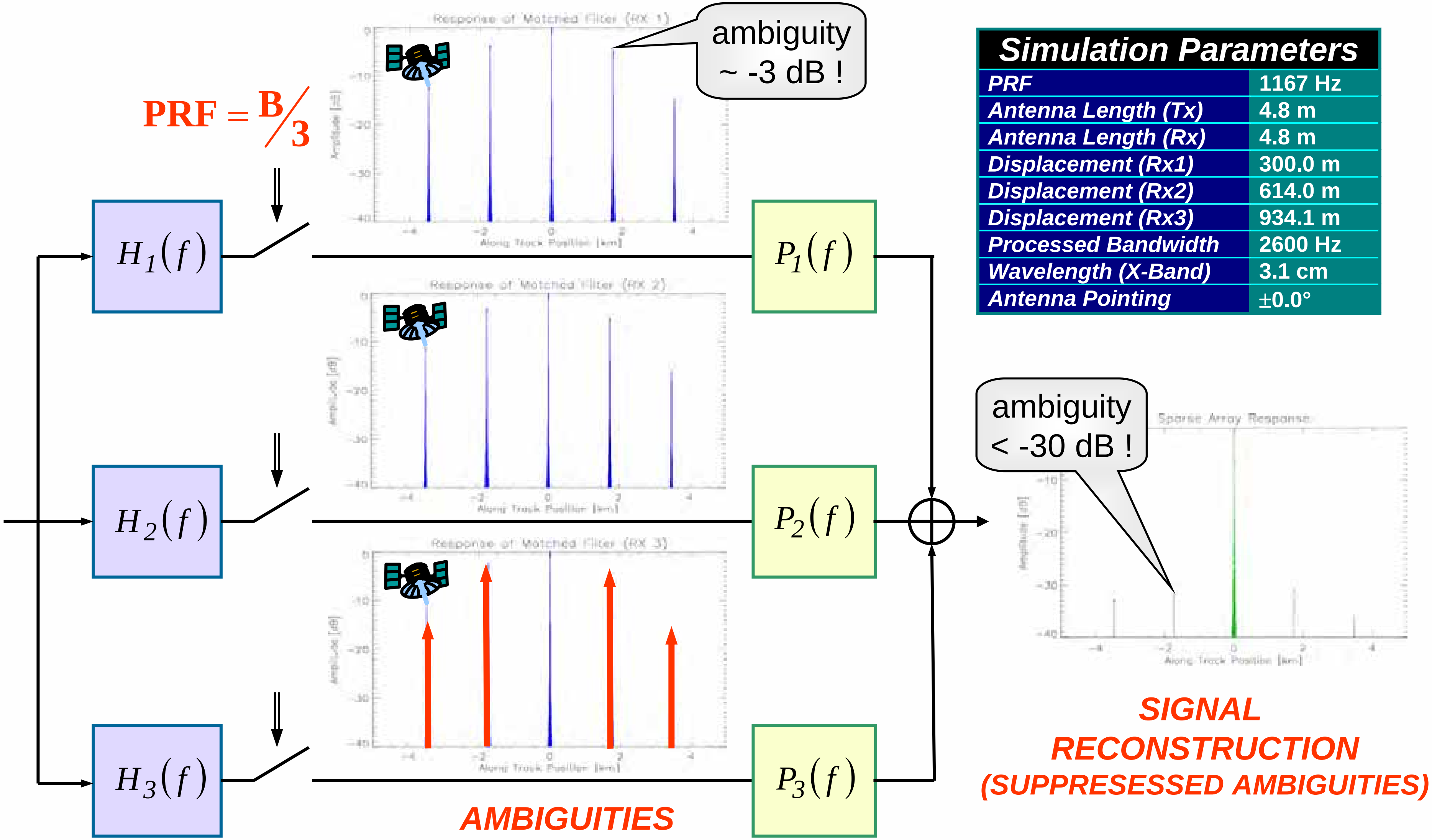

Sparse Array Reconstruction: Nonuniform Distance + Noise

Raw Data
(Point Target)

Processed Signal
(Matched Filter)

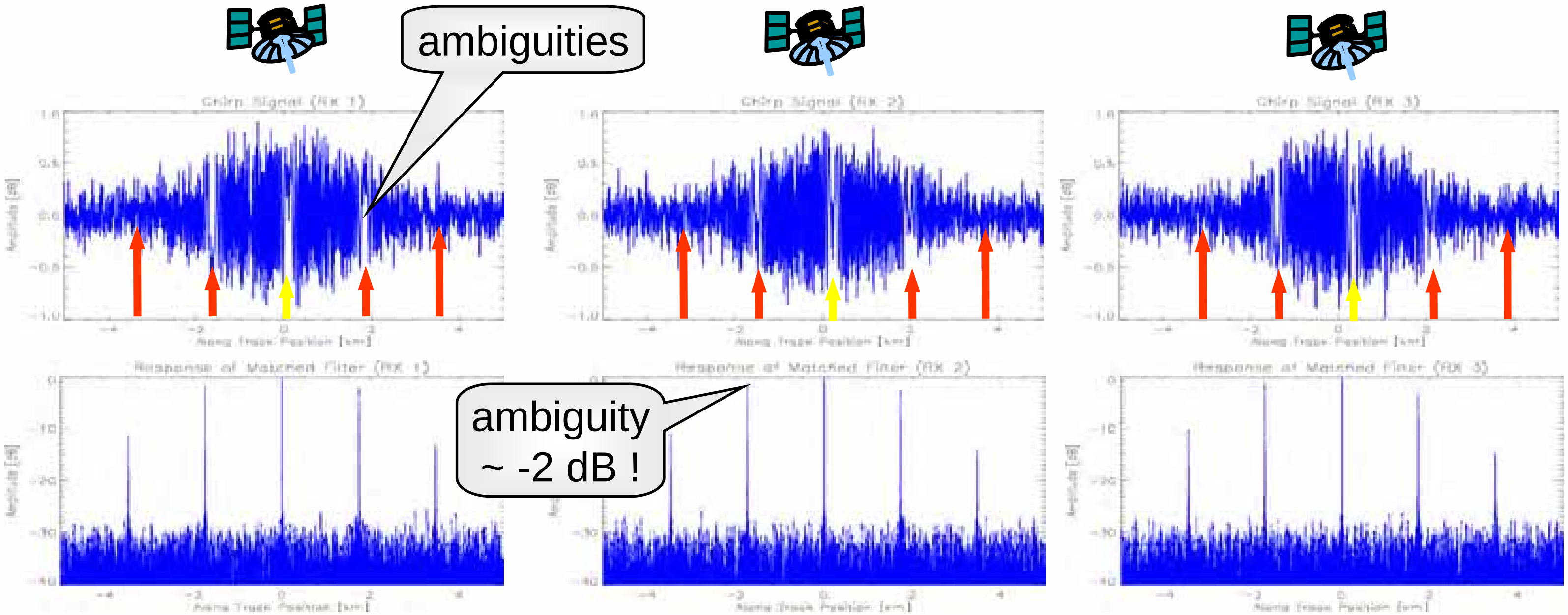

Sparse Array Processing

Signal Reconstruction & SAR Processing

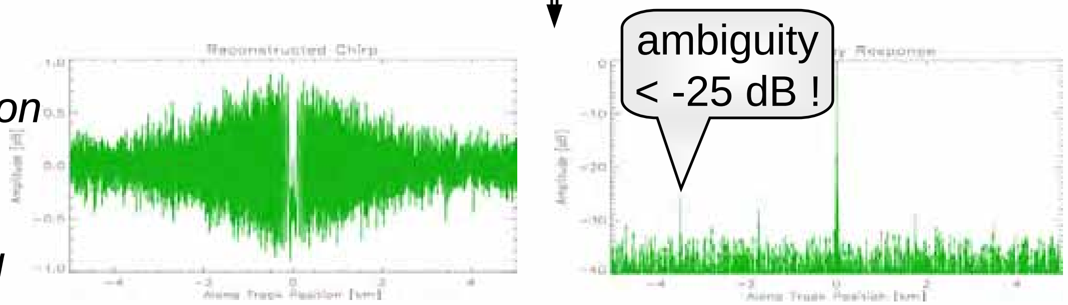

Simulation Parameters	
PRF	1167 Hz
Antenna Length (Tx)	4.8 m
Antenna Length (Rx)	4.8 m
Displacement (Rx1)	300.0 m + 1.7 m
Displacement (Rx2)	617.0 m + 0.4 m
Displacement (Rx3)	934.1 m + 1.3 m
Processed Bandwidth	2600 Hz
Wavelength (X-Band)	3.1 cm
Antenna Pointing	±0.01°
SNR	- 5 dB

Microwaves and Radar Institute
gerhard.krieger@dlr.de

Superresolution with Multistatic Satellite Arrays

Increased geometric resolution of SAR images by:

- along-track displacement of receiving satellites :
  - ⇒ different Doppler centroids
  - ⇒ super-resolution in azimuth by coherent combination of shifted Doppler spectra
- across-track displacement of receiving satellites:
  - ⇒ different incident angles
  - ⇒ super-resolution in range by coherent combination of images with different ground range spectra

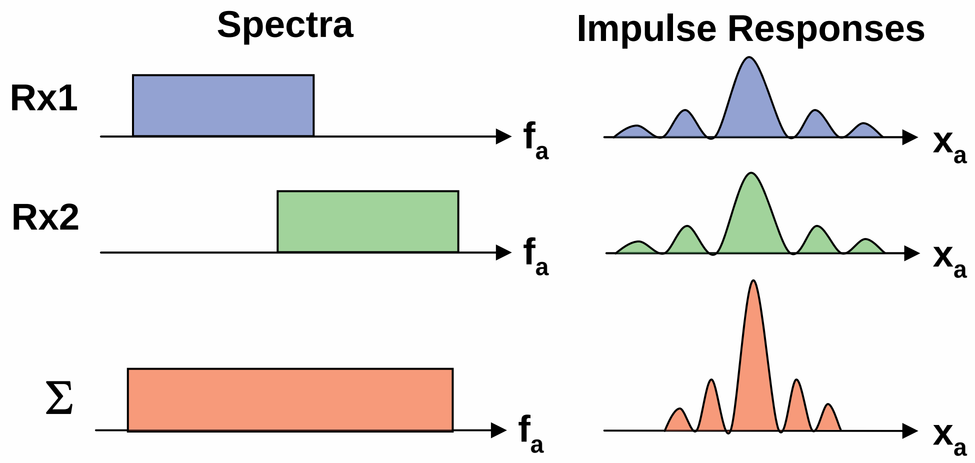

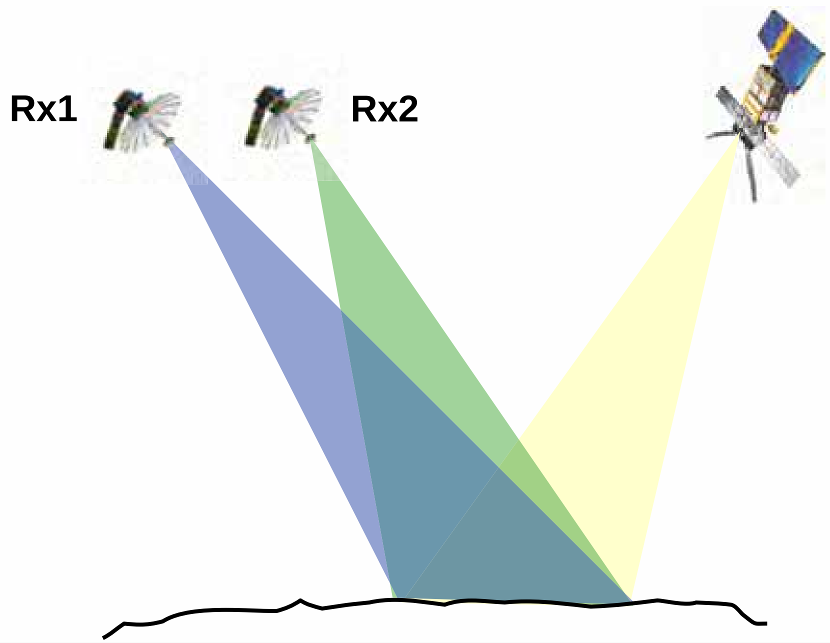

Microwaves and Radar Institute
gerhard.krieger@dlr.de

Challenges in Bistatic and Multistatic SAR Imaging

Orbit Control & Relative Position Sensing

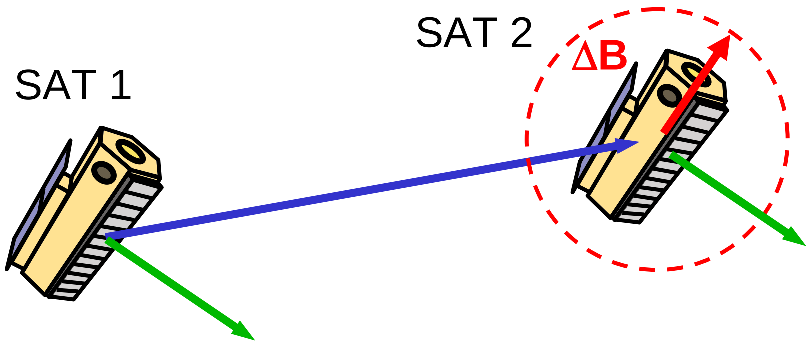

Bi- and Multistatic SAR Processing

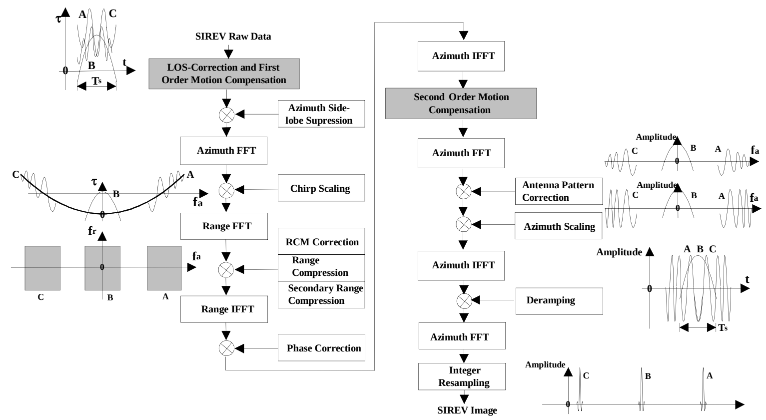

Bistatic Calibration & Antenna Co-Pointing

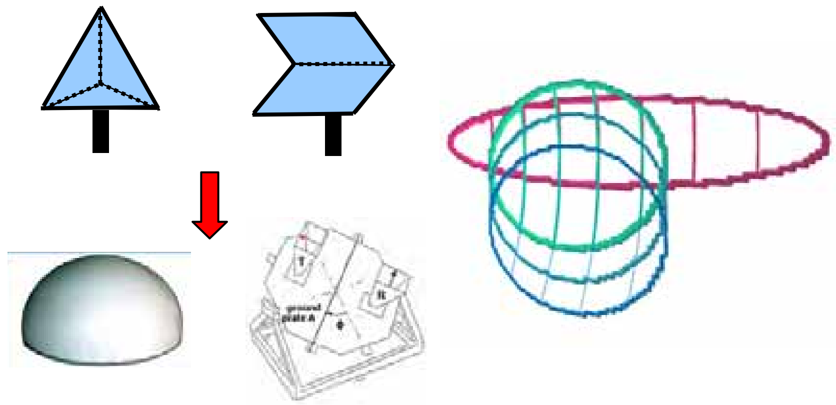

Time and Phase Synchronisation

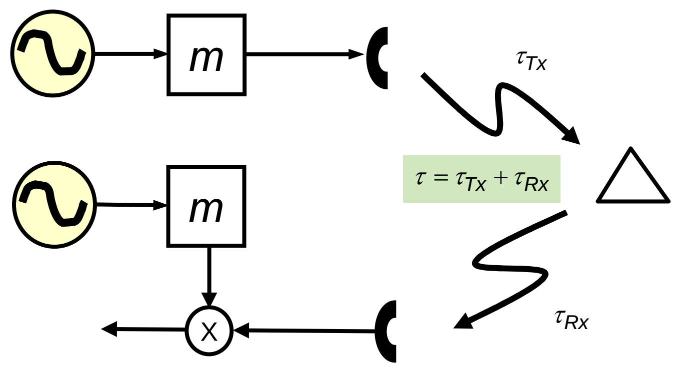

System Model for Bistatic Radar

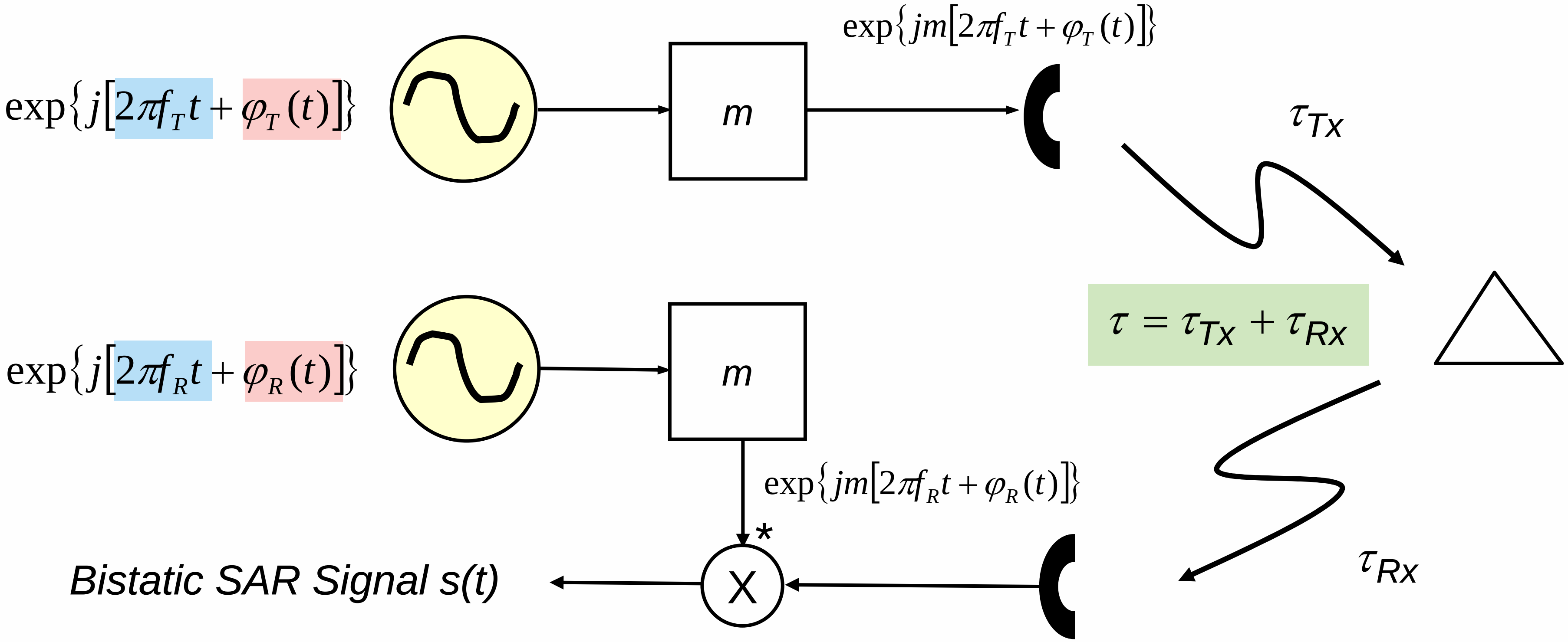

$$\mathbf{s}(t) = \exp\{jm[-2\pi f_T \tau + 2\pi(f_T - f_R)t + \varphi_T(t-\tau) - \varphi_R(t)]\}$$

Azimuth Modulation

Frequency Offset Δf

Phase Noise $\varphi(t)$

Degradation of Azimuth Impulse Response

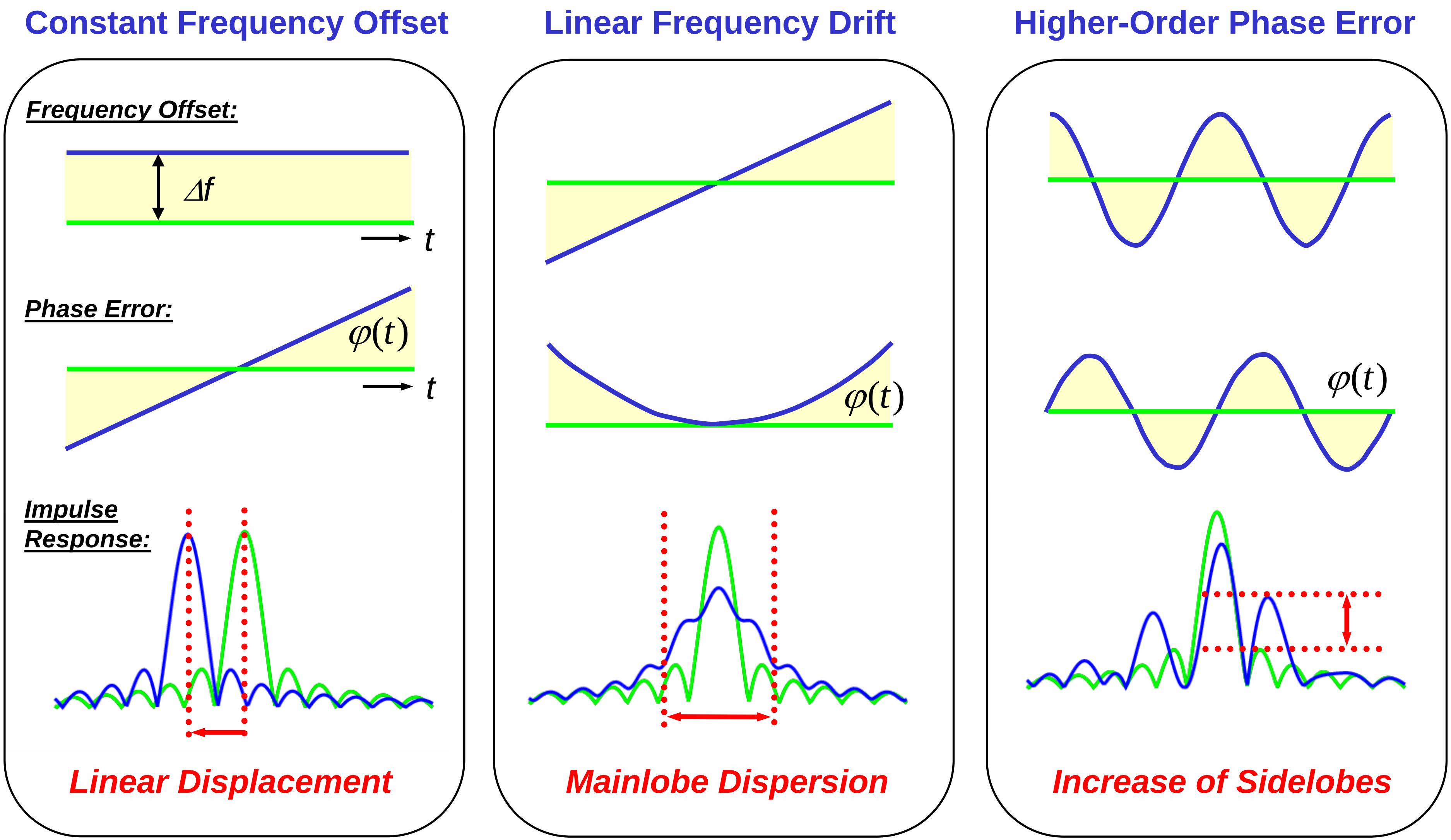

Microwaves and Radar Institute
gerhard.krieger@dlr.de

Model of Oscillator Phase Errors

- *$\varphi(t)$* is modelled by a stochastic process

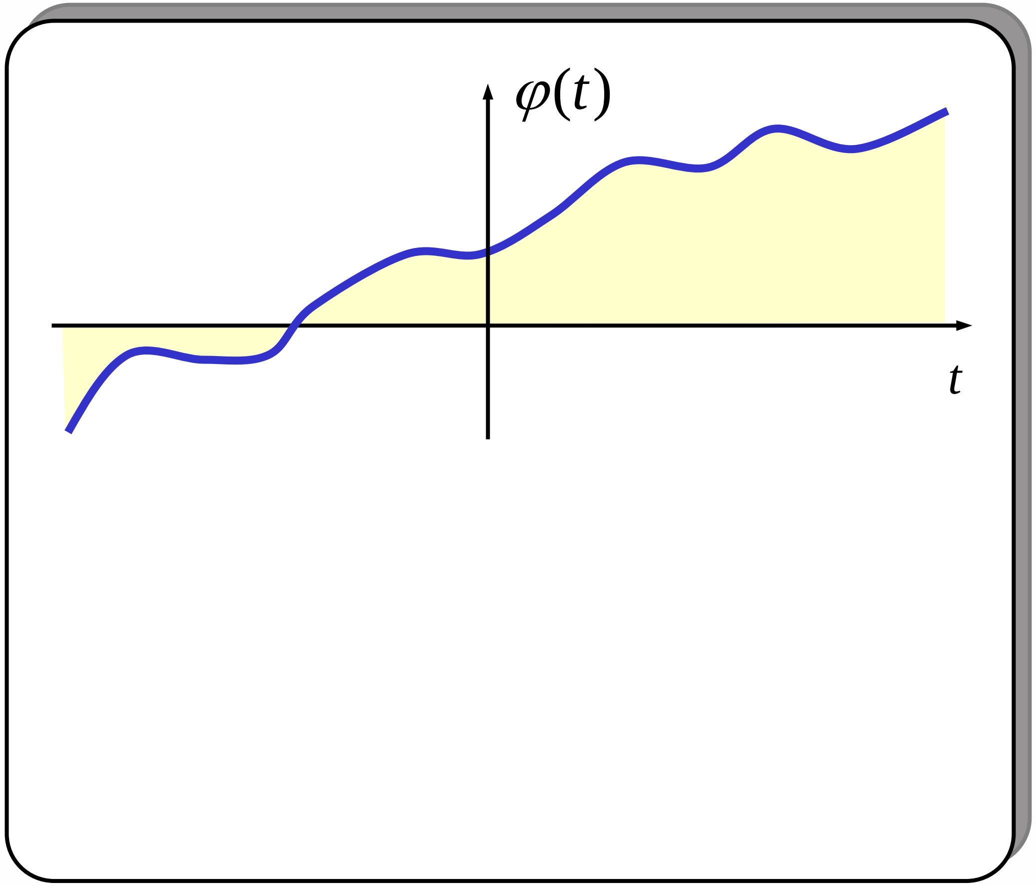

Microwaves and Radar Institute
gerhard.krieger@dlr.de

Model of Oscillator Phase Errors

- $\varphi(t)$ is modelled by a stochastic process with acf

$$R_\varphi(\tau) = \langle \varphi(t) \cdot \varphi(t+\tau) \rangle$$

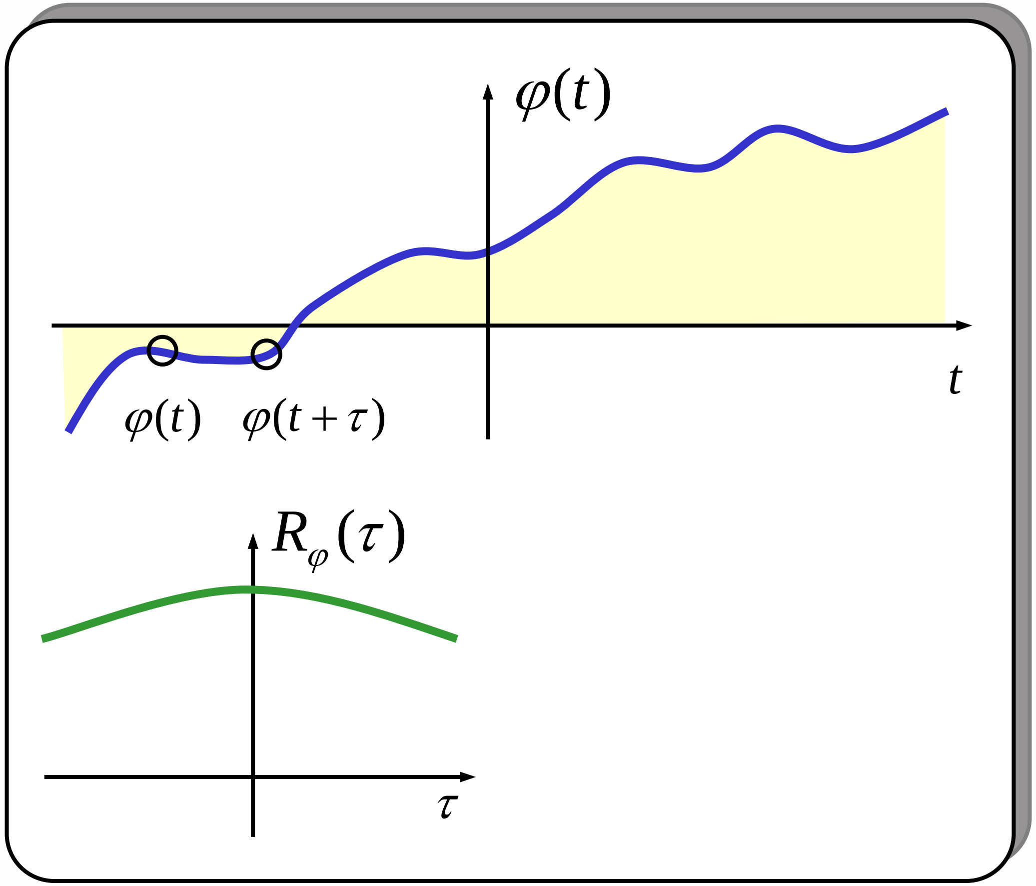

Model of Oscillator Phase Errors

- $\varphi(t)$ is modelled by a stochastic process with acf

$$R_\varphi(\tau) = \langle \varphi(t) \cdot \varphi(t+\tau) \rangle$$

- The phase spectrum

$$S_\varphi(f) \bullet\!\!-\!\!\circ\; R_\varphi(\tau)$$

describes phase fluctuations per Hertz bandwidth at Fourier frequency *f*

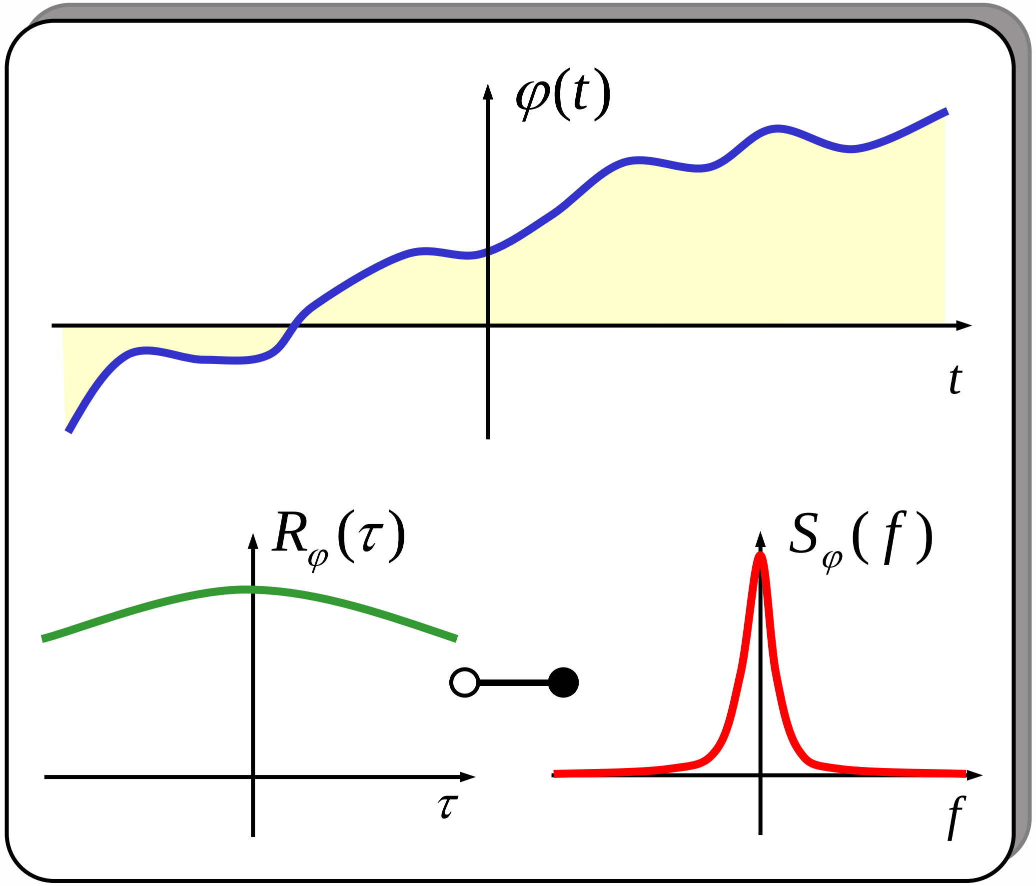

Model of Oscillator Phase Errors

- $\varphi(t)$ is modelled by a stochastic process with acf

$$\boxed{R_\varphi(\tau) = \langle\, \varphi(t)\cdot\varphi(t+\tau)\,\rangle}$$

- The phase spectrum

$$\boxed{S_\varphi(f) \bullet\!\!-\!\!\circ\; R_\varphi(\tau)}$$

describes phase fluctuations per Hertz bandwidth at Fourier frequency *f*

- $S_\varphi(f)$ is often approximated by:

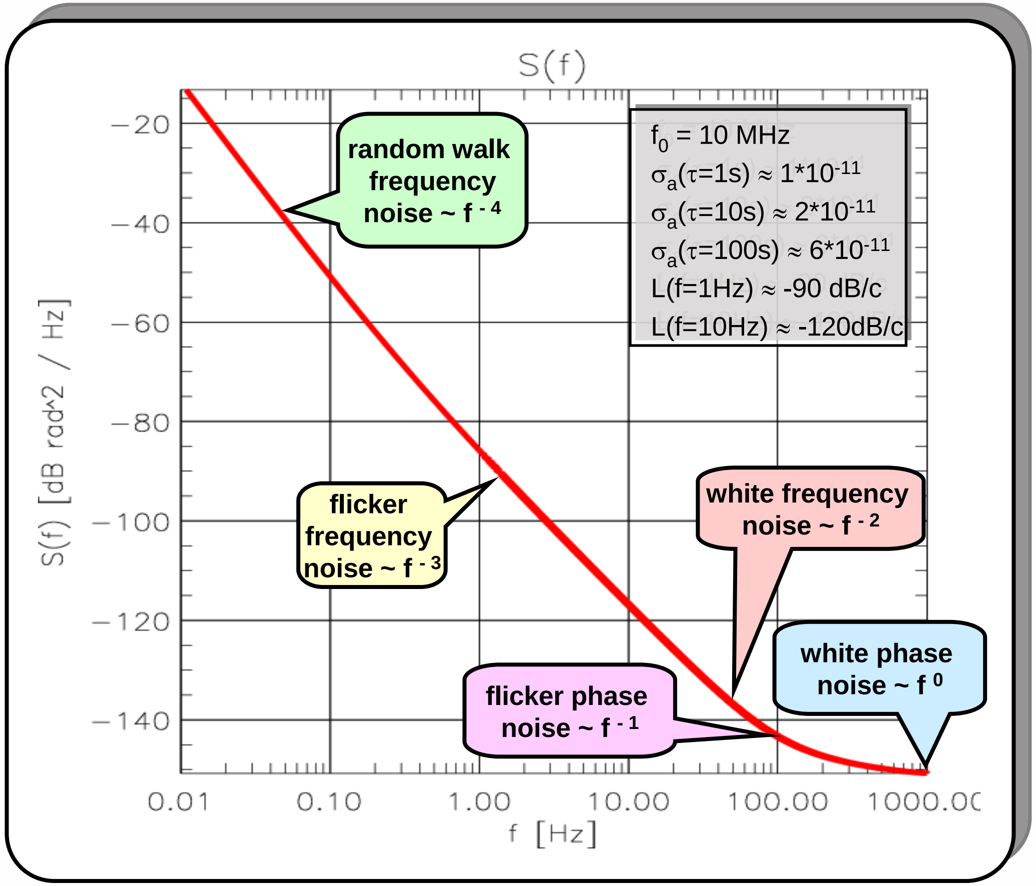

$$S_\varphi(f) = \underbrace{a\cdot f^{-4}}_{\text{random walk frequency noise}} + \underbrace{b\cdot f^{-3}}_{\text{frequency flicker noise}} + \underbrace{c\cdot f^{-2}}_{\text{white frequency noise}} + \underbrace{d\cdot f^{-1}}_{\text{flicker phase noise}} + \underbrace{e\cdot f^{0}}_{\text{white phase noise}}$$

Microwaves and Radar Institute
gerhard.krieger@dlr.de

Typical Realisations from $R_\varphi(\tau)$ $\circ\!\!-\!\!\bullet$ $S_\varphi(f)$

Realisations with φ(t=0) = 0°

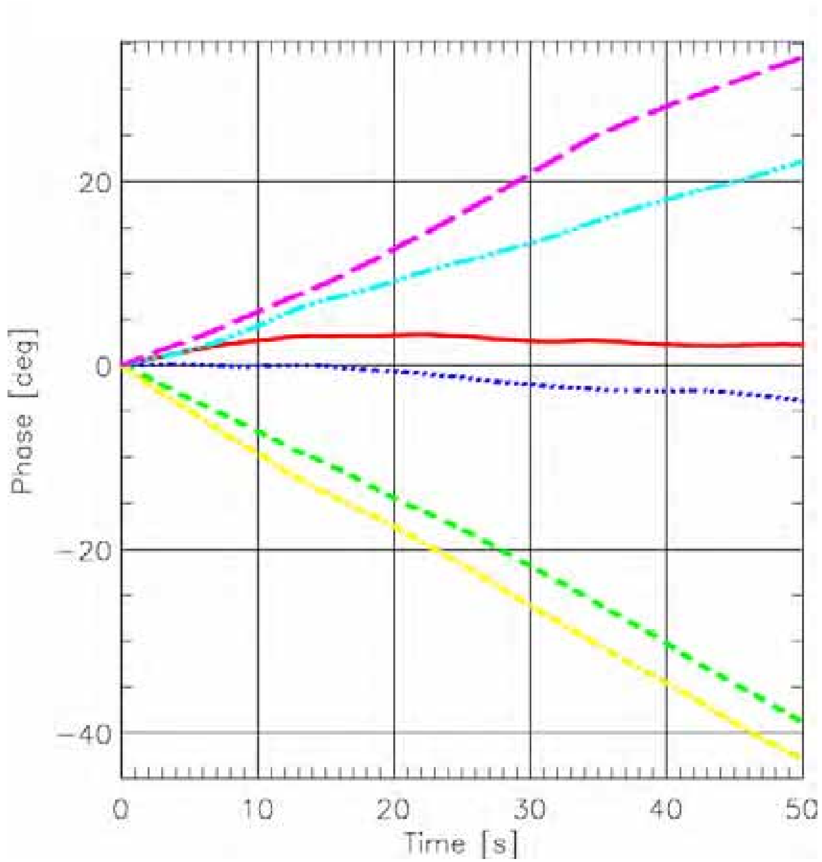

Constant phase ramp removed

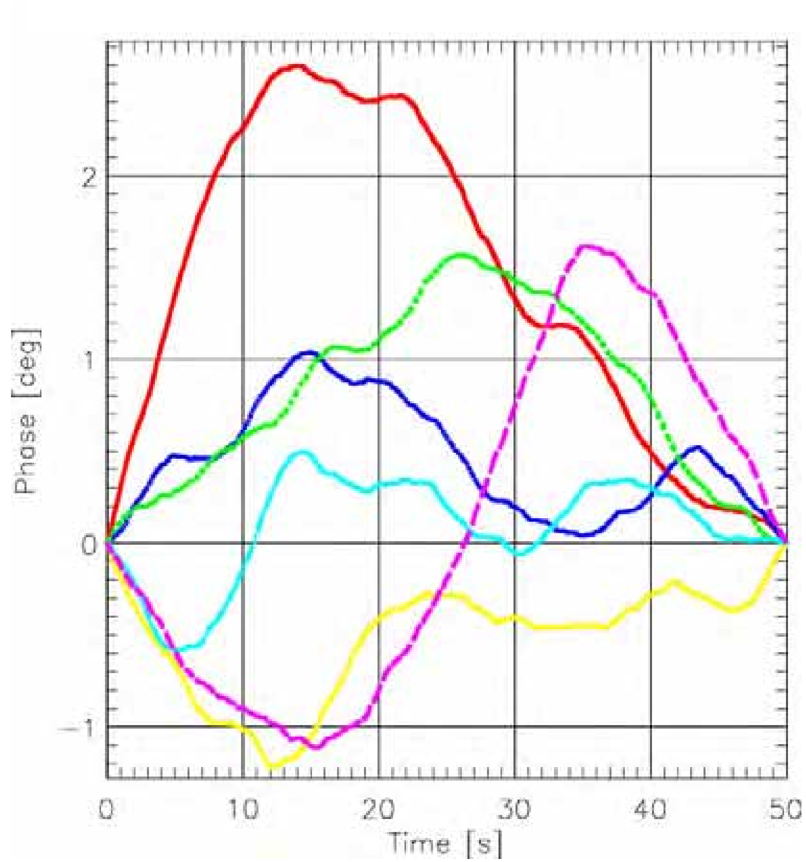

Microwaves and Radar Institute
gerhard.krieger@dlr.de

Bistatic SAR Response: Simulation Example

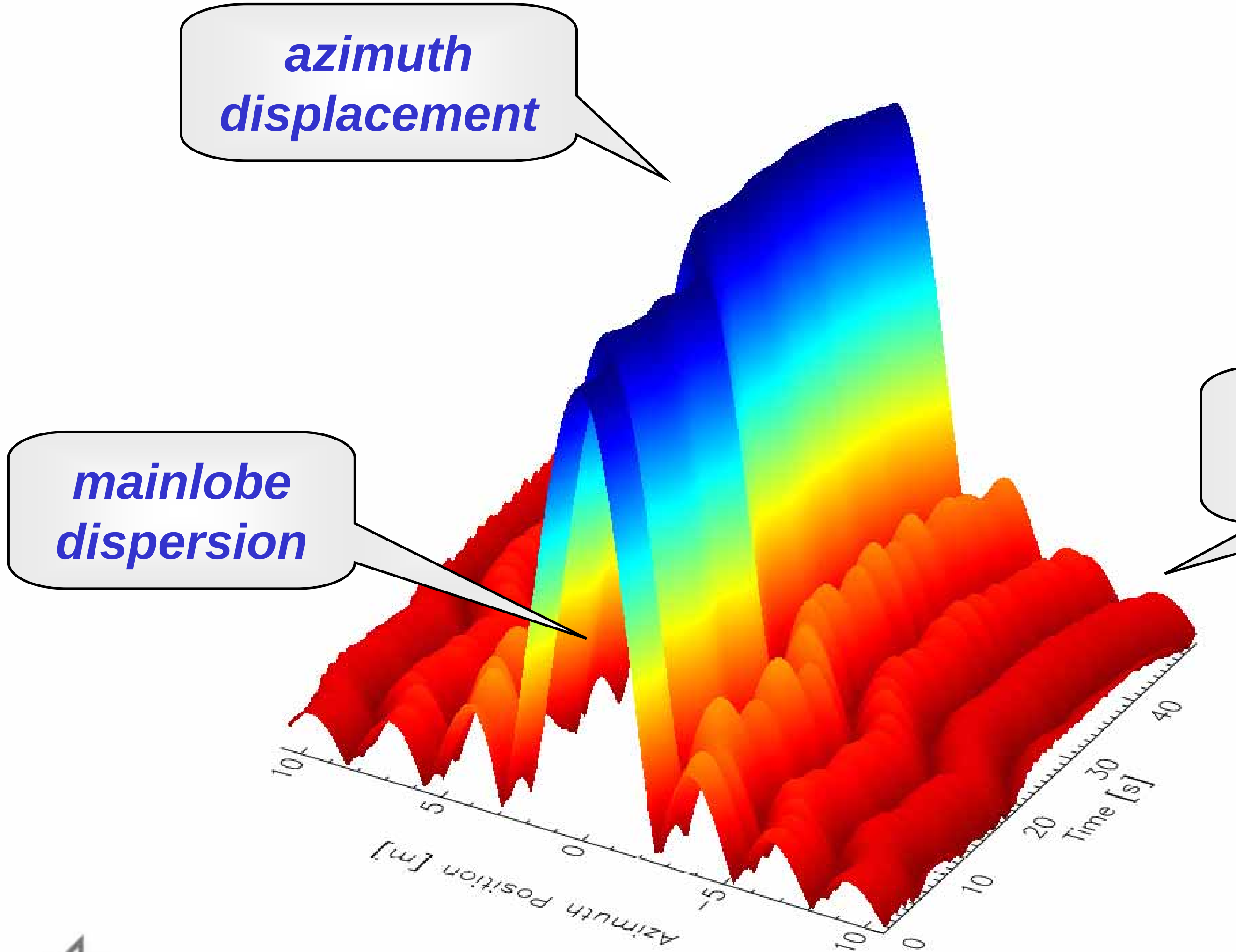

λ = 0.24 m
T_{az} = 4 sec
r_0 = 800 km
v = 7 km/s

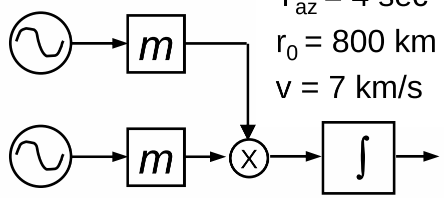

Microwaves and Radar Institute
gerhard.krieger@dlr.de

Bistatic SAR Response: Simulation Example

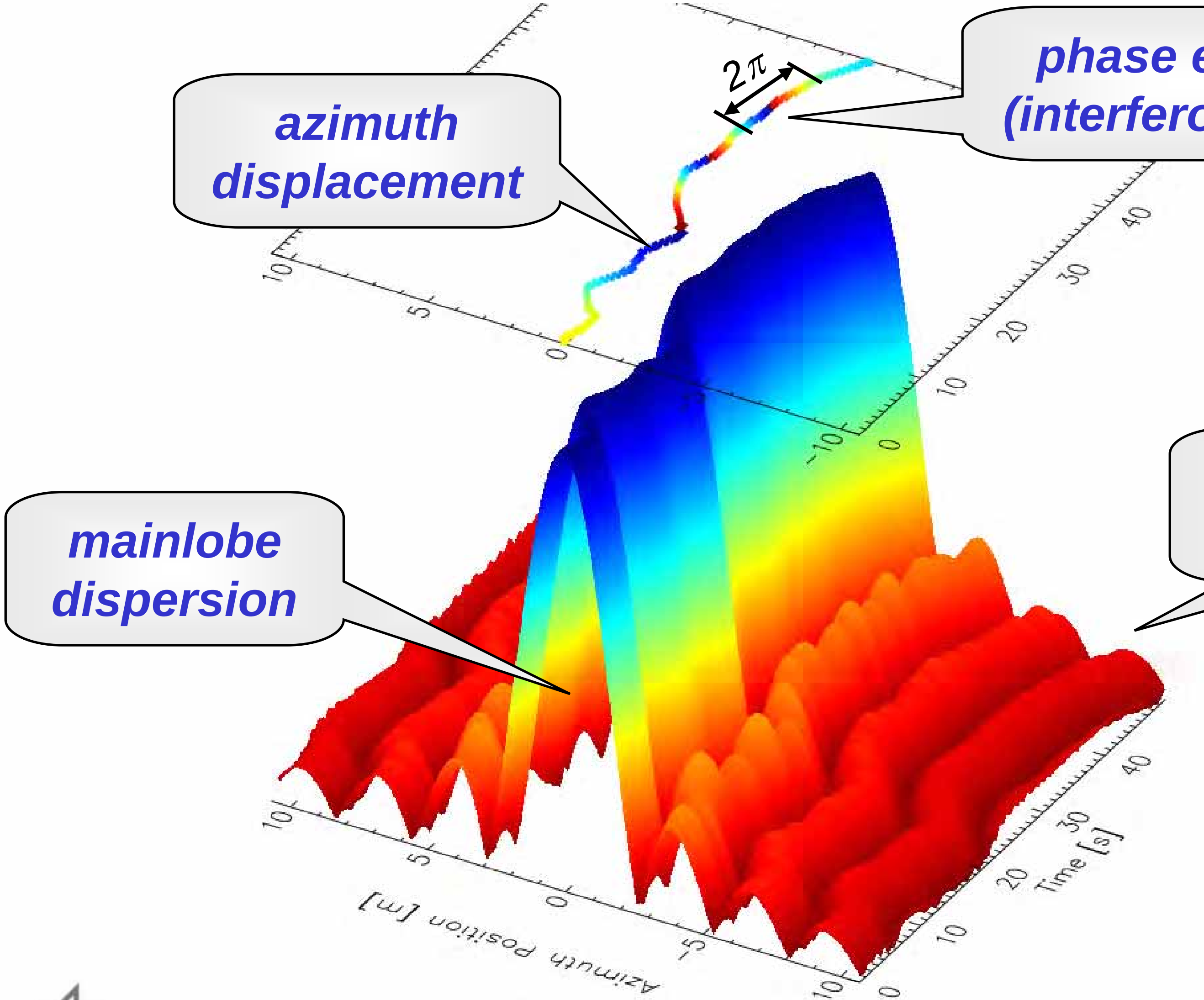

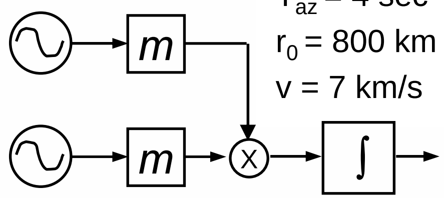

$\lambda = 0.24$ m

$T_{az} = 4$ sec

$r_0 = 800$ km

$v = 7$ km/s

Microwaves and Radar Institute
gerhard.krieger@dlr.de

Integrated Side-Lobe Ratio (ISLR)

Definition:

$$ISLR = \frac{\text{Signal Energy in Mainlobe}}{\text{Integrated Signal Energy in Sidelobes}}$$

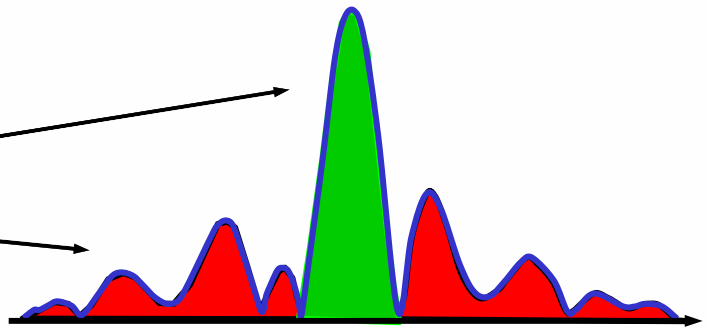

Derivation from Phase Spectrum $S_\varphi(f)$:

$$ISLR \approx 2 \cdot \left(\frac{f_0}{f_{osc}}\right)^2 \cdot \int_{1/T_a}^{\infty} S_\varphi(f) \cdot df$$

(for $\sigma_{\varphi,HF} << 1 rad$)

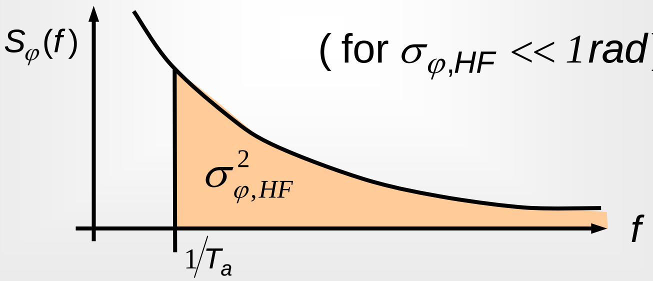

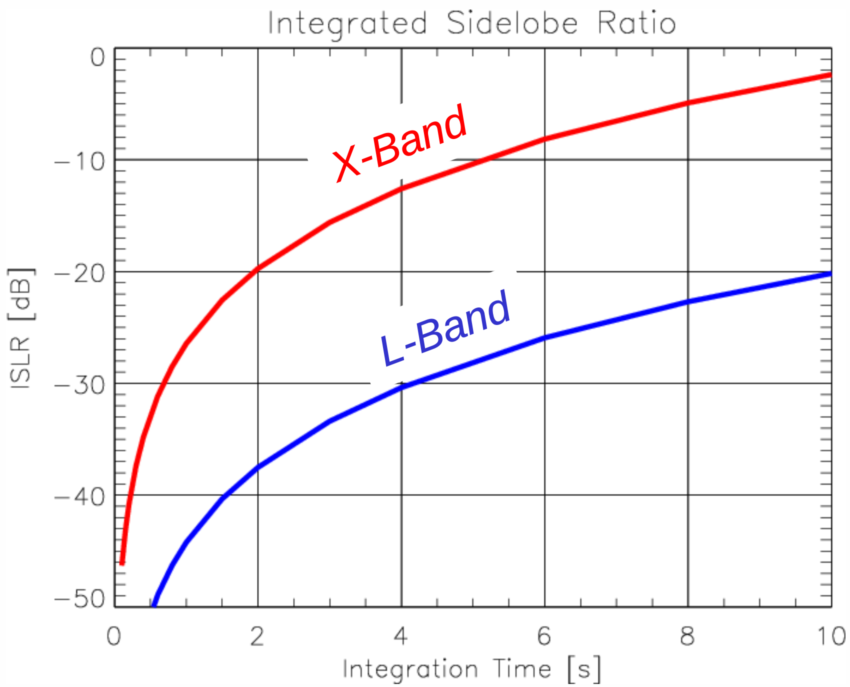

Microwaves and Radar Institute
gerhard.krieger@dlr.de

Mainlobe Dispersion

- mainlobe dispersion is mainly due to quadratic phase errors
- typical requirement: $\varphi_Q < 45°$ (~ 3 % dispersion)
- quadratic phase errors may be derived from second derivative of phase

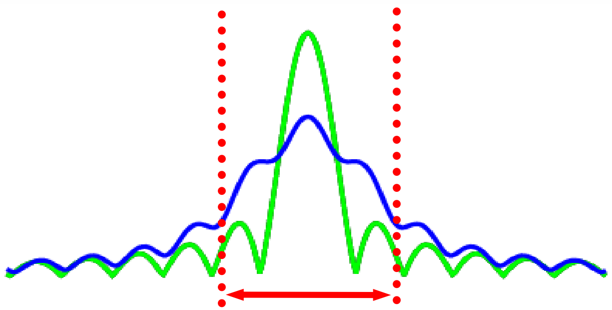

Quadratic Phase Errors:

$$\sigma_Q^2 = 2 \cdot \left(\frac{f_0}{f_{osc}} \right)^2 \cdot \frac{(\pi T_a)^4}{4} \cdot \int_0^{1/T_a} f^4 \cdot S_\varphi(f) \cdot df$$

Mainlobe Dispersion:

$$\frac{\Delta az_{bistat}}{\Delta az_{ideal}} \approx \sqrt{1 + \left(\frac{\sigma_Q}{\pi} \right)^2} \quad \text{for} \quad \varphi_Q < \pi$$

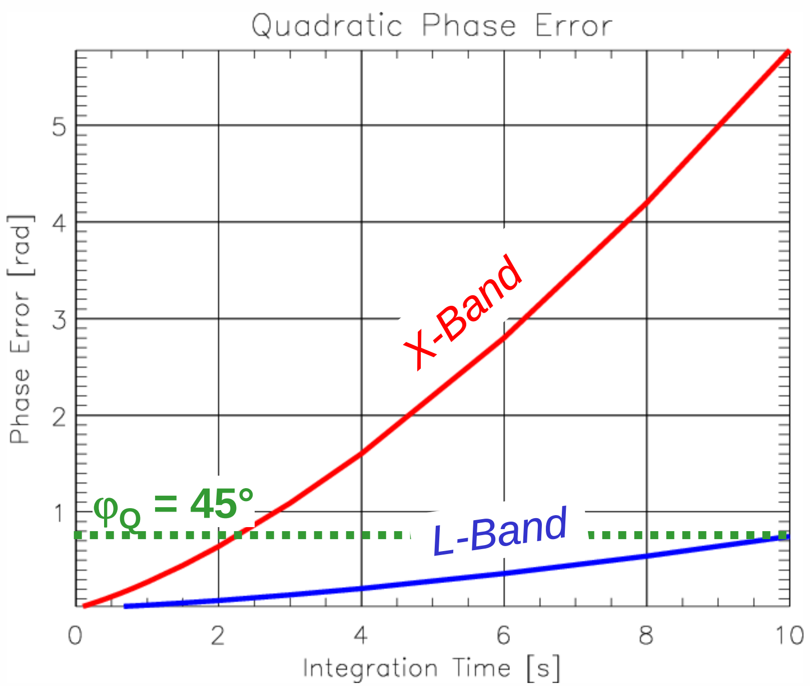

Microwaves and Radar Institute
gerhard.krieger@dlr.de

Azimuth Displacement

- small frequency offset → large azimuth displacement
- possible solutions:
    - use of ground control points
    - simultaneous mono- and bistatic data acquisition
    - relative phase referencing between Tx and Rx

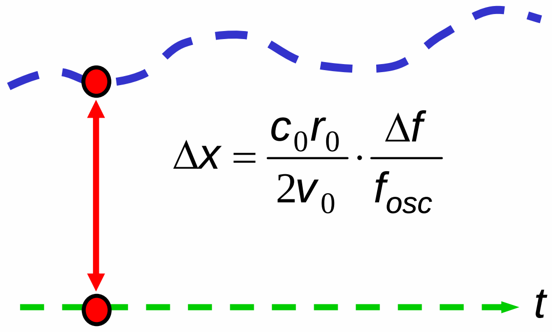

$$\Delta x = \frac{c_0 r_0}{2 v_0} \cdot \frac{\Delta f}{f_{osc}}$$

Residual Azimuth Displacement:

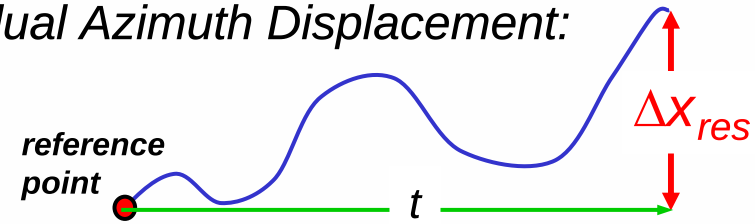

$$\sigma^2_{\Delta x\, res} = \left(\frac{c_0 r_0}{v_0}\right)^2 \cdot \int_0^\infty \frac{f^2}{f_{osc}^2} \cdot S_\varphi(f) \cdot \left[\frac{\sin(\pi T_a f)}{\pi T_a f}\right]^2 \cdot \left[1 - \left(\frac{\sin(2\pi f t)}{2\sin(\pi f t)}\right)^2\right] \cdot df$$

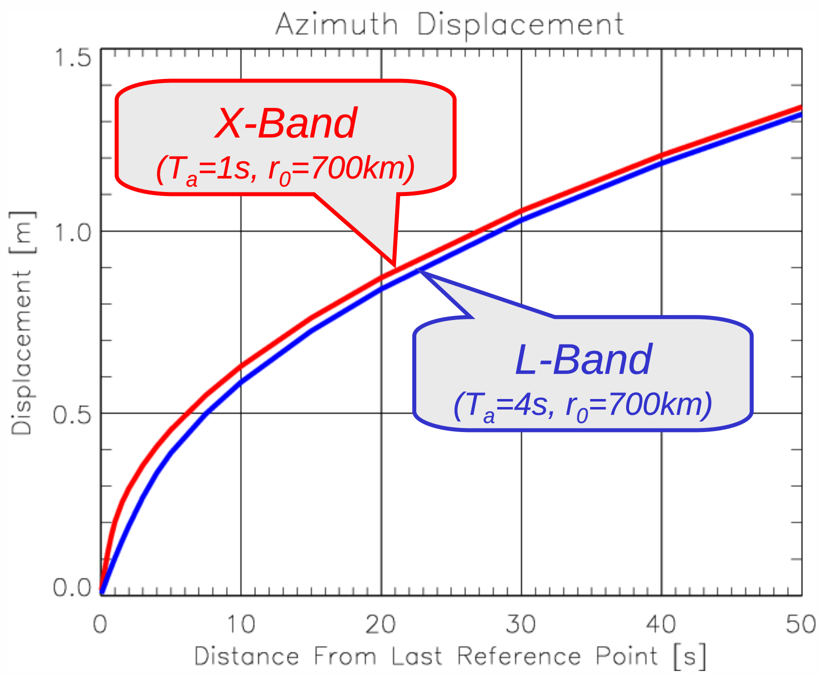

Microwaves and Radar Institute
gerhard.krieger@dlr.de

Pulse Synchronisation

LO frequency offset will lead to slightly different PRFs:

- $\rightarrow$ *range walk*
- $\rightarrow$ *shift of the receiving window*

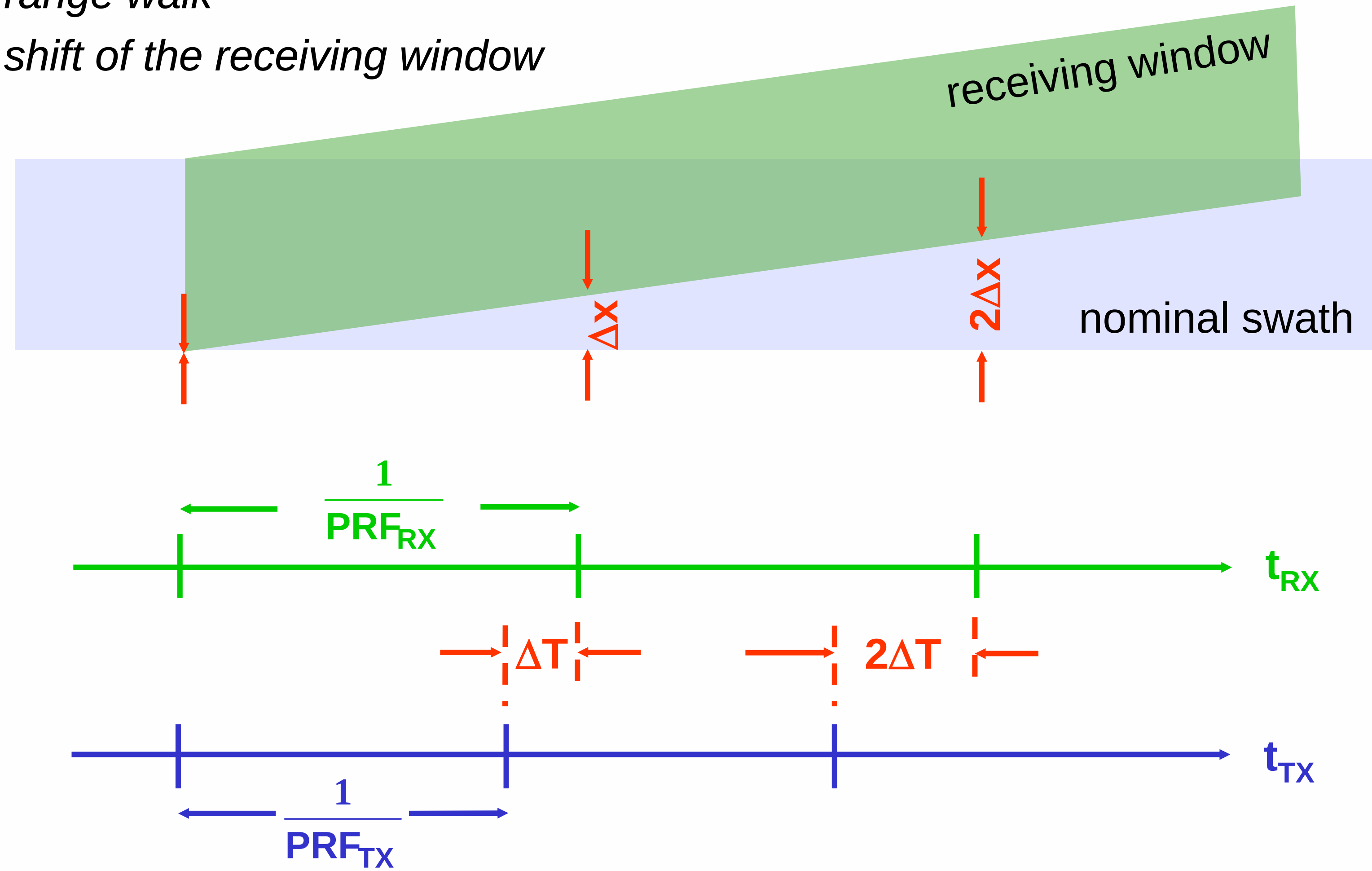

Microwaves and Radar Institute
gerhard.krieger@dlr.de

Pulse Synchronisation

Solutions to synchronization:

- *Pulse synchronization with link to common reference (e.g. GPS)*
- *Automatic detection of swath signal (e.g. by power analysis of received signal)*
- *Direct data link between transmitter and receiver*
- *Continuous recording*

Example for synchronization with GPS:

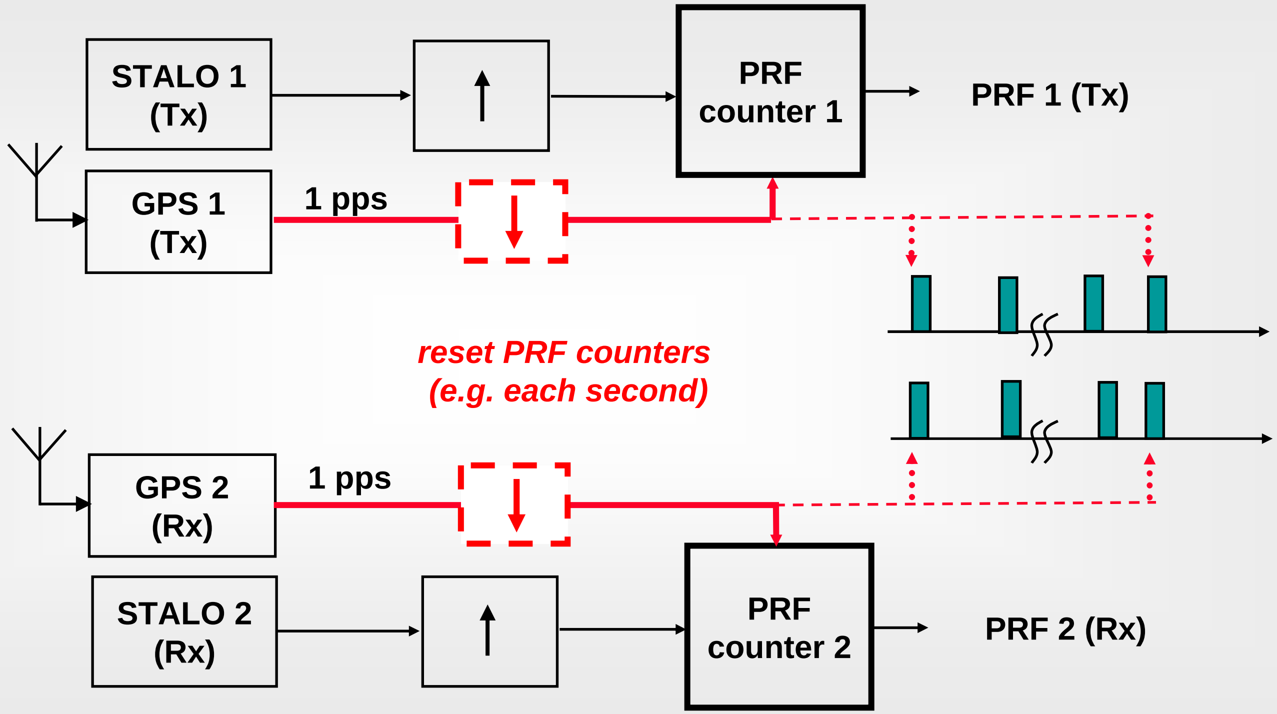

Microwaves and Radar Institute
gerhard.krieger@dlr.de

Solutions for Phase Referencing

Continuous USO Synchronisation

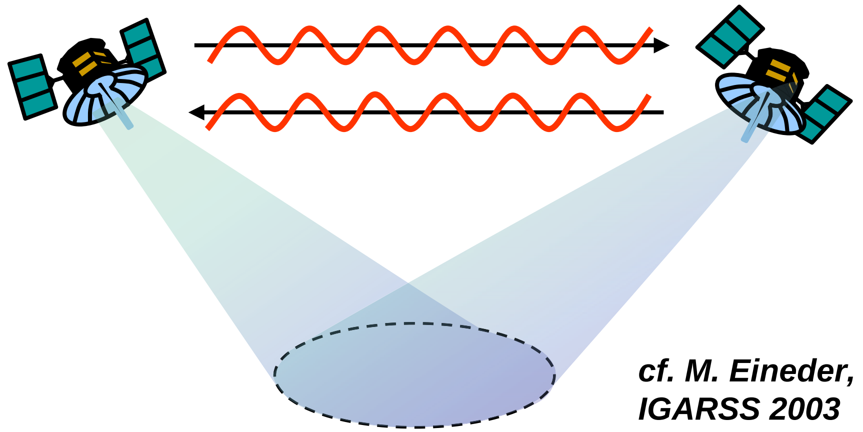

Mutual Exchange of Radar Pulses

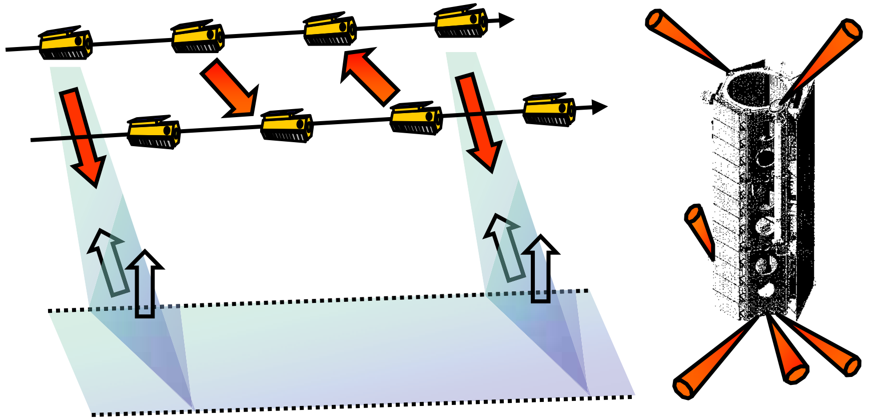

Ground Control Points + ‚Hyper-Stable' Oscillators

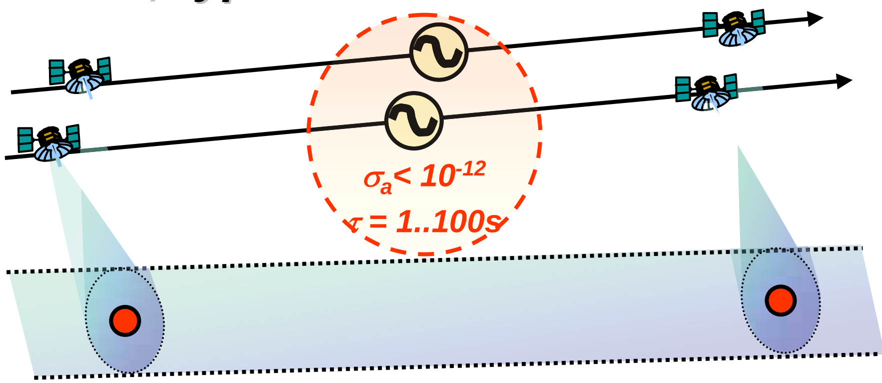

Alternating Transmit Mode

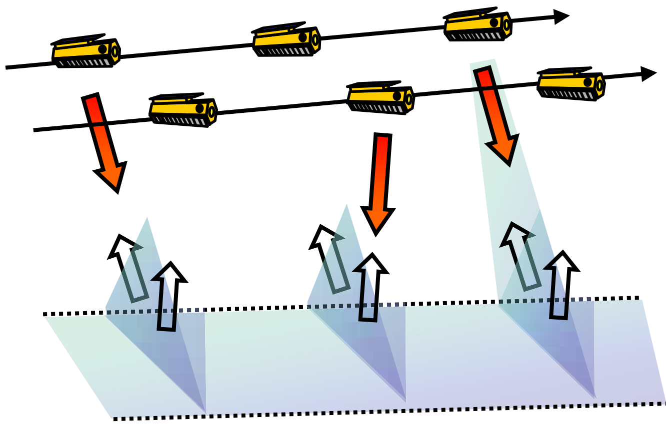

Microwaves and Radar Institute
gerhard.krieger@dlr.de

Derivation of Required Sync Frequency

Relative Phase

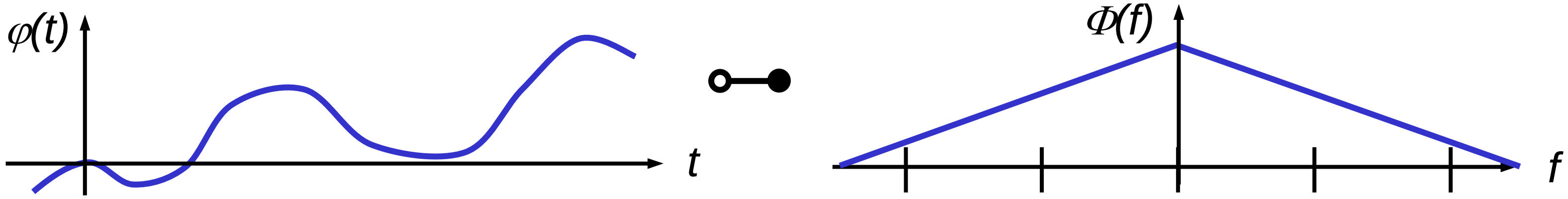

Deutsches Zentrum für Luft- und Raumfahrt e.V. in der Helmholtz-Gemeinschaft
Microwaves and Radar Institute
gerhard.krieger@dlr.de

Derivation of Required Sync Frequency

Relative Phase

Sampled Reference Signal

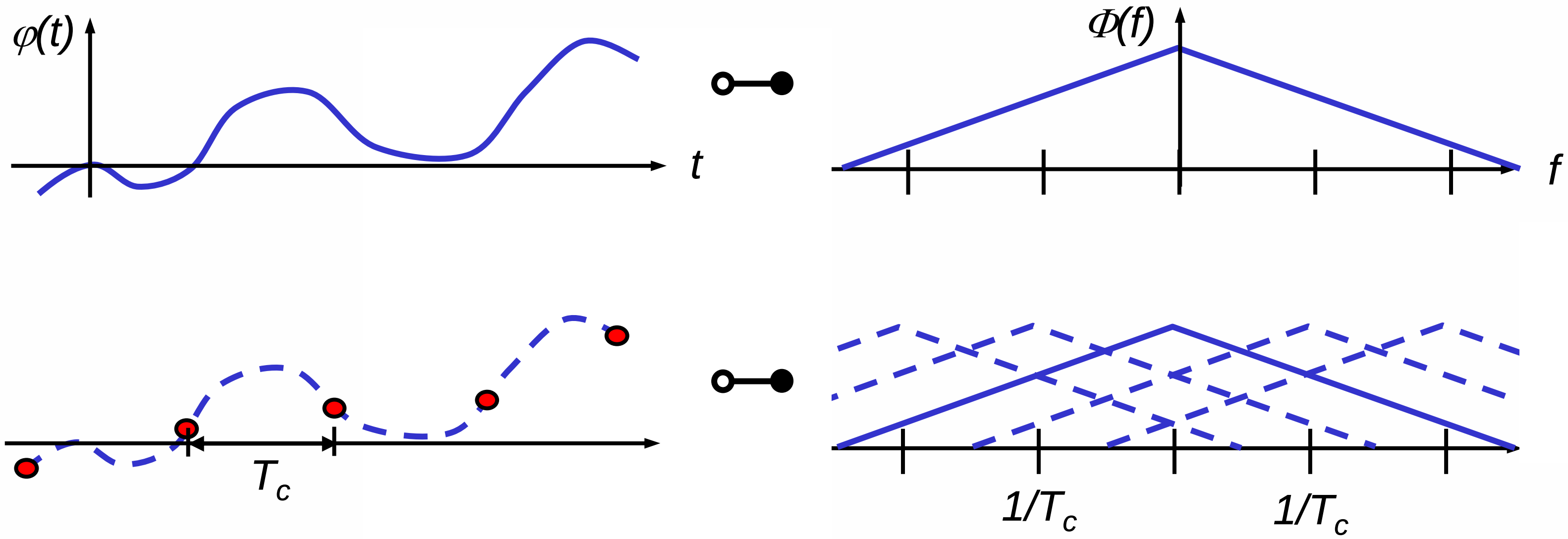

Microwaves and Radar Institute
gerhard.krieger@dlr.de

Derivation of Required Sync Frequency

Relative Phase

Sampled and Interpolated Reference Signal

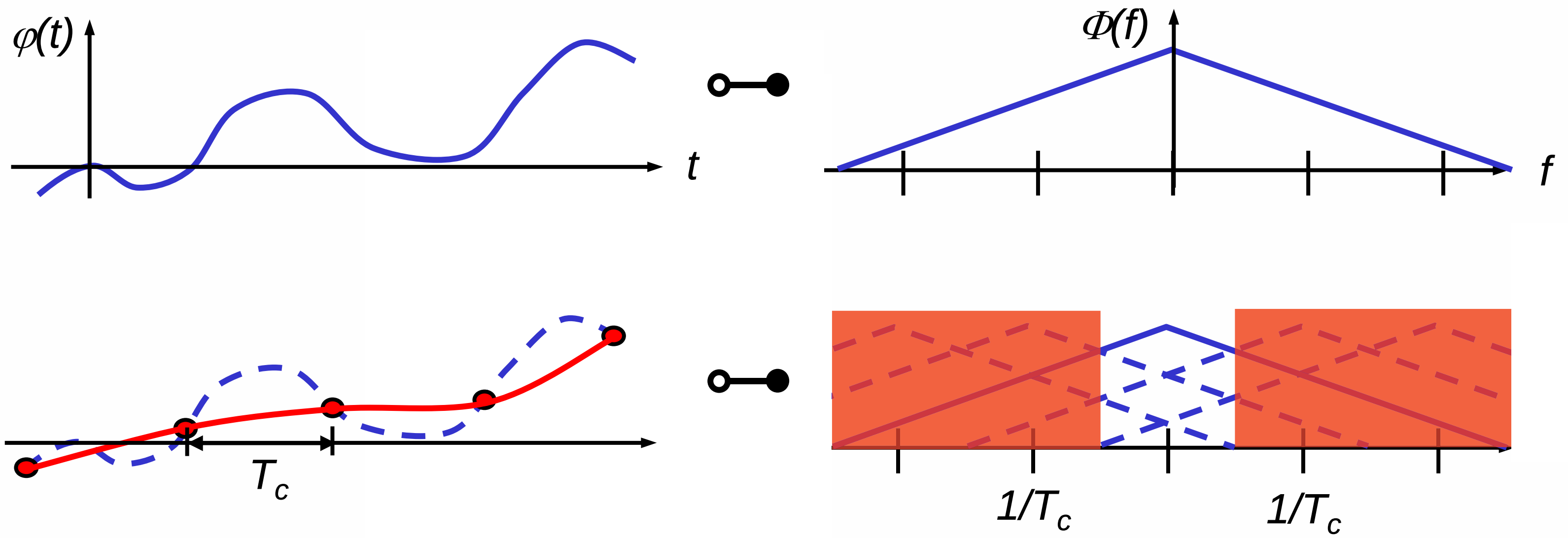

Microwaves and Radar Institute
gerhard.krieger@dlr.de

Derivation of Required Sync Frequency

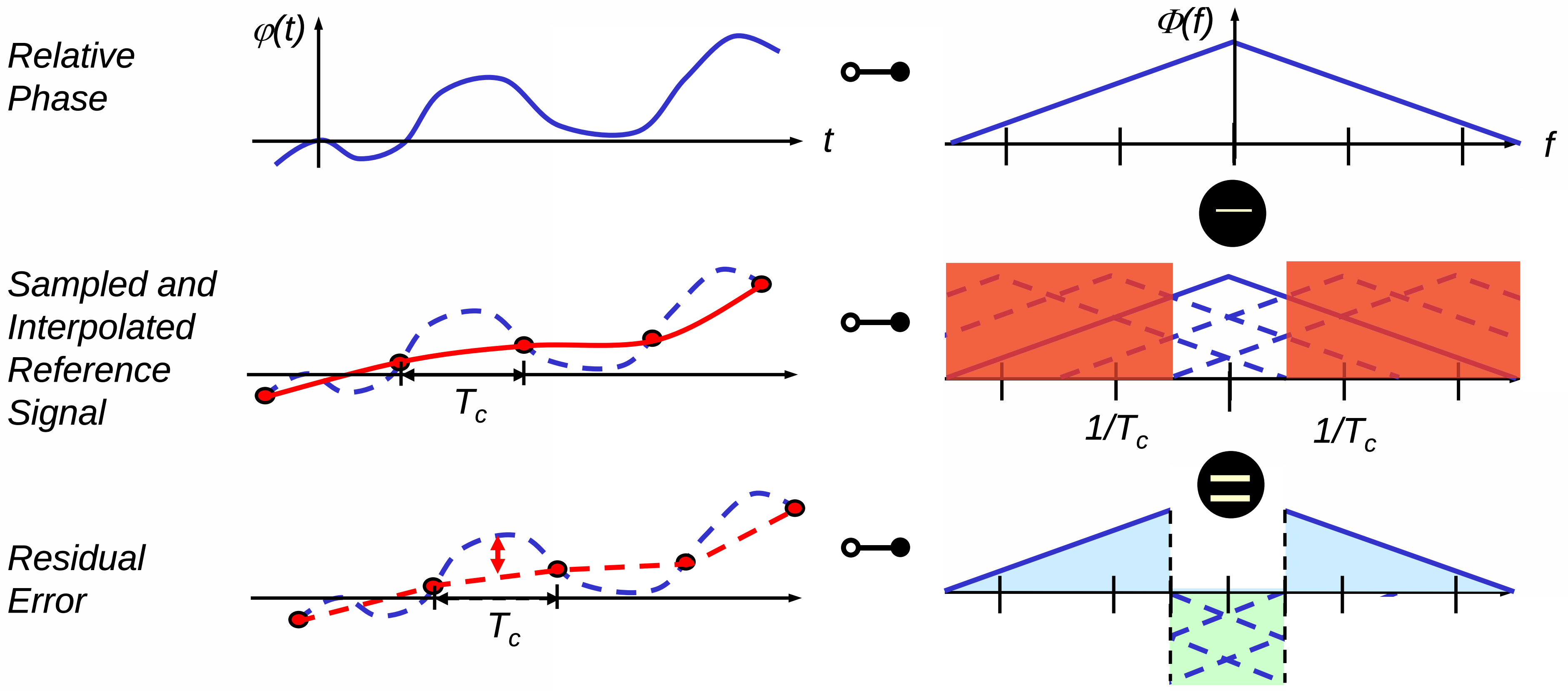

Microwaves and Radar Institute
gerhard.krieger@dlr.de

Derivation of Required Sync Frequency

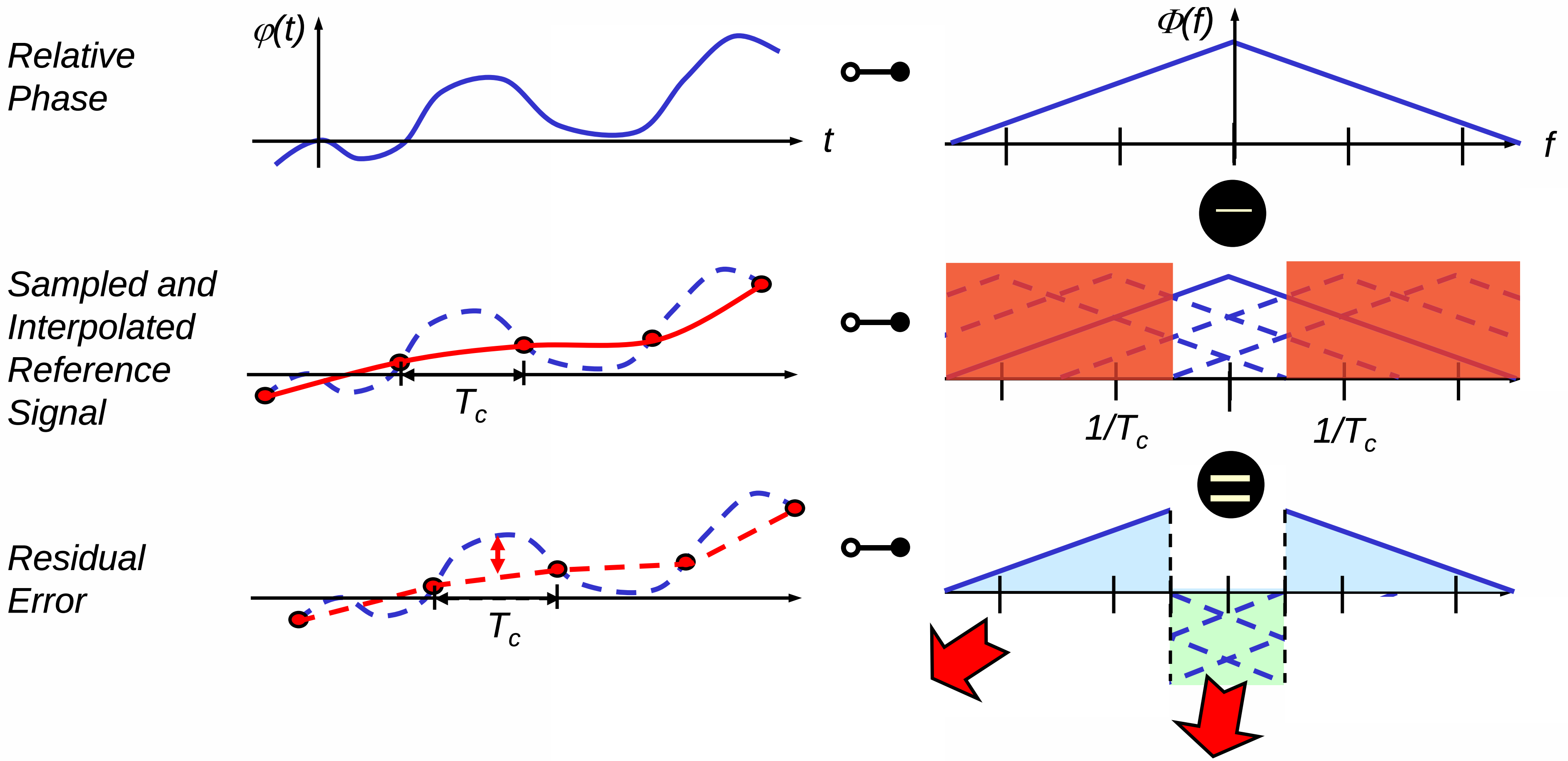

$$\sigma_{\varphi}^{2} = 2\cdot\left(\frac{f_0}{f_{osc}}\right)^2 \cdot \left[\int_{1/(2T_c)}^{\infty} S_{\varphi}(f)\cdot\left(\frac{\sin(\pi T_a f)}{\pi T_a f}\right)^2 \cdot df + \sum_{i=1}^{\infty}\int_{-1/(2T_c)}^{1/(2T_c)} S_{\varphi}\left(f+\frac{i}{T_c}\right)\cdot\left(\frac{\sin(\pi T_a f)}{\pi T_a f}\right)^2 \cdot df\right]$$

Microwaves and Radar Institute
gerhard.krieger@dlr.de

Predicted Phase Error

‚Normal USO‘

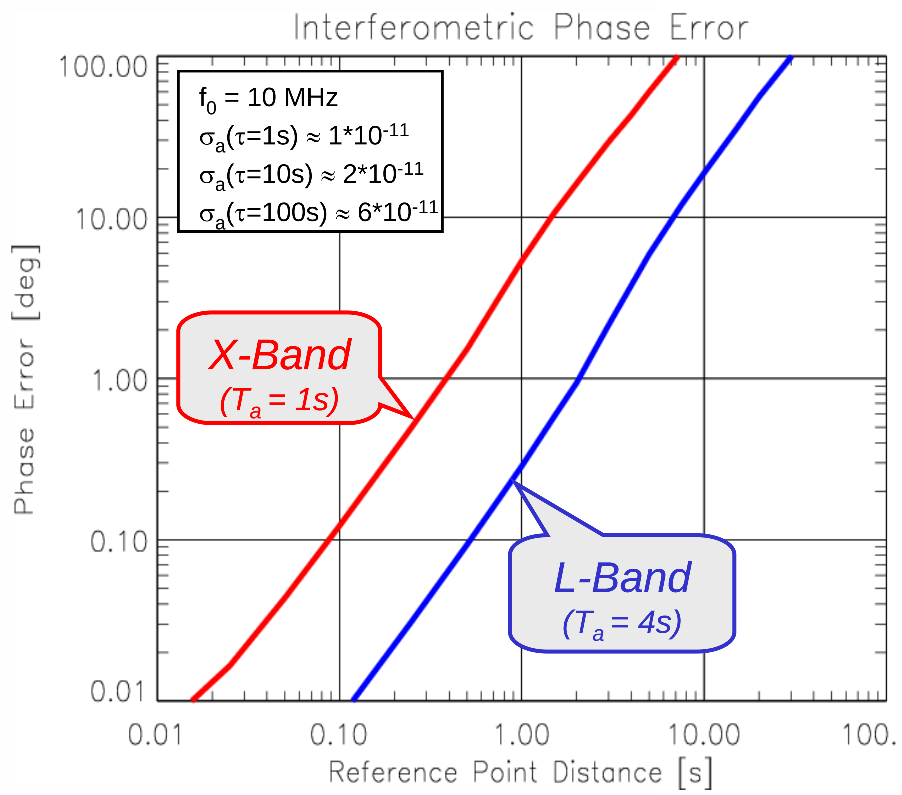

‚Hyper-Stable‘ Oscillator

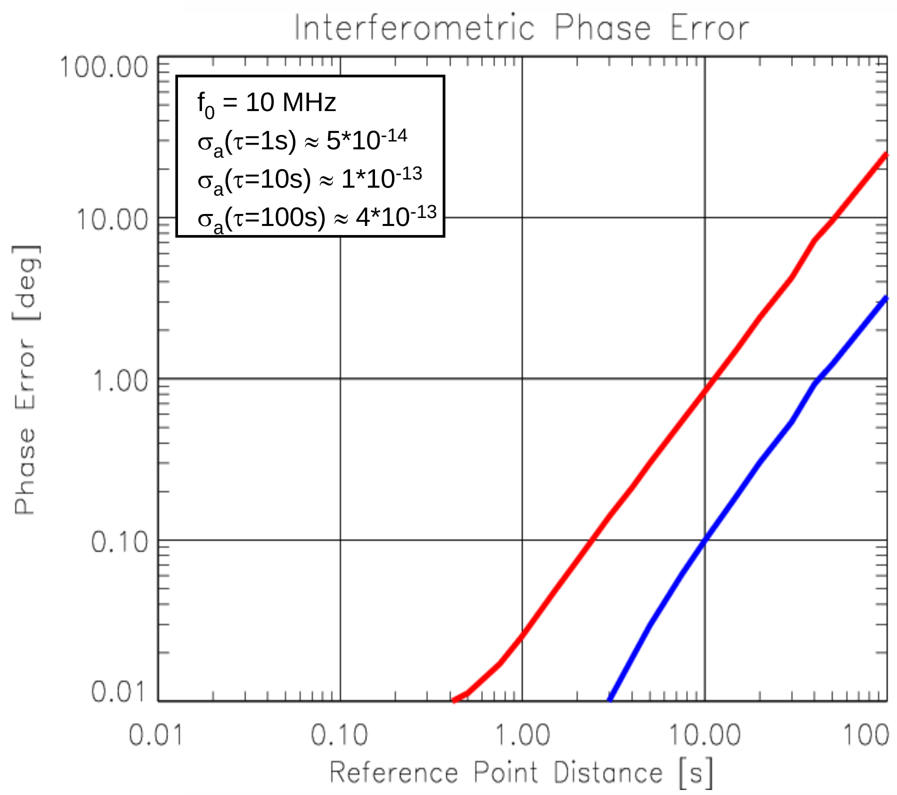

$$\sigma_\varphi^2 = 2\cdot\left(\frac{f_0}{f_{osc}}\right)^2\cdot\left[\int_{1/(2T_c)}^{\infty} S_\varphi(f)\cdot\left(\frac{\sin(\pi T_a f)}{\pi T_a f}\right)^2\cdot df + \sum_{i=1}^{\infty}\int_{-1/(2T_c)}^{1/(2T_c)} S_\varphi\left(f+\frac{i}{T_c}\right)\cdot\left(\frac{\sin(\pi T_a f)}{\pi T_a f}\right)^2\cdot df\right]$$

Predicted Phase Error

No Phase Referencing	T_C = 10 sec	T_C = 1 sec

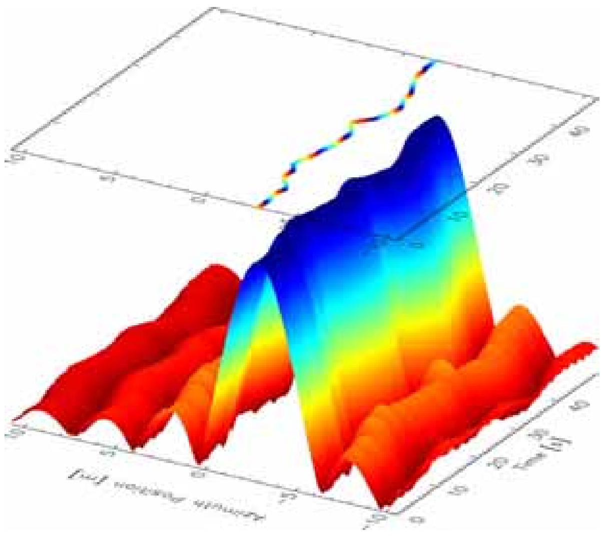

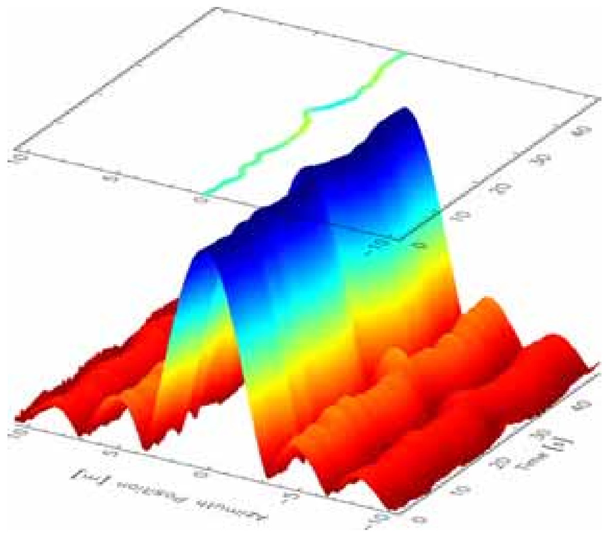

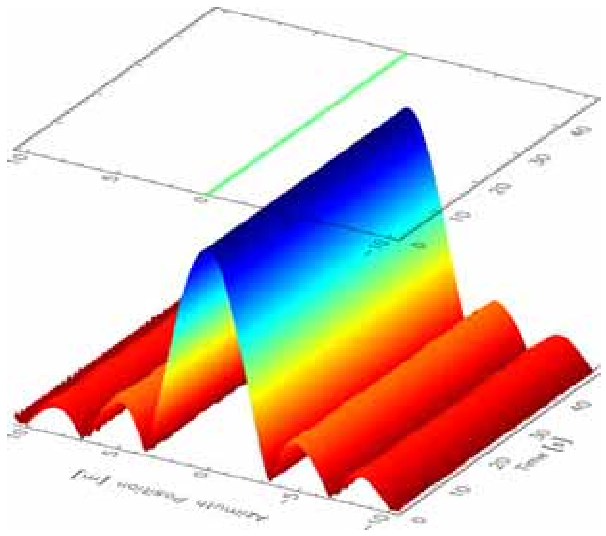

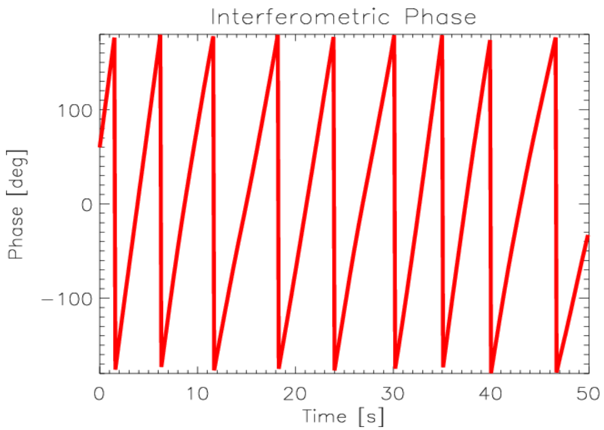

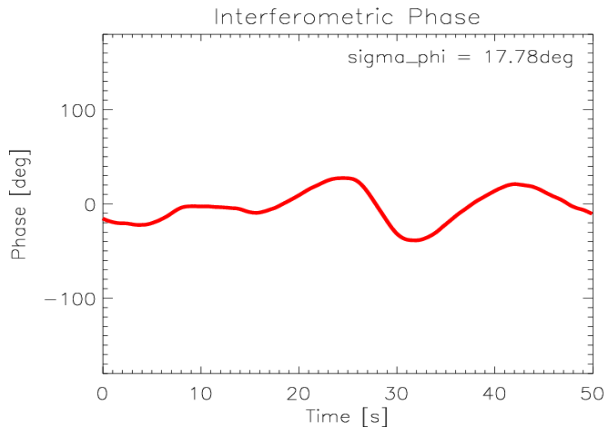

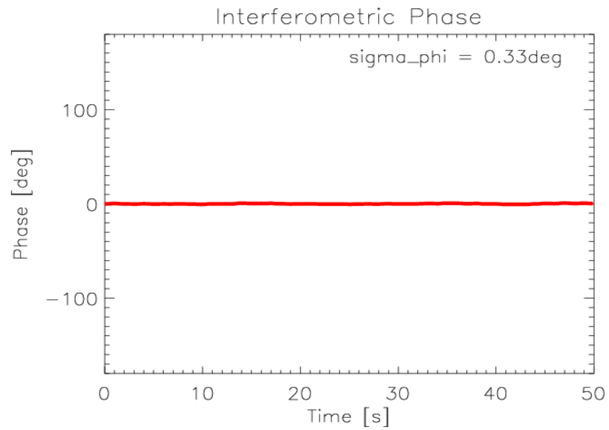

Microwaves and Radar Institute
gerhard.krieger@dlr.de

Close Formation Flight: Collision Avoidance

Autonomous Control

- *onboard computation of relative orbit maneuvers to ensure safe distance*
- *requires real-time relative position estimation and communication link between the satellites*

- *has to take into account fuel constraints (DART !)*

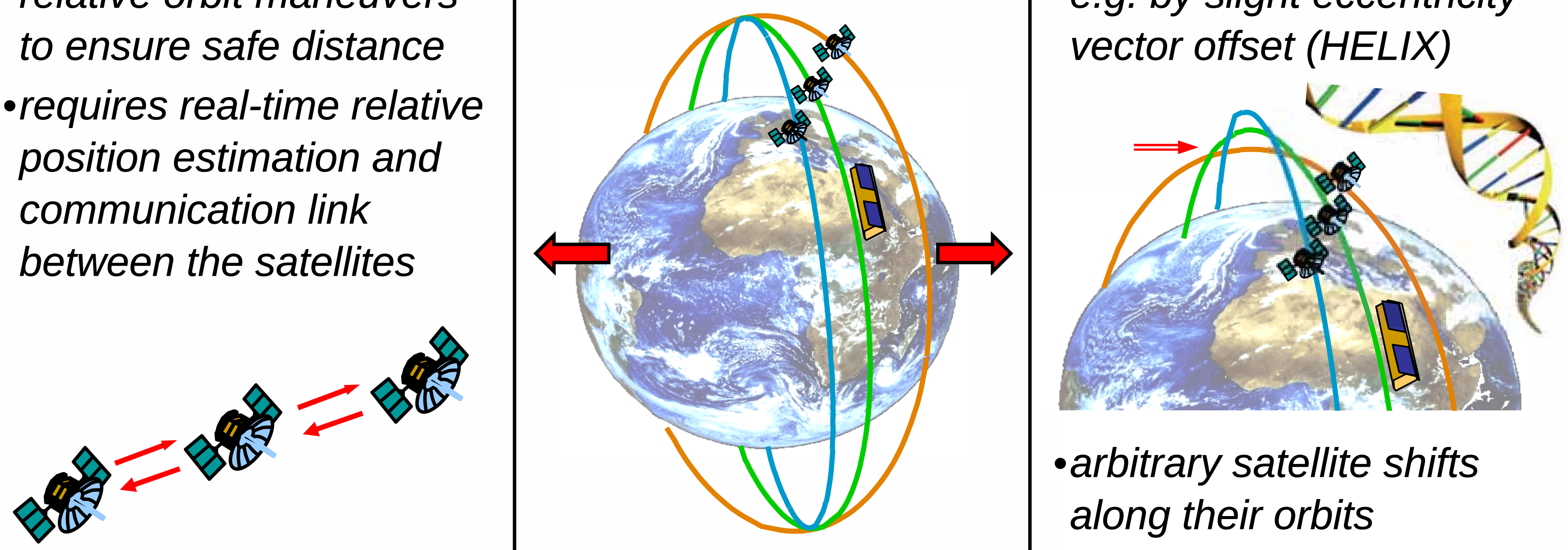

Safe Orbit Design

- *avoid orbit crossings, e.g. by slight eccentricity vector offset (HELIX)*

- *arbitrary satellite shifts along their orbits*
- *very short along-track baselines for a given latitude range*

Microwaves and Radar Institute
gerhard.krieger@dlr.de

Baseline Control and Baseline Estimation

- ***All satellites are exposed to almost identical orbit perturbations***
  - *precise baseline control with low fuel consumption (e.g. to ensure fixed baseline ratios)*
  - *very small differential acceleration (< 100 nm/s² → baseline error of less than 1 mm for 1000 km swath)*
- ***Precise baseline estimation by***
  - *double-difference GPS/Galileo carrier-phase measurements*
  - *accurate orbit propagation model*
  - *several studies predict a 3-D accuracy in the order of 1-2 mm*

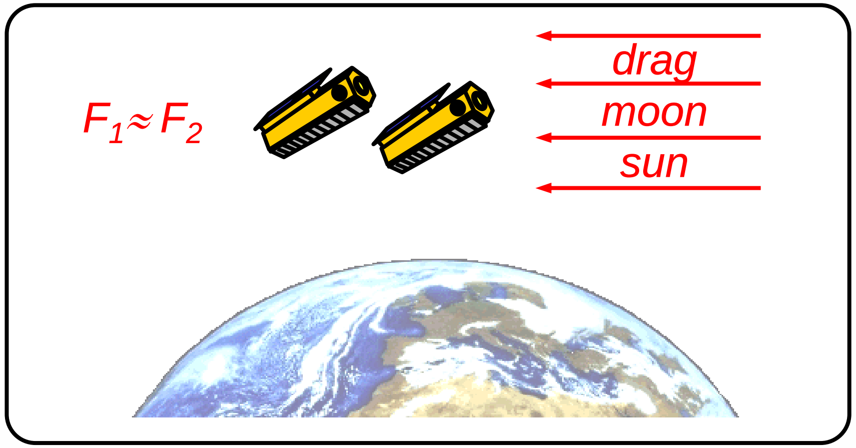

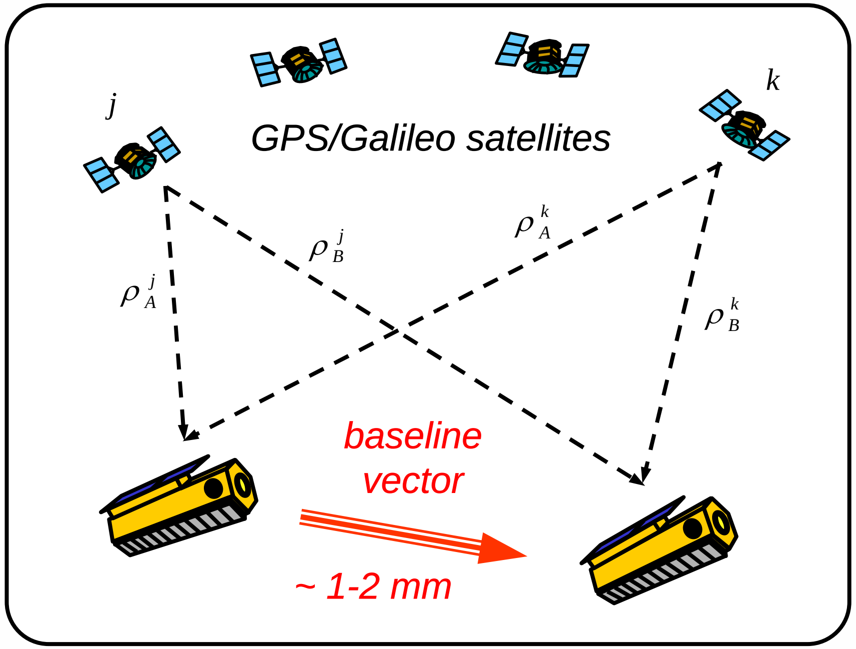

Microwaves and Radar Institute
gerhard.krieger@dlr.de

References: General

- IEE special issue on bistatic and multistatic radar, IEE Proceedings-F, Vol. 133, pp. 587-668, 1986.
- Hartl P, Braun HM, *Bistatic radar in space*, in "Space-based radar handbook", L.J. Cantafio, Artech House, Norwood, MA, 1989.
- Willis NJ, *Bistatic radar*, in Radar Handbook, MI Skolnik, editor, Chapter 25, Mc-Graw-Hill Publishing Co., 1990.
- Simpson RA, *Spacecraft studies of planetary surfaces using bistatic radar*, IEEE Transactions on Geoscience and Remote Sensing, Vol. 31, No. 2, pp. 465-482, 1993.
- Willis NJ, *Bistatic radar*, Artech House, Boston, 1995.
- Chernyak VS, *Fundamentals of multisite radar systems*. Amsterdam, Gordon & Breach, 1998.
- Moccia A, Chiacchio N, Capone A, *Spaceborne bistatic synthetic aperture radar for remote sensing applications*, Int. J. Remote Sens., Vol. 21, No. 18, pp. 3395-3414, 2000.
- Martin M, Klupar P, Kilberg S, Winter J, *Techsat 21 and revolutionizing space missions using microsatellites*, 15th American Institute of Aeronautics and Astronautics Conference on Small Satellites, Utah, USA, 2001.
- Griffiths HD, From a different perspective: principles, practice and potential of bistatic radar, Proc. International Radar Conference, Adelaide, Australia, 2003.
- Krieger G, Moreira A, *Spaceborne bi- and multistatic synthetic aperture SAR: potential and challenges*, IEE Proc. Radar Sonar Navigation, in print, 2006. (see also EUSAR 2004)
- Cherniakov M (editor), *Bistatic radars: emerging technology*, John Wiley & Sons, to appear in 2007.

References: Frequent Monitoring, Parasitic Radar

- Tomiyasu K, *Bistatic synthetic aperture radar using two satellites*, Eascon '78 Conference, IEEE, 1978.
- Hartl P, Braun HM, *A bistatic parasitical radar (BIPAR),* Proc. ISPRS, Kyoto, Japan, 1988.
- Guttrich GL, Sievers WE, *Wide area surveillance concepts basd on geosynchronous illumination and bistatic UAV or satellie reception*. IEEE Aerospace Conference, 1997.
- Ogrodnik RF, Wolf WE, Schneible R, McNamara J, Clancy J, Tomlinson PG, *Bistatic variants of space-based radar*. IEEE Aerospace Conference, 1997.
- Prati C, Rocca F, Giancola D, Guarnieri AM, *Passive geosynchronous SAR system reusing backscattered digital audio broadcasting signals*, IEEE Transactions on Geoscience and Remote Sensing, Vol. 36, No. 6, pp. 1973-1976, 1998.
- Martin-Neira M, Mavrocordatos C, Colzi E, *Study of a constellation of bistatic radar altimeters for mesoscale ocean applications*, IEEE Transactions on Geoscience and Remote Sensing, Vol. 36, No. 6, pp. 1898-1904, 1998.
- Cherniakov M, *Space-surface bistatic synthetic aperture radar - prospective and problems*. Proc. Radar Conference, pp. 22-25, Edinburgh, 2002.
- Krieger G, Fiedler H, Houman D, Moreira A, *Analysis of system concepts for bi- and multi-static SAR missions*, IEEE Geoscience and Remote Sensing Symposium (IGARSS), Toulouse, France, 2003.
- Sarabandi K, Kellndorfer J, Pierce L, *GLORIA: geostationary/low-earth orbiting radar image acquisition system: a multi-static GEO/LEO synthetic aperture radar satellite constellation for Earth observation*, IEEE Geoscience and Remote Sensing Symposium (IGARSS), Toulouse, France, 2003.
- Keydel W, *Perspectives and visions for future SAR systems*, IEE Proc. Radar Sonar Navigation, Vol. 150, No. 3, pp. 97-103, 2003.

References: Bistatic Scattering

- Kell RE, *On the derivation of bistatic RCS from monostatic measurements*, Proc. IEEE, Vol. 53, No. 8, pp. 983-987, 1965.
- Domville A, *The bistatic reflection from land and sea of X-band radio waves*, GEC Electr: Ltd: Stanmore, England, Memorandum SLM 1802, 1967.
- Ulaby F, van Deventer T, East J, Haddock T, Coluzzi ME, *Millimeter-wave bistatic scattering from ground and vegetation targets*, IEEE Trans. Geosci. Remote Sensing, Vol. 26, No. 3, pp. 229-243, 1988.
- Glaser J, *Some results in the bistatic radar cross section (RCS) of complex objects*, Proc. IEEE, Vol. 77, pp. 639-648, 1989.
- Ruffini G, Cardellach E, Rius A, Aparicio JM, *Remote sensing of the ocean by bistatic radar observation: a review*, IEEC Report ESD-iom019-99, Barcelona, Spain, 1999.
- Eigel R, Collins P, Terzuoli A, Nesti G, Fortuny J, *Bistatic scattering characterization of complex objects*, IEEE Trans. Geosci. Remote Sensing, Vol. 38, No. 5, pp. 2078-2092, 2000.
- Long MW, *Radar reflectivity of land and sea*, Artech House, 2001.
- Khenchaf A, *Bistatic Scattering and Depolarization by Randomly Rough Surfaces: Application to the Natural Rough Surfaces in X-Band*, Waves in Random Media, Vol. 11, pp. 61-89, 2001.
- Elfouhaily T, Thompson DR, Linstrom L, *Delay Doppler analysis of bistatically reflected signals from the ocean surface: theory and application*, IEEE Trans. Geosci. Remote Sens., Vol. 40, No. 3, pp. 560-573, 2002.
- Burkholder RJ, Gupta IJ, Johnson JT, *Comparison of monostatic and bistatic radar images*, IEEE Antennas and Propagation Magazine, Vol. 45, No. 3, pp. 41- 50, 2003.
- Nashashibi A, Ulaby F, *Millimeter-wave polarimetric bistatic radar scattering from rough soil surfaces*, IGARSS, Toulouse, France, 2003.
- Ceraldi E, Franceschetti G, Iodice A, Riccio D, *Estimating the soil dielectric constant via scattering measure-ments along the specular direction*, IEEE Trans. Geosci. Remote Sens., Vol. 43, No. 2, pp. 295-305, 2005.

References: SAR Interferometry

General Reviews about Interferometry:

- Bamler R, Hartl P, *Synthetic aperture radar interferometry*, Inverse Problems, Vol. 14, pp. 1-54, 1998.
- Rosen PA, Hensley S, Joughin IR, Li FK, Madsen SN, Rodriguez E, Goldstein R, *Synthetic aperture radar interferometry*, Proc. IEEE, Vol. 88, No. 3, pp. 333-382, 2000.
- Hanssen R, *Radar interferometry: data interpretation and error analysis,* Dordrecht, Kluwer Academic Publishers, 2001.

Interferometry with Multistatic Satellite Configurations:

- Moccia A, Vetrella S, A tethered interferometric synthetic aperture radar (SAR) for a topographic mission, IEEE Transactions on Geoscience and Remote Sensing, Vol. 30, No. 1, pp. 103-109, 1992.
- Zebker HA, Farr TG, Salazar RP, Dixon TH, *Mapping the world's topography using radar interferometry: the TOPSAT mission*, Proc. IEEE, Vol. 82, No. 12, pp. 1774-1786, 1994.
- Massonnet D, *Capabilities and limitations of the interferometric cartwheel*, IEEE Trans. Geosci. Remote Sensing, Vol. 39, No. 3, pp. 506-520, 2001.
- Girard R, Lee PF, James K, *The RADARSAT-2&3 topographic mission: an overview*. IEEE International Geoscience and Remote Sensing Symposium, Toronto, Canada, IEEE, 2002.
- Krieger G, Fiedler H, Mittermayer J, Papathanassiou K, Moreira A, *Analysis of multistatic configurations for spaceborne SAR interferometry*, IEE Proc. Radar Sonar Navigation, Vol. 150, No. 3, pp. 87-96, 2003.
- Zink M, Krieger G, Amiot T, *Interferometric performance of a cartwheel constellation for TerraSAR-L*, FRINGE Workshop, Frascati, Italy, 2003.
- Krieger G, Moreira A, Fiedler H, Hajnsek I, Eineder M, Zink M, Werner M, *TanDEM-X: a satellite formation for high resolution SAR interferometry*. ESA Fringe Workshop, Frascati, Italy, 2005.

Microwaves and Radar Institute
gerhard.krieger@dlr.de

References: Multi-Baseline Interferometry & Tomography

- Ferretti A, Monti Guarnieri A, Prati C, Rocca F, *Multi baseline interferometric techniques and applications*, in ESA Workshop on Applications of ERS SAR Interferometry, Zurich, Switzerland, 1996.
- Homer J, Longstaff ID, Callaghan G, *High resolution 3-D SAR via multi-baseline interferometry*, IGARSS 1996.
- Massonnet D, Reduction of the need for phase unwrapping in radar interferometry, *IEEE Transactions on Geosciene and Remote Sensing,* Vol. 32, No. 2**,** pp. 489-497, 1996.
- Reigber A, Moreira A, *First demonstration of airborne SAR tomography using multibaseline L-band data*, IEEE Trans. Geosc. and Remote Sens., Vol. 38, No. 5, pp. 2142-2152, 2000.
- Gini F, Lombardini F, Montanari M, *Layover solution in multibaseline SAR interferometry*, IEEE Trans. Aerospace and Electronic Systems, Vol. 38, No. 4, pp. 1344-1356, 2002.
- She Z, Gray DA, Bogner RE, Homer J, Longstaff ID, *Three-dimensional space-borne SAR imaging with multiple pass processing*, Intern. Journal of Remote Sensing, Vol. 23, No. 10, pp. 4357-4382, 2002.
- Fornaro G, Lombardini F, Serafino F, *Three-dimensional multipass SAR focusing: experiments with long-term spaceborne data*, IEEE Trans. Geosci. Remote Sens., Vol. 43, No. 4, pp. 702-714, 2005.
- Eineder M, Adam N, *A Maximum-likelihood estimator to simultaneously unwrap, geocode, and fuse SAR interferograms from different viewing geometries into one digital elevation model*, IEEE Trans. Geosci. Remote Sens., Vol. 43, No. 1, pp. 24-36, 2005.
- Lombardini F, *Differential tomography: a new framework for SAR interferometry*, IEEE Trans. Geosci. Remote Sensing, Vol. 43, No. 1, pp. 37-44, 2005.
- Krieger G, Moreira A, *Multistatic SAR satellite formations: potentials and challenges*, Proc. IGARSS, pp. 2680 – 2684, Seoul, Korea, 2005.
- Fornaro G, Monti Guarnieri A, Pauciullo A, Tebaldini S, *Joint multibaseline SAR interferometry*, EURASIP Journal Applied Signal Processing, Vol. 20, pp. 3194-3205, 2005.

Microwaves and Radar Institute
gerhard.krieger@dlr.de

References: Polarimetric SAR Interferometry

General Papers about Polarimetric SAR Interferometry:

- Cloude SR, Papathanassiou KP, *Polarimetric SAR interferometry*, IEEE Transactions on Geoscience and Remote Sensing, Vol. 36, No. 5, pp. 1551-1565, 1998.
- Treuhaft RN, Siqueira PR, *The vertical structure of vegetated land surfaces from interferometric and polarimetric radar*, Radio Science, Vol. 35, No. 1, pp. 141-177, 2000.
- Papathanassiou KP, Cloude SR, *Single-baseline polarimetric SAR interferometry*, IEEE Transactions on Geoscience and Remote Sensing, Vol. 39, No. 11, pp. 2352-2363, 2001.
- Cloude SR, Papathanassiou KP, *Three-stage inversion process for polarimetric SAR interferometry*, IEE Proceedings - Radar, Sonar and Navigation, Vol. 150, No. 3, pp. 125-134, 2003.

Polarimetric SAR Interferometry with Multistatic Satellite Array:

- Massonnet D, Moreira A, Bamler R, Souyris JC, *Voice: volumetric interferometry cartwheel experiment*, proposal to European Space Agency for a mission to retrieve vegetation structure parameters and above ground forest biomass using a passive polarimetric SAR interferometry cartwheel configuration, 2002.
- Moreira A, Papathanassiou K, Krieger G, *Polarimetric SAR interferometry with a passive polarimetric micro-satellite concept*. 27th general assembly of the international union of radio science (URSI). Maastricht, Netherlands, 2002.
- Krieger G, Papathanassiou K, Cloude S, Moreira A, Fiedler H, Völker M, *Spaceborne polarimetric SAR interferometry: performance analysis and mission concepts*. 2nd international workshop on applications of polarimetry and polarimetric interferometry (PolInSAR), Frascati, Italy, ESA, 2005.
- Krieger G, Papathanassiou K, Cloude S, *Spaceborne polarimetric SAR interferometry: performance analysis and mission concepts*, EURASIP Journal on Applied Signal Processing, Vol. 20, pp. 3272-3292, 2005.

Microwaves and Radar Institute
gerhard.krieger@dlr.de

References: Along-Track Interferometry and GMTI

- Goldstein RM, Zebker HA, *Interferometric radar measurement of ocean surface currents*, Nature, Vol. 328, No. 20, pp. 707-709, 1987.
- Romeiser R et al., *Study on concepts for radar interferometry from satellites for ocean (and land) applications*, http://www.ifm.uni-hamburg.de/~wwwrs/project_koriolis.htm.
- Moccia A, Rufino G, *Spaceborne along-track SAR interferometry: performance analysis and mission scenarios*, IEEE Trans. Aerospace Electronic Systems, Vol. 37, No. 1, pp. 199-213, 2001.
- Gill E, Runge H, *A tight formation flight for along-track SAR interferometry*, Proc. of Formation Flying Symposium 2004, Washington, USA.
- Carande R, *Dual baseline and frequency along-track interferometry*, Proc. IGARSS 1992, Houston, Texas, USA.
- Lombardini F, Bordoni F, Gini F, Terrazzani L, *Multibaseline ATI-SAR for robust ocean surface velocity estimation*, IEEE Tran. Aerospace Electron. Systems, Vol. 40, No. 2, pp.417-433, 2004.
- Marais K, Sedwick R, *Space based GMTI using scanned pattern interferometric radar*, IEEE Aerospace Conference, 2001.
- Goodman NA, Stiles JM, *A general signal processing algorithm for MTI with multiple receive apertures*, IEEE Radar Conf., Atlanta, pp. 315-320, 2001.
- Ender J, *Spacebased SAR/MTI using multistatic satellite configurations*, EUSAR 2002, pp. 337-340, Cologne, Germany.
- Cerutti-Maori D, Ender, J, *Performance analysis of multistatic configurations for spaceborne GMTI based on the auxiliary beam approach,* IEE Radar Sonar & Navigation, Vol. 153, No. 2, pp. 96-103, 2006.

References: High Resolution and Wide Swath SAR Imaging

- Prati C, Rocca F, *Improving slant-range resolution with multiple SAR surveys*, IEEE Trans. Aerospace Electronic Systems, Vol. 29, pp. 135-143, 1993.
- Gatelli F, Guamieri AM, Parizzi F, Pasquali P, Prati C, Rocca F, *The wavenumber shift in SAR interferometry*, IEEE Transactions on Geoscience and Remote Sensing, Vol. 32, No. 4, pp. 855-865, 1994.
- Goodman NA, Lin SC, Rajakrishna D, Stiles JM, *Processing of multiple-receiver spaceborne arrays for wide area SAR*, IEEE Trans. Geosci. Remote Sensing, Vol. 40, No. 4, pp. 841-852, 2002.
- Krieger G, Moreira A, *Potentials of digital beamforming in bi- and multistatic SAR*, IGARSS, Toulouse, France, 2003.
- Aguttes JP, *The SAR train concept: required antenna area distributed over n smaller satellites, increase of performance by n*, IGARSS, Toulouse, France, 2003.
- Younis M, *Digital beam-forming for high-resolution wide swath real and synthetic aperture radar*, PhD-thesis, Karlsruhe, Germany, 2004.
- Krieger G, Gebert N, Moreira A, *Unambiguous SAR signal reconstruction from nonuniform displaced phase center sampling*, IEEE Geoscience and Remote Sensing Letters, Vol. 1, No. 4, pp. 260-264, 2004.
- Li Z, Wang H, Su T, Bao Z, *Generation of wide-swath and high-resolution SAR images from multichannel small spaceborne SAR systems*, IEEE Geoscience and Remote Sensing Letters, Vol. 2, No. 1, pp. 82-85, 2005.

Microwaves and Radar Institute
gerhard.krieger@dlr.de

References: Bistatic SAR Processing

- Soumekh M, *Bistatic synthetic aperture radar inversion with application in dynamic object imaging*, IEEE Transactions on Signal Processing, Vol. 39, No. 9, 2044-2055, 1991.
- Ding Y, Munson DC, *A fast back-projection algorithm for bistatic SAR imaging*. IEEE International Conference on Image Processing, 2002.
- D'Aria D, Guarnieri AM, Rocca F, *Focusing bistatic synthetic aperture radar using dip move out*, IEEE Transactions on Geoscience and Remote Sensing, Vol. 42, No. 7, pp. 1362-1376, 2004.
- Loffeld O, Nies H, Peters V, Knedlik S, *Models and useful relations for bistatic SAR processing*, IEEE Transactions on Geoscience and Remote Sensing, Vol. 42, No. 10, pp. 2031-2038, 2004.
- Rigling BD, Moses RL, *Polar format algorithm for bistatic SAR*, IEEE Transactions on Aerospace and Electronic Systems, 40 (4), 1147-1159, 2004.
- Neo Y, Wong F, Cumming I, *Focusing bisatic SAR images using non-linear chirp scaling*, Radar Conference, Toulouse, France, 2004.
- Cantalloube H, Wendler M, Giroux V, Dubois-Fernández P, Krieger G, *Challenges in SAR processing for airborne bistatic acquisitions*, Proceedings of EUSAR, Ulm, Germany, 2004.
- Walterscheid I, Ender JHG, Brenner AR, Loffeld O, *Bistatic SAR processing using an Omega-K type algorithm*, IEEE Geoscience and Remote Sensing Symposium, Seoul, Korea, 2005.
- Natroshvili K, Loffeld O, Nies H, Medrano Ortiz, A, *First steps to bistatic focusing*, IEEE Geoscience and Remote Sensing Symposium, Seoul, Korea, 2005.
- Giroux V, Cantalloube H, Daout F, *An omega-K algorithm for SAR bistatic systems*, IGARSS, Seoul, 2005.
- Rodriguez-Cassola M, Krieger G, Wendler M, *Azimuth-invariant, bistatic airborne SAR processing strategies based on monostatic algorithms*, IGARSS, Seoul, Korea, 2005.
- Sanz-Marcos J, Prats P, Mallorqui JJ, *Bistatic fixed-receiver parasitic SAR processor based on the back-propagation Algorithm*, IGARSS, Seoul, Korea, 2005.
- Bamler R, Boerner E, *On the use of numerically computed transfer functions for processing of data from bistatic SARs and high squint orbital SARs*, IGARSS, Seoul, Korea, 2005.

References: Bistatic SAR Experiments & Synchronisation

- Auterman JL, Phase Stability Requirements for a Bistatic SAR. IEEE Nat. Radar Conference, Atlanta, USA, 1984.
- Martinsek D, Goldstein R, Bistatic radar experiment, European Conference on Synthetic Aperture Radar (EUSAR), Friedrichshafen, Germany, pp. 31-34, 1998.
- Wendler M, Krieger G, Horn R, Gabler B, Dubois-Fernandez P, Vaizan B, du Plessis O, First results of a joint bistatic airborne SAR experiment. International Geoscience and Remote Sensing Symposium (IGARSS), Toulouse, France, IEEE, 2003.
- Eineder M, Oscillator clock drift compensation in bistatic interferometric SAR, IEEE Geoscience and Remote Sensing Symposium (IGARSS), Toulouse, France, 2003.
- Walterscheid I, Brenner AR, Ender JHG, Results on bistatic synthetic aperture radar, Electronics Letters, Vol. 40, No. 19, pp. 1224-1225, 2004.
- Weiß M, Synchronisation of bistatic radar systems, IEEE Geoscience and Remote Sensing Symposium (IGARSS), Anchorage, USA, IEEE, 2004.
- Dubois-Fernandez P, Cantalloube H, Vaizan B, Krieger G, Horn R, Wendler M, Giroux V, ONERA-DLR bistatic SAR campaign: planning, data acquisition, and first analysis of bistatic scattering behavior of natural and urban targets, IEE Proceedings - Radar, Sonar and Navigation, in print, 2006. (see also EUSAR 2004)
- Yates G, Horne AM, Blake AP, Middleton R, Andre DB, Bistatic SAR image formation, IEE Proceedings - Radar, Sonar and Navigation, in print, 2006. (see also EUSAR 2004)
- Krieger G, Younis M, Impact of oscillator noise in bistatic and multistatic SAR, IEEE Geoscience and Remote Sensing Letters, in print, 2006. (see also IGARSS 2005)
- Younis M, Metzig R, Krieger G, Performance prediction of a phase synchronization link for bistatic SAR, IEEE Geoscience and Remote Sensing Letters, in print, 2006.

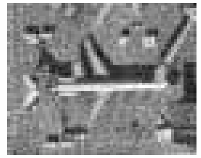

Microwaves and Radar Institute
gerhard.krieger@dlr.de